RECLAMATION

Managing Water in the West

Arroyo de las Cañas Geomorphic, Hydraulic, and Sediment Transport Analysis

Middle Rio Grande Project, New Mexico
Albuquerque Area Office

U.S. Department of the Interior
Bureau of Reclamation

September 2016

Mission Statements

The mission of the Department of the Interior is to protect and provide access to our Nation's natural and cultural heritage and honor our trust responsibilities to Indian Tribes and our commitments to island communities.

The mission of the Bureau of Reclamation is to manage, develop, and protect water and related resources in an environmentally and economically sound manner in the interest of the American public.

RECLAMATION
Managing Water in the West

Arroyo de las Cañas Geomorphic, Hydraulic, and Sediment Transport Analysis

Middle Rio Grande Project, New Mexico
Albuquerque Area Office

Report Prepared by
Aubrey Harris, E.I.T., M.S.C.E., Hydraulic Engineer and
Jonathan AuBuchon, P.E, Hydraulic Engineer

Report Reviewed by
Tony Lampert, P.E., Civil (Hydraulic/Hydrologic) Engineer,
Robert Padilla, P.E., D.WRE, Supervisory Civil (Hydraulic/Hydrologic) Engineer
Reclamation River Analysis Group,
Technical Services Division

Acknowledgements

This work has been greatly benefited by the persistent data collection of the US Geological Survey and technical work members of the River Analysis Group in Reclamation's Albuquerque Area Office. Recent works by T. Massong, P. Makar, and others have provided insight into the geomorphic, hydraulic and technical analyses that were necessary to achieve this work.

Contents

Page

Executive Summary

The Bureau of Reclamation (Reclamation) has authority for river channel maintenance on the Rio Grande between Velarde, New Mexico, and the headwaters of the Caballo Reservoir. Reclamation regularly monitors changes in the river channel and evaluates channel and levee capacity in an effort to identify river maintenance sites where there is concern about possible damage to riverside facilities. The Rio Grande surrounding the Arroyo de las Cañas confluence was identified as an area of river maintenance concern as the river is confined by a levee system and the Low Flow Conveyance Channel (LFCC) to the West. The Arroyo de las Cañas influences the Rio Grande by transporting and depositing sediment at its confluence. The sediment has locally stabilized the confluence, exacerbating the erosion of the Rio Grande's western bank. The tributary's sediment supply may also be contributing to downstream sandbar formation.

This report provides an analysis of geomorphic and hydraulic observations within the Cañas reach. This helps evaluate changes that have and are occurring in the riverine system and aids in understanding viable future activities and potential future channel responses.

Flow and sediment supply are the two main drivers of geomorphic change on the Rio Grande (Makar and AuBuchon, 2012). An analysis of the magnitude, frequency, and duration of discharge in the Rio Grande and sediment supply provide indications of how the drivers have changed, providing insight into observation of geomorphic change. Major findings related to the drivers of geomorphic changes within the Cañas reach are summarized as follows:

- Local precipitation, annual average between 5 and 15 inches, primarily occurs from July through September via high magnitude but short duration events (2.2.1.2 *Precipitation* p. 11).
- Largest discharges within the reach are driven by snow melt. Water operations have caused the Rio Grande to change from being dry about a third of the year to being wet all year long. (2.2.3 *Duration* p. 14).
- Suspended sediment concentration increases downstream of San Acacia, a trend that has been decreasing in magnitude since the drought began in 1999 (2.3.1 *Suspended Sediment* p.16).
- An analysis of recent data suggests that the winter months at San Acacia and the monsoonal flow at San Marcial are more effective in transporting the suspended sediment load than the spring runoff flows. (2.3.2.2 *Seasonal Suspended Sediment Load,* p.24).
- Sediment continues to coarsen, with the largest suspended sediment concentrations occurring during the monsoon season. Sand sized particles are more prevalent in flows greater than 100 cfs. Seasonality trends were observed in the composition of suspended sediment at San Acacia, while San Marcial is more uniform. (2.3.2.3 *Suspended Sediment Load based on Particle Size*, p.25).

Geomorphic change within the Cañas reach have been assessed using six parameters: width, slope, sinuosity, planform, channel topography, and bed material size. A summary of the major observations for the six analyzed geomorphic parameters are as follows:

- Width decreased from 1918 to 2000 but has stayed constant from 2006-2012. Variability in the width has continued to decrease, resulting in a more uniform channel (3.1.2 *Longitudinal Channel Width*, p. 31).
- Channel planform has moved from a braided, predominantly bed load system circa 1918-1949 to a single channel planform from the 1960s to the present indicating a mixed bed and suspended sediment load system. Accompanying this change has been an increase in vegetation and a loss of in-channel bars, with some channel bars becoming attached to the river channel banks. Vegetation since the 1990s has been relatively constant. Sand bars upstream of the Arroyo de las Cañas have stabilized more than those downstream of the Cañas due to woody vegetation. Bend migration and island/bar formation are more dynamic downstream of the Arroyo de las Cañas (3.2 *Channel Location and Planform,* p. 34)
- River bed slope has decreased in recent years with the channel length increasing above the Arroyo de las Cañas. The slope has increased slightly downstream of the Arroyo de las Cañas with a pivot point for the transition approximately at Arroyo del Tajo (3.3.2 *Mean Bed Profiles over Time,* p. 42).
- Sinuosity has stayed relatively constant since 1949, with a slight increase upstream of Arroyo de las Cañas and a slight decrease downstream (3.4 *Channel Sinuosity,* p. 46).
- Bed material has coarsened over time in the reach, with bed material size decreasing in the downstream direction. River bed samples are generally not stable due to the shear stresses that develop in the channel at flows greater than 1,000 cfs. Bed material samples from Arroyo de las Cañas indicate a higher stability relative to Rio Grande bed material samples, suggesting that larger arroyo particles may provide armoring near the arroyo confluences (3.5.2 *Bed Particle Stability,* p. 49).
- Channel topography changes between 1992 and 2013 show that the channel has deepened and narrowed. Upstream of the Arroyo de las Cañas, the floodplain terrace has increased the height above the river bed compared to the topography downstream of the arroyo. (3.6 *Channel Floodplain Topography,* p. 51)

The trends in the observed geomorphic parameters indicate the Rio Grande through the Arroyo de las Cañas reach is narrowing and degrading, with the channel becoming more incised upstream of the confluence. Coupled with this are signs of bed material coarsening, slope decreasing, and a slight sinuosity increase in recent years. These are all similar expected reactions that Lane (1954) and Schumm (1977) found in their general riverine relationships when the sediment supply is decreased. Some of these parameter changes are further predicted to be amplified by Lane and Schumm's relationships when the peak discharge is decreased. Knighton (1998) also observed that the larger the ratio of peak flow to mean flow, the larger variation in active channel width. The increase in summer flow duration, coupled with the peak flow cuts for flood control has resulted in a reduction in this ratio. Based on Knighton's ratio this would predict a narrower channel, which is consistent with reach observations (4.0 Future Channel Response p.63).

If the sediment load to the reach continues to decrease, the planform may shift to be more meandering and have less mobility of river bed sediments due to armoring. More bank erosion from lateral migration may also occur as the river continues to reduce its slope. The section downstream from the Arroyo de las Cañas may become narrow and meandering, following a similar response as the upstream section. If the peak flow decreases, say by increased diversion upstream or drier hydrologic regimes, and the duration of low flows continue to persist throughout most of the year: the bed material would be expected to coarsen and fines will be winnowed out of the bed material. Arroyo confluences, with their supply of coarse particles, may stabilize part of the river channel, causing local incision or erosion in the unprotected portions of the river channel. Localized incisions would exacerbate the disconnection between the main river channel and its floodplain.

Maintenance and channel restoration efforts that take these trends into account will likely be successful in the future. Apart from changing system drivers that promote a resetting of the channel and floodplain connection, channel restoration may only be temporary. The planform evolution models of Massong et al. (2010) suggests that if enough outside energy is brought to bear on the system (increase flow magnitudes, durations, frequency) the system may eventually reset and provide better connection between the active channel and its floodplain. Given observed trends in the water supply, a system reset is unlikely. Mechanical intervention could reset this connection through terrace lowering or streambed raising, with the latter more representative of the sediment reworking from a large flood event.

Without some mechanical resetting of historic conditions, it is estimated that the channel will become more uniform and homogeneous. Overflow and inundation will be less frequent as channel incision continues. Some of these trends may be temporarily reversed with a mechanical resetting, creating more river-floodplain interaction, and potentially causing localized aggradation, bed material fining, and increase in slope. A similar response may also occur through clearing vegetation at some of the eastern tributary confluences, allowing for additional sediment to be brought into the system, causing an increase in sediment load. While this may temporarily produce desirable outcomes for the observed geomorphic parameters, it would likely be temporary without concomitant changes in water operations that have a pronounced effect on the water supply (magnitude, duration, and frequency).

1.0 Background

The Arroyo de las Cañas location on the Rio Grande is currently classified as a Class 2 river maintenance site (Maestas et al., 2014). The study area for this analysis encompasses aggradation-degradation (agg-deg) lines 1364 to 1455, approximately 11 river miles from RM 101 to RM 89. The confluence of the Arroyo de las Cañas (Figure 1) is approximately at agg-deg 1374, near RM 95.5. Within this reach the Rio Grande is close to the western spoil levee for the Low Flow Conveyance Channel (LFCC). The LFCC spoil levee, constructed in the 1950s, protects the LFCC and the Socorro Main Canal. The construction of the LFCC made it necessary to shift the river to the east which also narrowed the floodplain (Massong 2006). Massong (2006) further noted that from a review of the aerial photography, this channel modification was the only anthropogenic activity in the reach from the 1930s to 2006. There has been increased vegetation observed within the study reach since 2002, which helps to stabilize and narrow the channel (Makar et al. 2006). Makar and AuBuchon (2012) identified Arroyo de las Cañas as a potential local bed grade control on the Rio Grande but there is some uncertainty as to the extent of bed elevation control (Massong, 2006).

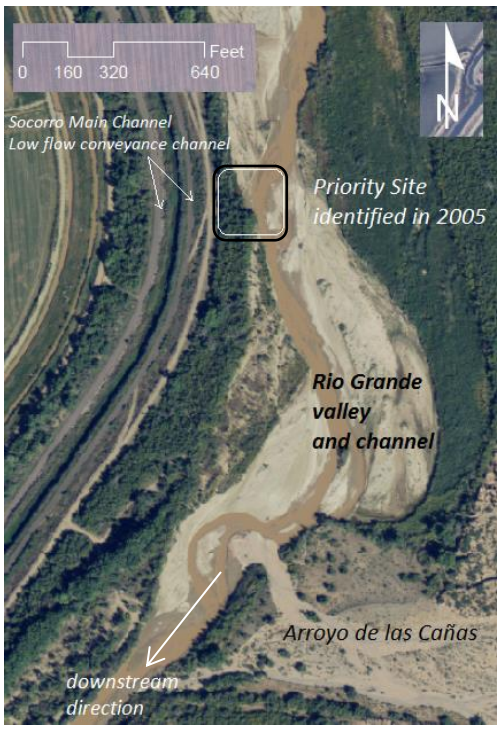

Figure 1 Aerial photograph of the Arroyo de las Cañas river maintenance site and surrounding geographic features circa 2006.

In 2005, a river maintenance site was identified near the Arroyo de las Cañas confluence (Figure 1). The site is located south of Socorro and north of US Route 380, between River Mile 95 and 96 (based on 2002 River Mile demarcations) and about 1,000 feet upstream of the confluence of the Arroyo de las Cañas (Massong 2006). In 2005, significant bank erosion was observed at this site and plans were initiated for constructing a river maintenance design. The design was poised to be constructed when the 2008 spring snow-melt runoff moved the river's alignment away from the spoil levee. The change reduced the probability of damage to the spoil levee and a decision was made to stop work at this site and monitor the area in case future work is warranted (Nemeth, 2008). With aid of findings in this report, a project may be pursued to provide protection for the LFCC's spoil levee, while exploring habitat restoration potential in the vicinity.

The Arroyo de las Cañas, with a drainage area of about 32 square miles (Bullard, 2004) enters from the east. Arroyo de las Cañas is one of many arroyos in this reach that are the result of the Joyita Uplift, a geological feature creating highly faulted rock formations that can deliver sediment to the Rio Grande through a width reduction in the Santa Fe formation (MEI, 2002).

The purpose of this report is to document geomorphic, hydraulic and sediment transport analyses within the study area in order to identify whether the river is currently adjusting, whether the

principal drivers of sediment and water in the vicinity have changed, and to identify expected future channel responses.

2.0 Drivers of Change in the Arroyo de las Cañas Project Site

Flow and sediment supply are the two main drivers of geomorphic change on the Rio Grande (Makar and AuBuchon, 2012). An analysis of sediment supply and the magnitude, frequency and duration of discharge in the Rio Grande provide indications of how the drivers have changed, as well as observations of geomorphic change. The extent by which the drivers affect the geomorphology within a reach of the Rio Grande are controlled by factors such as bank stability, bed stability, base level, floodplain lateral confinement, and floodplain connectivity (Makar and AuBuchon, 2012). This section assesses the changes in the main drivers on the Rio Grande in recent decades. Data used in the analyses of the drivers are from the U.S. Geological Survey (USGS) field sampling sites at the San Marcial (USGS 08358400) and San Acacia Rio Grande Floodway (USGS 08354900), National Water Information System, which includes two precipitation gages in Socorro (GHCN US1NMSC0001 and GHCN US00296387), Bosque del Apache (GHCN USC00291138) (Figure 2). The USGS gages are about 27 miles downstream and 18 miles upstream of the Arroyo de las Cañas respectively. The San Antonio gage (USGS 08355490) was also used in this analysis; this gage came into operation in 2006 and is about 6 miles downstream of the Arroyo de las Cañas.

Summary of major findings in the analysis of drivers:

- The early 1990s, 2005, and 2008 were high flow and long duration spring snowmelt discharge years.
- The study reach is a losing stream.
- Local precipitation trend has a generally decreasing annual average. Events are episodic however, with annual rainfall between 5 and 15 inches.
- Local precipitation primarily occurs in July through September, via high magnitude but short duration events; while the largest discharge events are still primarily driven by snow melt in the higher elevations of the Rio Grande watershed.
- The suspended sediment concentration increases downstream of San Acacia Diversion Dam.
- Sand sized particles are more prevalent in the suspended sediment load when discharges are above 140 cfs than at lower flows, where silts and clays are dominant.
- The duration of discharges between 0-1,000 cfs has increased between 1990 and 2014.
- The duration of discharges greater than 2,000 cfs has decreased between 1990 and 2014.
- There is evidence of suspended sediment and bed material coarsening throughout the study reach over time.
- The discharges moving the most suspended sediment at San Acacia are 1,000 cfs during the winter months and at 4,000 cfs during spring run-off. The winter effective discharge moves twice as much sediment as during spring runoff.

- The discharges moving the most suspended sediment at San Marcial are 2,000 cfs during monsoonal events and 4,500 cfs during spring runoff. Monsoon season is the most effective at transporting sediment.

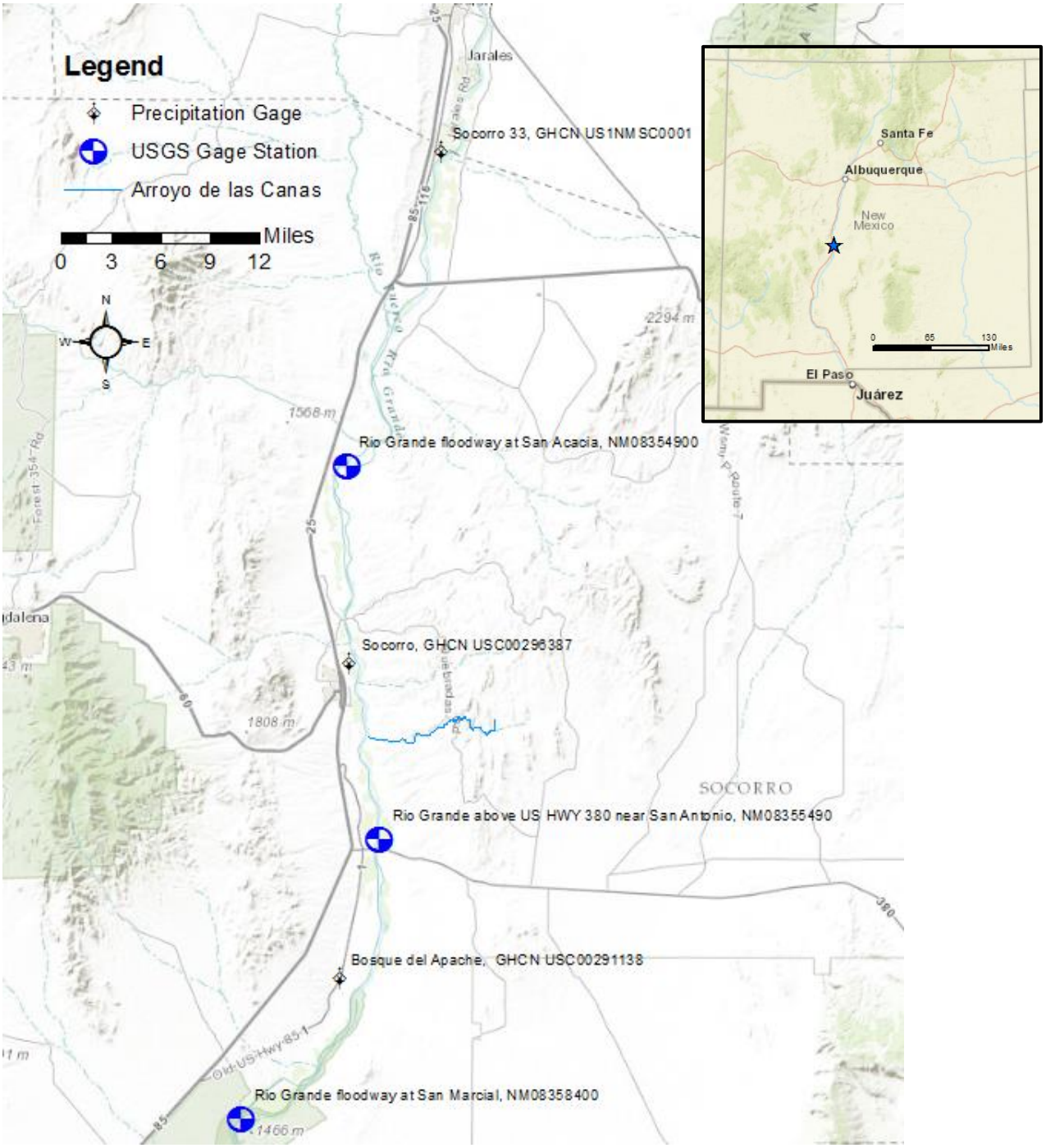

Figure 2 Map of the study area and surrounding gages used for discharge data. Inset: New Mexico with the study area location.

2.1 Brief History of Water Operations within the Study Area

Reclamation and the U.S. Army Corps of Engineers (USACE) are authorized to address water delivery, flooding, and sediment management needs on the Middle Rio Grande (MRG). Historically this was pursued by performing channelization, levee, and dam projects (Figure 3). These anthropogenic actions had an influence on the drivers of change and also the morphology of the river (Owen et al, 2012).

Within this study reach the construction and operation of the Low Flow Conveyance Channel (LFCC) affected the water supply in the Rio Grande. The LFCC and its spoil levee was constructed and fully operational in 1959, and was used to fulfill water agreements between New Mexico and Texas. From the 1960s and 70s, the majority of river flow was diverted at San Acacia, New Mexico and sent via the LFCC directly to Elephant Butte Reservoir. Diversions from the Rio Grande into the LFCC were suspended in 1985, except for a few experimental test operations in the early 1990s.

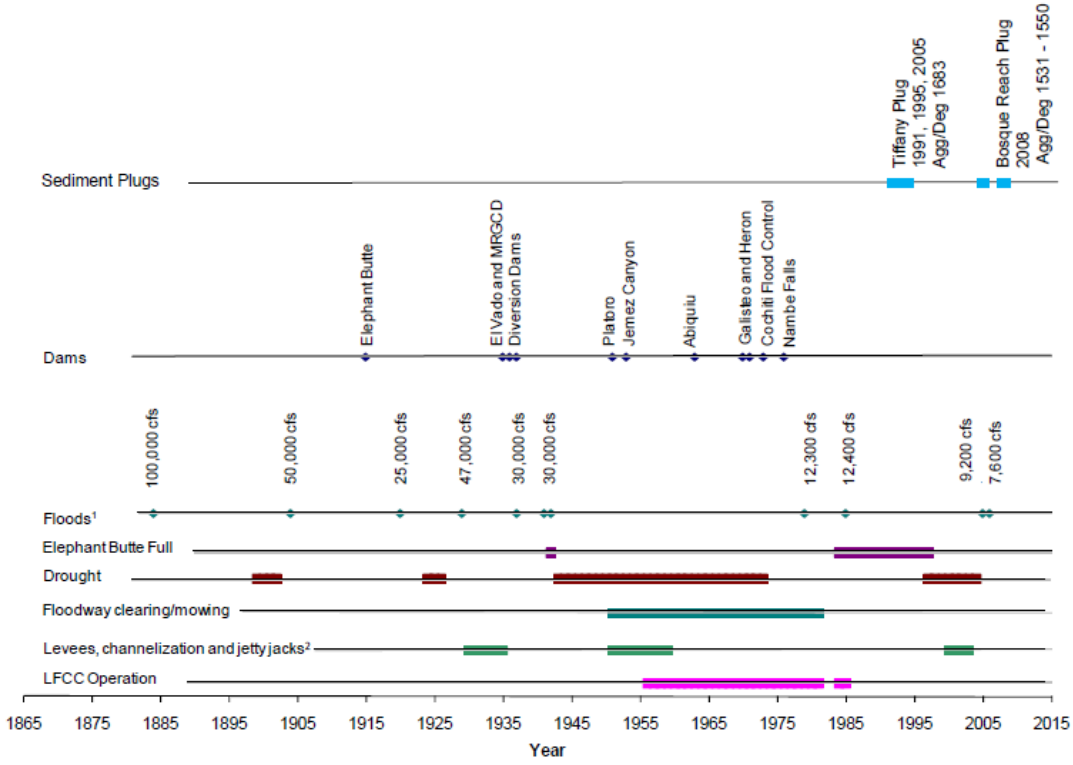

Figure 3 Historical timeline of the Middle Rio Grande (Makar and AuBuchon, 2012)

In addition to anthropogenic influences, climatic cycles have also had an influence on the drivers of change, which in turn also likely had an effect on the river's morphology. Over the last century there was a significant drought from 1943 to 1974 that caused the Elephant Butte Reservoir to be depleted. Since the late 1970s the reservoir began to fill again, and was essentially full from the mid-1980s to the late 1990s. These were wet years, and in 1979 New Mexico was able to fulfill previous debits to water compacts to Texas and Mexico, and even accrue water credits. Starting in 1999, long-term drought began to impact the reservoir level that has had an impact continuing into the current time frame (Owen et al, 2011). The annual mean,

maximum, and minimum reservoir water surface levels (Figure 4) may affect the deposition of sediment upstream, as shown in a study of the Rio Grande from Elephant Butte to San Marcial, (at the downstream end of this study reach) which affects the energy gradient of upstream water (Owen et al, 2012).

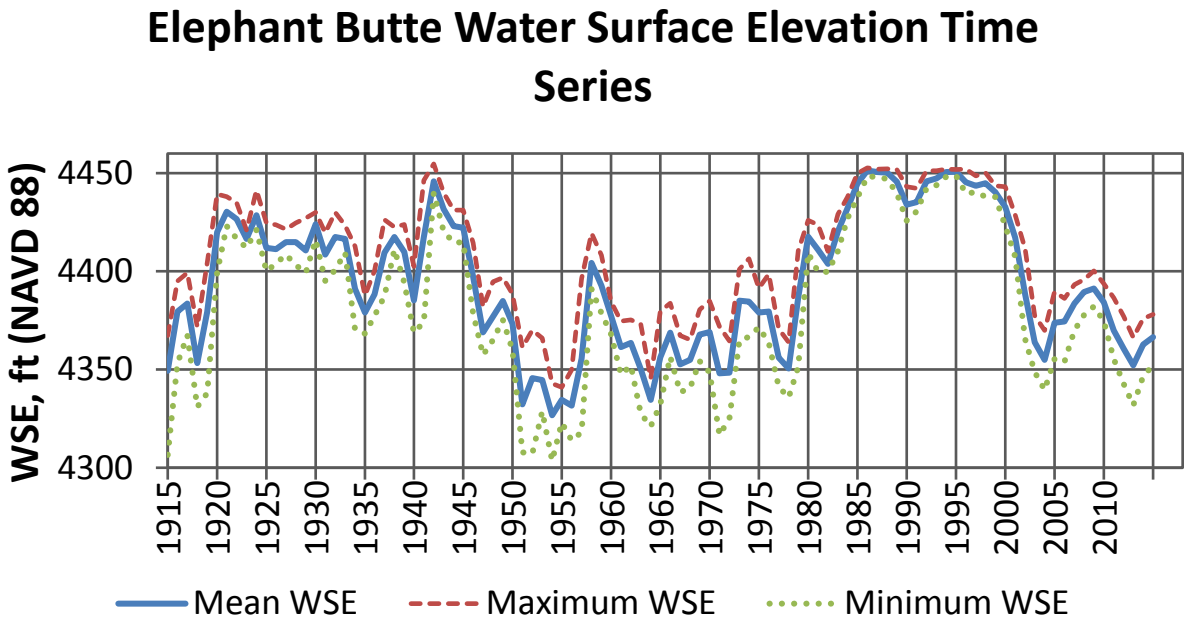

Figure 4 Annual average, maximum and minimum Elephant Butte Reservoir levels over time (modified from Owen et al, 2012)

2.2 First Driver: Rio Grande Discharge or Flow

2.2.1 Magnitude of Discharge

2.2.1.1 Cumulative Discharge

The magnitude of discharge was evaluated by comparing the discharge entering and exiting the study reach over time, as well as the quantity of discharge. The USGS water gage at San Acacia (08354900) measures the discharge before entering the study reach; the USGS water gage at San Marcial (08358400) measures the discharge downstream of the study reach (Figure 5 and 6). The period of record for San Acacia covers 1937 to the current time, except from 1965 to 1973, where no data was recorded. Throughout the 1930s and 1964, the gages showed similar discharge patterns, where a spike at one gage would correspond with a spike at the other. After the closing of Cochiti Dam, in 1973, when San Acacia monitoring resumed, there was period where San Marcial showed more discharge, and from approximately 1982 to 2001, San Acacia flows exceed that of San Marcial. The maximum exceedance, or the difference in discharge from one year, occurs in 1986 by almost 460,000 acre-ft, and from that point in time onward, the exceedance decreases to an average of about 100,000 acre-ft around 1996.

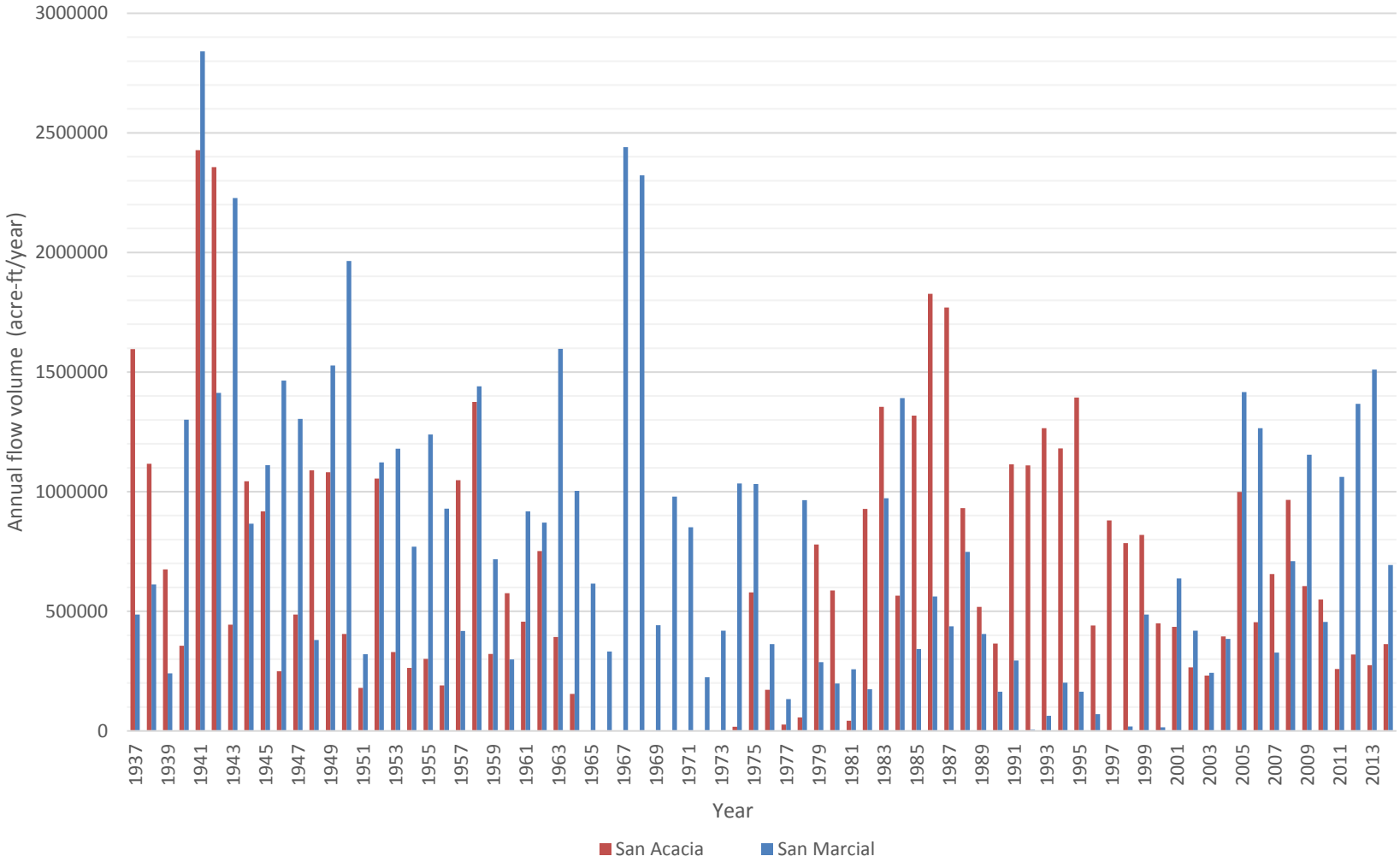

Figure 5 Annual discharge at the San Acacia (USGS 08354900) and San Marcial gages (USGS 08358400).

The evaluation period for the cumulative discharge reflects the continuous record from 1974 to 2014 (Figure 6). Because the gauge at San Acacia had no data collected from 1965 to 1973, it would be inappropriate to graph in a cumulative discharge against San Marcial, which has a continuous period of record from 1900 to current.

It was found that from 1974 to 1991, the USGS gage at San Marcial (USGS 08358400) had greater cumulative discharge than the upstream gage at San Acacia (USGS 08354900). At this period, flow was diverted to the LFCC above the San Acacia gage and returned downstream of the San Marcial gage. The flows at this time period may indicate that arroyos, drains, and/or groundwater base flow were contributing water at a greater rate than evaporation losses and the cumulative diversion at the LFCC. In 1982, the annual discharge at San Acacia begins to exceed that of San Marcial, and by 1991 the cumulative discharge at San Acacia exceeds that of San Marcial, as observed by a higher value in cumulative discharge in Figure 6. There appears to be three different time periods during the analysis period where the slope of cumulative discharge at San Acacia is steeper than at San Marcial (Figure 6). While the slope increases for both of the gaging stations, the larger increase at the San Acacia gage than the San Marcial gage is likely associated with evaporation, transpiration, or groundwater losses between the gage stations. The slope shift beginning in 1982 at San Acacia is probably due to the change in LFCC operations (Reclamation, 1985; Reclamation, 2000), where diversions were curtailed due to environmental concerns and eventually suspended in 1985. The inclusion of San Juan –Chama waters into the Rio Grande may have been a possible contributor to a slight increase of flows through this reach during this time period as well.

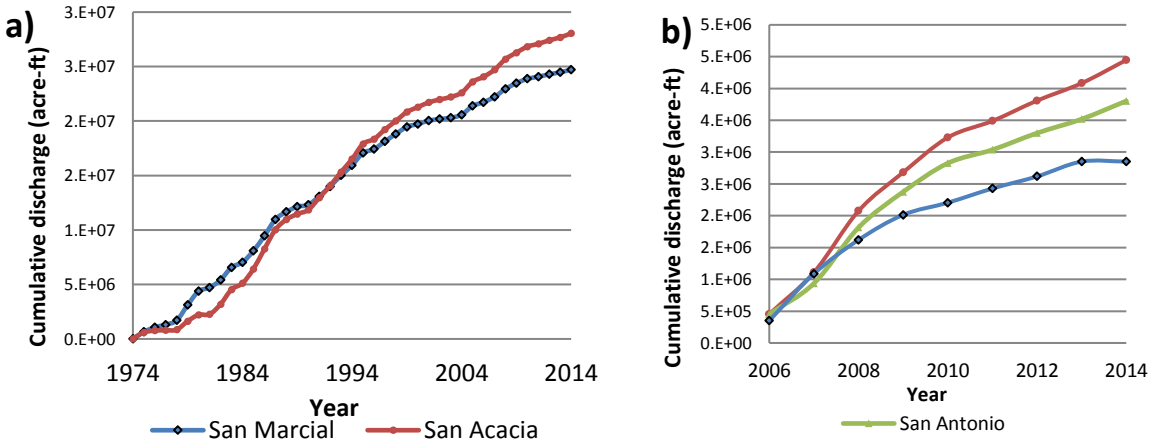

Figure 6 Cumulative water discharge at USGS water gages in San Acacia (USGS 08354900), San Antonio (USGS 08355490), and San Marcial (USGS 08358400).

After 1993, the upstream gage, San Acacia (USGS 08354900), has a cumulative discharge that exceeds the cumulative discharge at San Marcial (USGS 08358400) indicating that losses from evapotranspiration or groundwater infiltration are greater than contributing flows. Figure 6b shows the three USGS gages within the study area, the third one being the San Antonio gage, about six miles downstream from the Arroyo de las Cañas, which began operation in 2006. The San Antonio gage is about 24 miles downstream from the San Acacia gage and 21 miles upstream from the San Marcial gage. The San Antonio gage is 57% of the distance between San Acacia gage and San Marcial gage, but on average over the 8 year data period, it had 53% of the discharge, with some years varying to be 12% more than the expected discharge or 16% less.

The loss of discharge in the Rio Grande is, on average, greater below San Antonio to San Marcial than between San Acacia and San Antonio.

2.2.1.2 Precipitation

The Rio Grande receives a lot of water from snow melt runoff in the spring, where the precipitation that has accumulated as snow pack in the high mountains melts and drains into the headwaters of the watershed. Precipitation is a major contributor to surface water runoff in the immediate project area, and following rain events the discharge in the Rio Grande may increase rapidly. The majority of rain events occur during the late summer and early fall, reflecting monsoonal weather events. The gages local to the study area (see Figure 2 for a map) reflect precipitation from the monsoons.

Observing precipitation data can provide some indication of how river discharge was affected year to year. The National Climatic Data Center releases monthly summaries for location within the Global Historical Climatology Network (GHCN). There are over 40,000 stations within this network all over the world. Some gages had records which are offline or incomplete, so multiple gages, those closest in proximity to the previous gage locations, were used to complete the data set for this study area.

These sites were used to extend data curated by previous works (Massong 2006):

- Socorro USC00296387 (1998-2007; 2013-2015);
- Socorro 33 NNE, NM US1NMSC0001 (2008-2012);
- Bosque del Apache, NM USC00291138 (1998-2014).

From 1962 to 1997, the average precipitation at Bernardo was about 8.2 inches per year, with the highest annual amount at 13.74 inches in 1974. At the Socorro gages, the trend was a general decrease in average annual precipitation by a rate of 0.10 inches per year, with rainfall exceeding 13 inches in 1986, 1997, and 2006 (Figure 7).

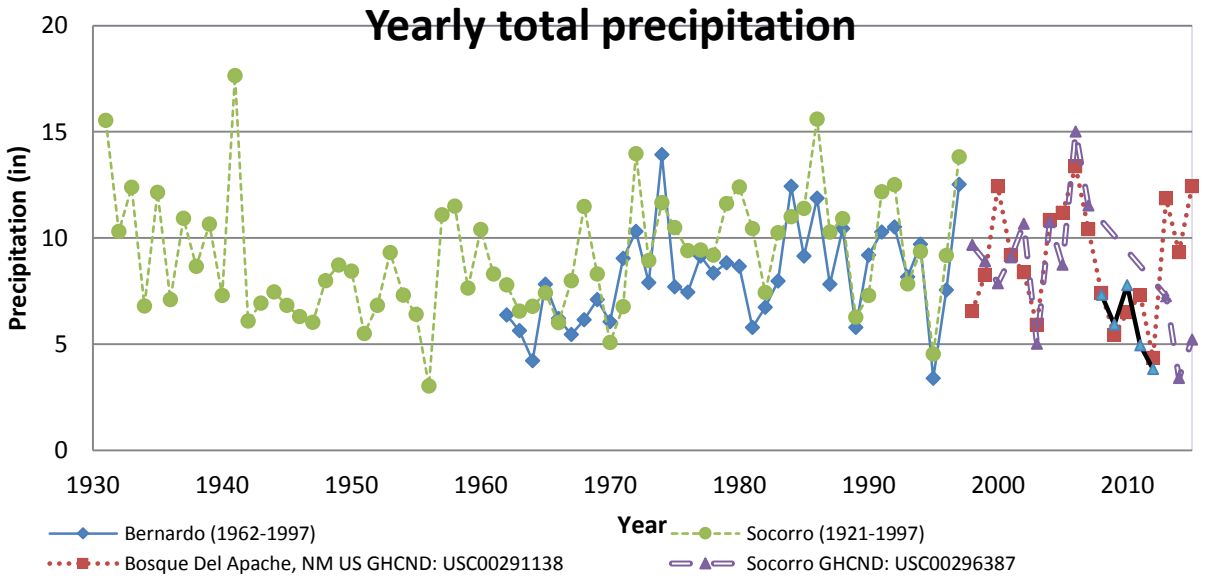

Figure 7 Total annual precipitation from gage sites near the study area.

Monthly precipitation at Socorro is shown by month in Figure 8 from 1931 to 2014 at the Socorro gages. The peak precipitation occurs from July through October, with the peak monsoon events occurring earlier in the calendar year since the 1986.

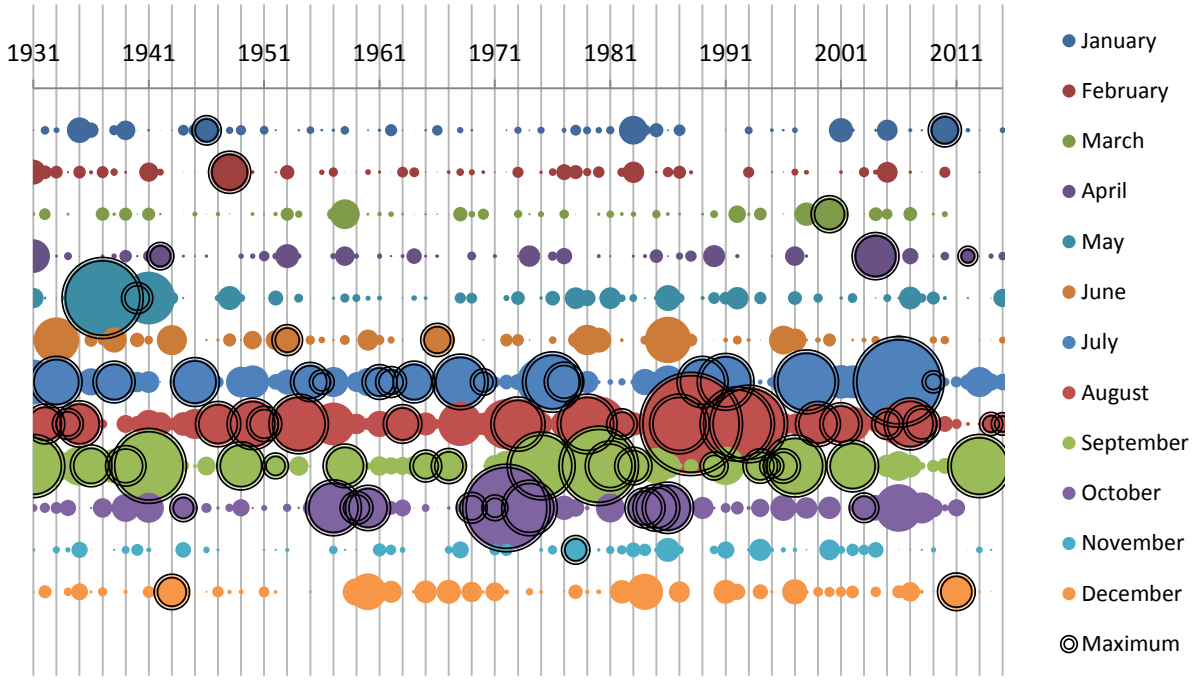

Figure 8 Monthly precipitation volume at the Socorro gages, with the maximum of that year indicated by a double circle around the data point; the data marker size represents the inches in precipitation, some of these values are indicated in boxes.

2.2.1.3 Peak Discharge

Peak discharge was evaluated based on the maximum daily average flow occurring every year. Observing the trends in peak discharge can give information about the magnitude of flow the reach experiences. In Figure 9, the black bars indicate the measured peak discharge for each year. The striped bars indicate when the annual peak discharge was greater at San Marcial (USGS 08358400) than San Acacia (USGS 08354900). The increase in discharge may come from intervening arroyos, drains, groundwater seepage, or other contributions to surface water flow. The T-bars indicate years at which the magnitude of peak discharge at San Acacia had greater maximum peak discharge than the downstream gage at San Marcial.

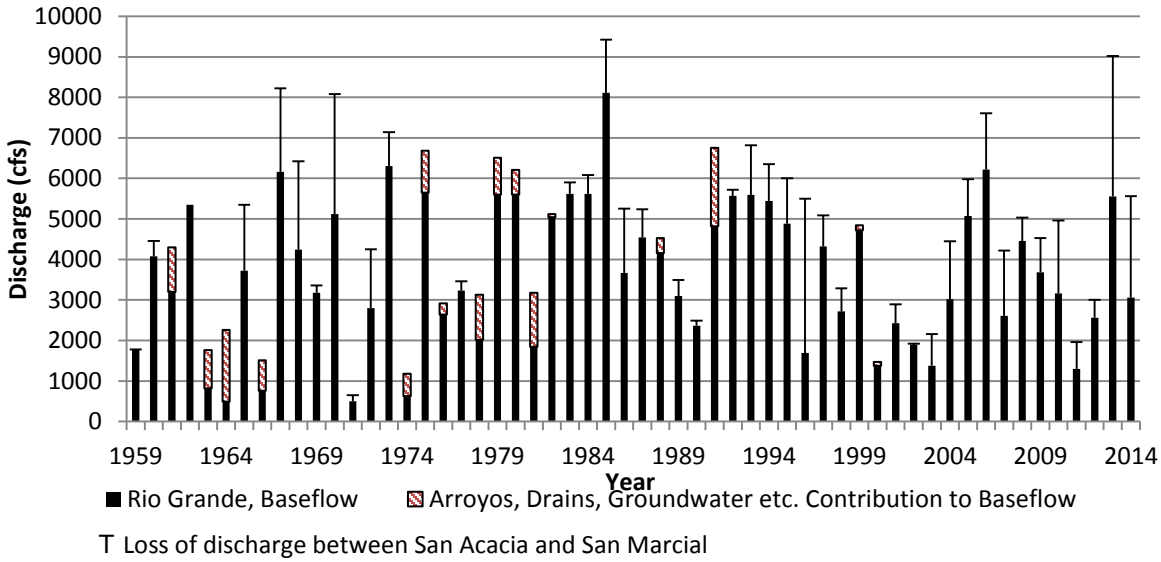

Figure 9 Peak annual discharge on the Rio Grande between San Acacia (USGS 08354900) and San Marcial (USGS 08358400).

One interesting observation from Figure 9 is that before 2000, there would be periods of years where there would be greater peak discharges at San Marcial, which is below San Acacia. Extended periods of this trend were from 1961-1966 and 1974-1982. After 2000, the peak discharge at San Acacia exceeded the annual peak discharge at San Marcial every year. This trend confirms the observation made from Figure 6, where the gap in cumulative discharge between San Acacia and San Marcial continues to increase in magnitude. Figure 9 shows that the Rio Grande was increasing in discharge during a drought period at the same time the LFCC was in operation.

2.2.2 Flood Frequency Analysis

Flood frequency indicates the magnitude and frequency of discharge events that happen between specific time periods. Flow frequency/flow duration analyses for the study area can be summarized from four reports: Bui (2014), Wright (2010), MEI (2002), and Bullard and Lane (1993). Bullard and Lane, MEI, and Wright extracted the annual peak flow from available USGS gage data to estimate return period flow. All three assumed a log Pearson Type III probability distribution. Wright and Bullard and Lane used the same analysis approach and combined the flows based on tributary inputs during the monsoon season with flows in the Rio Grande during the spring run-off season. This was to develop flood frequencies that represented a maximum combined flow. Bui, as well as MEI, performed statistical analyses based on the historical USGS gage observations of mean daily flows, resulting in a percent exceedance for the period of analysis. Bui's work provides probabilities and potential return intervals for particular discharges, but her original analysis is intended for characterizing seasonal flow regimes within a year, corresponding to the life cycle of the Silvery Minnow. Bui (2014) does not fit a probability distribution.

Table 1 provides the various analyses periods for each of the sources cited in this review.

Table 1. Analysis period for USGS gaging stations for flood frequency analysis.

Citation Source	Analysis Period	
	San Acacia*	San Marcial**
Bullard and Lane (1993)	1936–1989	1895-1988
MEI (2002)	1973-1991	1973-1991
Wright (2010)	1936-2008	1925-2008
Bui (2014)	1993-2013	1993-2013

Notes: * – San Acacia USGS gage stations 08355000 and 08354900
** – San Marcial USGS gage stations 08358500 and 08358400

For this analysis four of the USGS gages from Bui's (2014) analysis and two from MEI's (2002) analysis were reviewed. These include the gages at San Acacia (USGS 08354900), Escondida Bridge (USGS 08355050), US HWY 380 (USGS 08355490), and San Marcial (USGS 08358400). The gages at Escondida and US Hwy 380 were not used by MEI and have only been in operation from 2005 to 2013, which were drier years and may not demonstrate a full range of flood frequencies. This may have contributed to the lower discharge at Escondida at the ninety ninth percentile of discharge exceedance. The ninety ninth percentile of discharge represents the maximum discharge that occurs within the reach over the observation period. The percent exceedance can then be obtained as 100% minus the discharge percentile.

A decrease in the 99th percentile flows is apparent when comparing the MEI's (2002) analysis to Bui's (2014). MEI's analysis also indicates an increase in the flows at the 25th and 75th discharge percentile after 1985. This is likely due to the discontinuation of the LFCC (Reclamation, 1985; Reclamation, 2000). Bui's analysis shows a decrease in the frequency of even these flows over the last two decades, which may be attributed to the drought that began in 1999. Because this analysis is based on daily average flows, it probably does not reflect high, flashy peaks that have a short temporal duration.

Table 2 Discharge at different discharge percentiles for an entire years flow within the study area (modified from Bui 2014 and MEI 2002).

Discharge (cfs)	Bottom 25th Percentile	75th Percentile	99th Percentile
San Acacia 1973-1985 (MEI 2002)	5	800	~6,000
San Acacia 1985-1999 (MEI 2002)	500	2000	~6,000
San Acacia (Bui 2014)	200	750	4,550
Escondida Bridge (Bui 2014)	100	675	3,750
US Hwy 380 (Bui 2014)	50	600	4,250
San Marcial 1973-1985 (MEI 2002)	1	~1,050	~5,000
San Marcial 1985-1999 (MEI 2002)	250	1,500	~4,000
San Marcial (BUI 2014)	50	600	4,250

Shown in Table 3 are return period discharges from Wright (2010), MEI (2002), and a new analysis at San Acacia and San Marcial using the same time period as Bui (2014) (1993-2013).

The new data resulted from log Pearson type III distribution analysis, with input data from annual peak flows from USGS gages at San Acacia (skew coefficient = -0.700) and San Marcial (skew coefficient = -0.434). Each analyses represented in Table 3 assumes a log Pearson type III probability distribution, but evaluates a different period from the flow record. Wright calculated regulated peak flows at the USGS gages in San Acacia (USGS 08354900) and San Marcial (USGS 08358400) and incorporated the influence of reservoir regulation within the MRG. The operation at dams and reservoirs affect the rivers' discharge and therefore the peak flood intensity. Wright also combined peak flows from tributaries during the monsoon season with peak flows in the Rio Grande during spring run-off. Both MEI (2002) and the current analysis evaluate the period of time after the closure of Cochiti Dam. The current analysis also looks at a period of time after the cessation of flows in the LFCC (Reclamation, 1985; Reclamation, 2000).

Table 3 Discharge at different flood frequencies for the study area modified from Wright (2010) and MEI (2002)). Annual peak flow from the USGS was used in analysis.

Discharge (cfs)	2 Year	5 Year	10 Year	25 Year	50 Year	100 Year
San Acacia (Wright (2010)	7,800	12,000	14,500	17,400	19,300	20,100
San Acacia, 1993-2013	4,410	6,380	7,570	8,920	9,820	10,600
San Marcial (Wright 2010)	7,700	12,600	15,600	19,200	21,600	22,900
San Marcial, 1973-1999(MEI (2002)	4,160	6,290	7,610	8,810	10,300	11,300
San Marcial, 1993-2013	3,280	4,890	5,910	7,150	8,024	8,860

It is shown that Wright's peak discharge results were greater than more recent analyses (MEI and the current analysis) by a factor of two. This indicates that the combined tributary inputs and the spring run-off flows do not occur at a significant frequency to affect the flood return period. MEI's results over 1973 to 1999 show a greater discharge at all of the return frequencies than what was observed from USGS data from 1993-2013. The fifty year return period for MEI's analysis was similar to the 1993-2013 one hundred year return period. The decreasing return period can be attributed to the lower peak flows that have occurred in since 1993 (Figure 9).

2.2.3 Flow Duration

The duration of discharge is another parameter that helps characterize the flow regime. Persistent high flows with long durations have the power to redistribute sediment and contribute to the MRG's geomorphic adjustment. For the duration analysis, the daily discharge was evaluated from 1959 to 2014 at the San Acacia (USGS 08354900) and San Marcial (USGS 08358400) gages. The number of days within a range of discharges, i.e. 500 cfs to 999 cfs; 1,000 to 1,999 cfs, etc. were counted and plotted in an area graph (Figure 10). The frequency of discharges for each range is stacked on top of each other, so that the height of the peak indicates the number of "wet" days per year at the USGS gage station and downstream reach of the Rio Grande. Therefore drier years have a lower duration for flows experienced, while more frequent discharge ranges will appear as thick bands on the graph.

It was found that prior to 1985, the Rio Grande would occasionally run dry at the San Acacia gage, but since then there has been a consistent discharge greater than 1 cfs flow, even frequently greater than 100 cfs flow, in the Rio Grande at this location. Flows greater than 2,000 cfs have occurred about 52 days out of the year, on average once every three years between 1986 and 2013. The number of days where the flow exceeds 2,000 cfs has not increased over the study

period, with exception for 1986, where there was over 300 days that exceeded 2,000 cfs in the course of that year. The change may be attributed to the addition of San Juan-Chama waters to the system, as well as intentional water operations to prevent the Rio Grande from going dry.

Generally San Marcial (USGS 08358400) mirrored San Acacia (USGS 08354900) by having higher discharges in the same years, though the magnitude and flow duration of the discharge was generally less. The Rio Grande would often run dry at the San Marcial gage. The occurrence of dry days at San Marcial generally ended in 1997, due to the supplemental flows from San Juan-Chama and pumping from the LFCC. Between 1975 and 1981, San Marcial gage measured discharges of greater magnitude than experienced throughout the year at San Acacia. This is a strong indicator of arroyo and other inputs of flow in this reach.

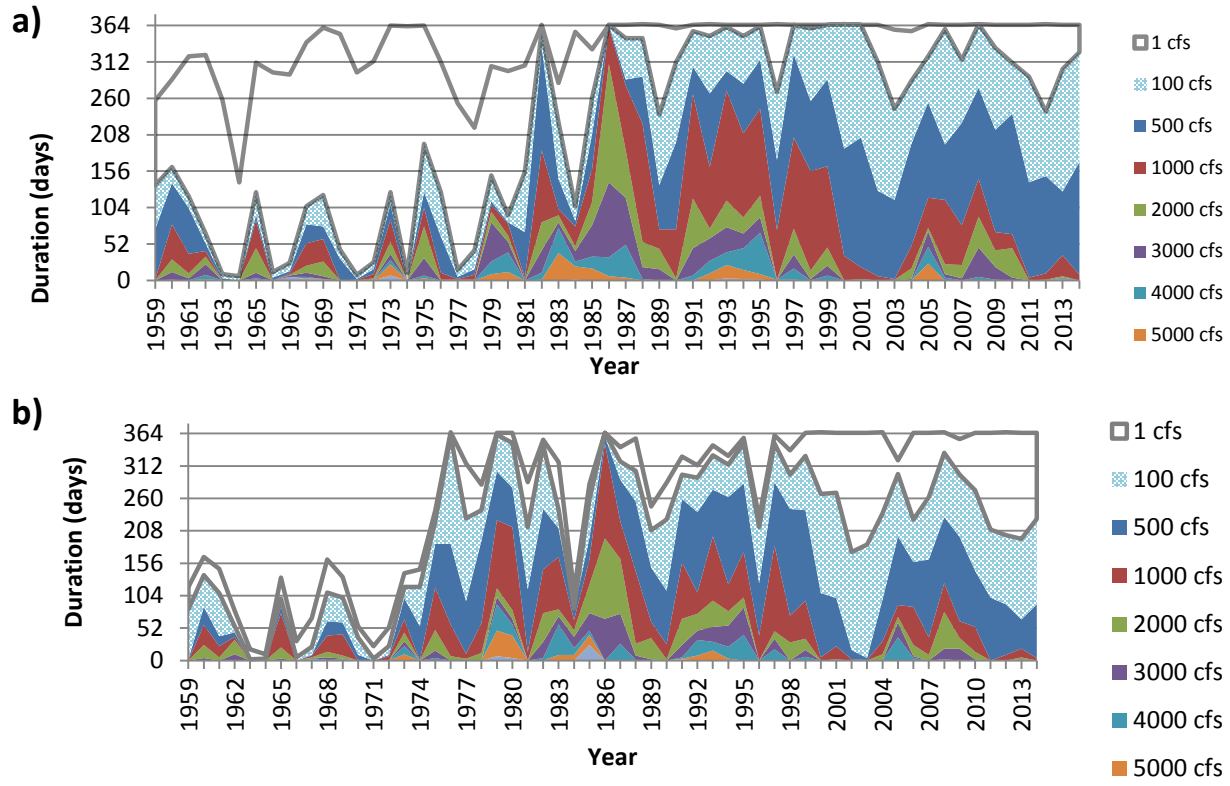

Figure 10 The duration of discharges on the Rio Grande between 1959 and 2014 at a) San Acacia (USGS 08354900) and b) San Marcial (USGS 08358400) gages.

In another representation (Figure 11), it is apparent those higher discharge periods (greater than 3,000 cfs) occur more frequently at the San Acacia gage than downstream at San Marcial. The periods of higher discharge, i.e. from 1982 to 1999 were consistent between the two gages.

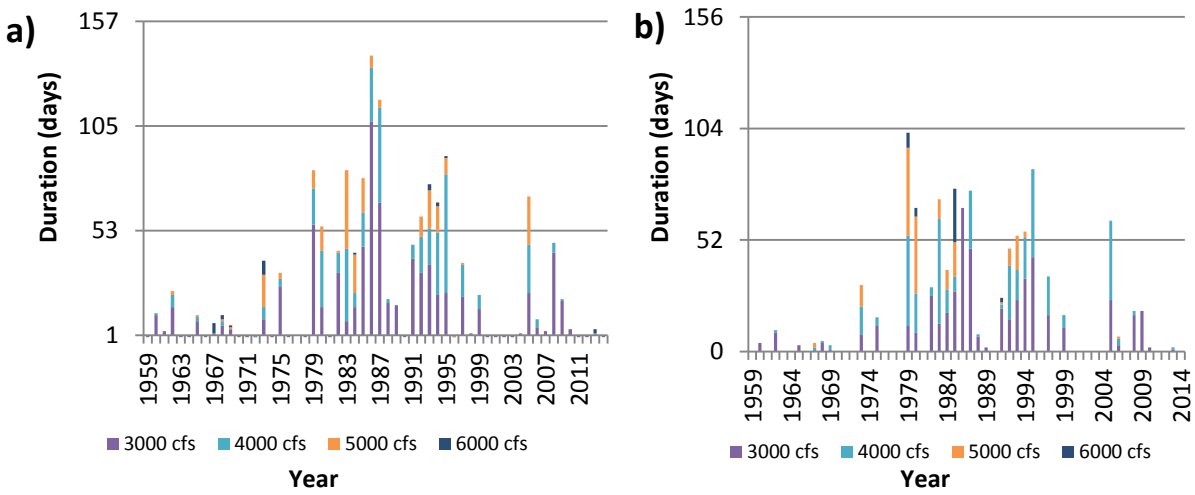

Figure 11 The duration of higher discharge periods (greater than 3,000 cfs) on the Rio Grande between 1959 and 2014 at a) San Acacia (USGS 08354900) and b) San Marcial (USGS 08358400) gages.

In general, the duration of higher discharge levels was less at San Marcial (USGS 08358400) than at San Acacia (USGS 08354900). The number of days and the magnitude of discharge both decrease as waters travel downstream on the Rio Grande. In 2002 and 2003 both San Acacia and San Marcial experienced a dry period, with San Marcial not exceeding a flow of 1,000 cfs in either year. For 2005, it was a wet year with high intensity discharges, with 48 days of discharge greater than 3,000 cfs at the San Acacia gage. Tables of durations can be found in the Appendix.

2.3 Second Driver: Sediment Supply on the Rio Grande

2.3.1 Suspended Sediment

2.3.1.1 Cumulative Sediment Discharge

The USGS reports the suspended sediment load for the Rio Grande at several of its gaging stations. The amount is estimated based on discharge and suspended sediment concentrations from field samples. The evaluation period for the cumulative discharge reflects the continuous record of the San Marcial and San Acacia gages from 1974 to 2014. Shown in Figure 12, the volume of suspended sediment is greater at the downstream gage at San Marcial (USGS 08358400) than at San Acacia (USGS 08354900). This is an indication that either sediment is eroding from the active channel or that arroyos and other sources of water increase the sediment load at San Marcial.

It is apparent that the cumulative suspended sediment transport rate increased, as indicated by an increase in slope, in certain years, namely 1982, 1985, 1991, 1993, 1999 and 2006 (Figure 12). Both San Marcial and San Acacia experience these higher loads, though with exception of 1982 and 1993, San Marcial has a higher magnitude of change in these sediment spikes. Between 1976 and 1982 the differential sediment transport rate between San Acacia and San Marcial is widening and then it narrowed again by 1991. The time period during an increase in the gap correlates with Rio Grande floodway clearing and mowing, where a decrease in vegetation may allow for bank erosion. The period also correlates to a time of high intensity and high magnitude

floods. There appears to be a similar trend of an increasing gap that started in 1991 and went to about 1999. Since 1999 the gap between the two lines seems to be decreasing. This is interesting since it seems to correlate with the drought that occurred in the late 1990s. In general, the USGS gage at San Marcial (08358400) experiences a greater suspended load than at San Acacia (USGS 08354900).

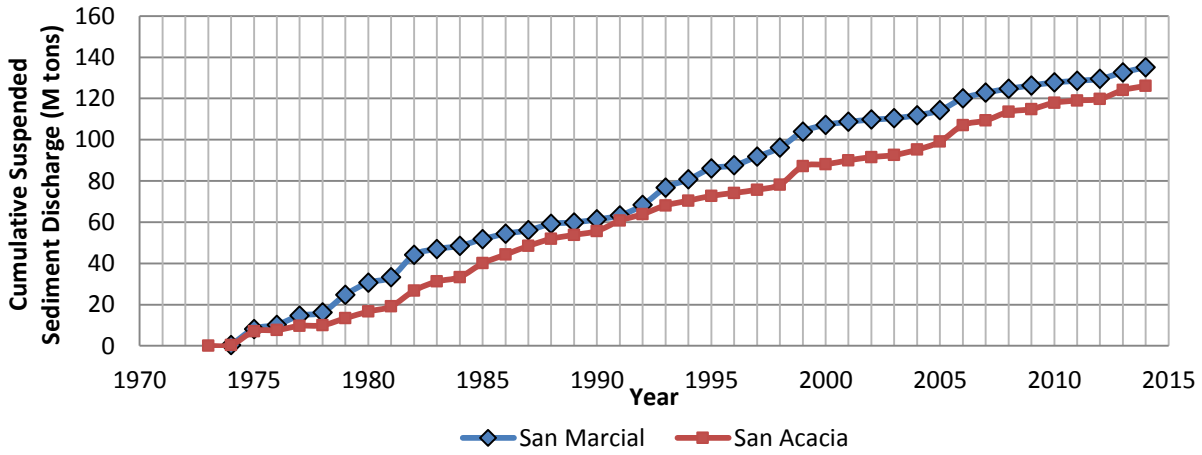

Figure 12 Cumulative sediment discharge according to USGS water gages at San Acacia (USGS 08354900) and San Marcial (USGS 08358400).

Throughout the period of record there are eras of time that appear to have the same slope, or the same amount of sediment discharged each year. Years with sediment discharges greater than 5.5 million (M) tons were removed from the analysis. These high sediment volumes constitute less than 20% of the measurements within the data and would skew analysis. Outliers are listed below in Table 4.

Table 4 Average suspended sediment volume throughout different periods. High concentration years (below) were removed from the analysis.

San Acacia Periods	**1974-1978**	**1979-1988**	**1989-1990**	**1991-2014**	--
Average Concentration	0.84 M tons/year	3.5 M tons/year	1.9 M tons/year	2.4 M tons/year	--
# of Years Exceeding 5.5 M (Excluded from average)	1	2	0	2	--
San Marcial Periods	**1974-1988**	--	**1989-1991**	**1992-2000**	**2001-2014**
Average Concentration	2.4 M tons/year	--	1.4 M tons/year	4.0 M tons/year	1.7 M tons/year
# of Years Exceeding 5.5 M (Excluded from average)	4	--	0	2	1

Table 5 Sediment years that exceeded 5.5 million tons for the San Acacia and San Marcial USGS gages.

High Sediment Years (Outliers)

San Acacia	San Marcial
• 1975 (7.3 M tons) -- -- • 1982 (7.6 M tons) • 1985 (6.7 M tons) -- • 1999 (8.9 M tons) • 2006 (8.0 M tons)	• 1975 (7.8 M tons) • 1979 (8.5 M tons) • 1980 (5.9 M tons) • 1982 (10.7 M tons) -- • 1993 (8.3 M tons) • 1999 (7.7 M tons) • 2006 (5.8 M tons)

It was found that the high sediment years that were excluded from the average suspended sediment load in Table 4, have higher peak flows than preceding years.

2.3.1.2 Double Mass Curve: Suspended Sediment and Water Discharge

Cumulative suspended sediment may be plotted against the water discharge to analyze the effectiveness of sediment transport over time. Shown in Figure 13, the cumulative suspended sediment per cumulative water discharge at San Marcial (USGS 08358400) exceeds that of San Acacia (USGS 08354900), with the disparity increasing since 1991. This is an indication that per acre foot of water, more sediment is transported by the Rio Grande at San Marcial rather than San Acacia. There was a great difference between cumulative discharge in the 1970s and 1980s, which equilibrated by 1991, corresponding with the operation of the LFCC, which was in operation until 1985 (Reclamation, 1985). After 1991 it becomes evident that San Marcial is experiencing a higher concentration of suspended sediment than San Acacia as the curves separate. This is during the time when Elephant Butte was filling or was at capacity. At the onset of drought in 1999, the sediment curves begin to trend towards one another again.

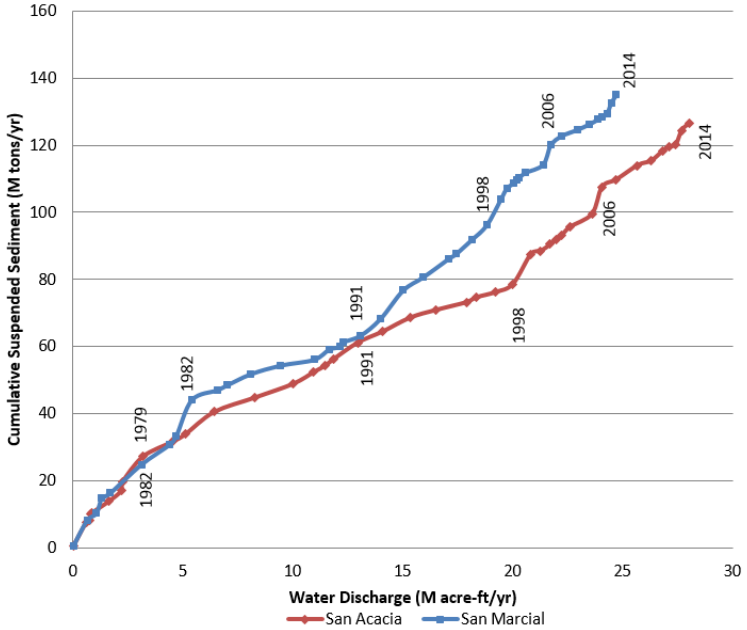

Figure 13 Double mass curve comparing cumulative water discharge to suspended sediment load from 1974 to 2014 at San Acacia (USGS 08354900) and San Marcial (USGS 08358400) gages.

Average annual sediment concentration was calculated based on the annual sediment discharge over the annual water discharge. Generally the sediment concentration at San Marcial exceeds that at San Acacia (Figure 14); there are some exceptions, for example the period of 1983-1992, 2006, and 2008-2012. Elephant Butte Reservoir was essentially at capacity from 1985 to 1999 (Owen et al, 2011), and this may have decreased the energy at San Marcial causing sediment to settle and creating lower sediment concentrations. Higher sediment concentration spikes at San Acacia tend to correlate with spikes at San Marcial, but spikes at San Marcial do not necessarily indicate increased concentrations at San Acacia. This is especially true in 1982, 1993, and 2014.

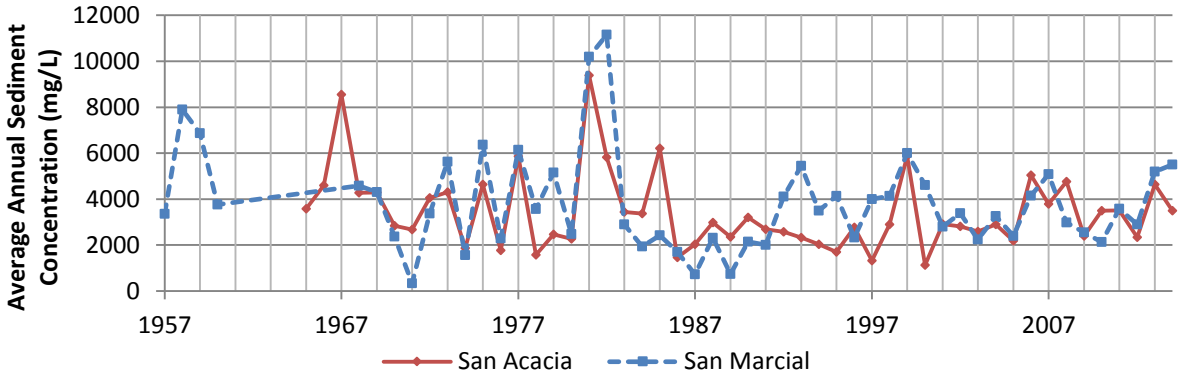

Figure 14 Suspended sediment concentration at USGS gages at San Acacia (USGS 08354900) and San Marcial (USGS 08358400) from the period of record 0f 1957 to 2014.

2.3.1.3 Analyses of the Average Monthly Suspended Sediment Discharge

In order to better understand the sediment budget of the Rio Grande in the study reach, it is possible to compare the inflow and outflow conditions of the suspended sediment by comparing San Acacia (USGS 08354900) and San Marcial (USGS 08358400) suspended sediment concentration data. This comparison theoretically can give information about the sediment movement in the reaches between them. Analysis was conducted based on USGS field measurements: suspended sediment concentration (80154) and suspended sediment discharge (80155). The range of years evaluated (1990 to 2013) represents the time after the end of LFCC operation. The LFCC diversion operation may have interfered with flow and sediment discharge patterns in earlier field measurements, and since the operation is not in effect now, analysis of earlier data is not necessary. The data was collected daily and condensed to monthly statistics by the USGS or an agency partner. The range of years were then further condensed to one monthly average to represent the study period.

In Table 5 and Figure 15, monthly averages of the suspended sediment measurements at the USGS gages are shown. The annual average at San Marcial (USGS 08358400) was 8,318 tons/day; the annual average at San Acacia (USGS 08354900) was 7,995 tons/day. Throughout the year, the suspended sediment concentration at San Marcial (Figure 15b) is persistently at higher concentrations when compared to San Acacia. In April, August and September, however, San Acacia has a higher suspended sediment load. This may reflect the influence of sediment discharge from the Rio Puerco (RM 126.5) and Rio Salado (RM 118.5) on the San Acacia gage. Both arroyos are upstream of the San Acacia Diversion Dam (RM 116.2). The suspended sediment load throughout the year is generally greater at San Marcial, which confirms the trend identified in the Double Mass Curve (Figure 13) that suspended sediment load increases throughout the study reach. The highest suspended sediment concentrations occur during the

time periods with the lowest monthly discharge. This is indicative of the flashy, low duration and high intensity flows of the monsoon period.

Table 6 Average monthly values for discharge and suspended sediment concentration and load at a) the San Acacia gage (USGS 08354900) and b) the San Marcial gage (USGS 08358400) from 1990 to 2013.

A) SAN ACACIA MONTHLY AVERAGE	Discharge (cfs)	Suspended Sediment Concentration (mg/L)	Suspended Sediment Load (tons/day)
JANUARY	858	887	2197
FEBRUARY	893	1044	2862
MARCH	843	580	1730
APRIL	1230	1078	6059
MAY	1989	1164	9045
JUNE	1585	791	4121
JULY	590	6371	12092
AUGUST	583	9471	28227
SEPTEMBER	428	8199	16329
OCTOBER	401	2276	3766
NOVEMBER	929	2457	6026
DECEMBER	913	1425	3494

B) SAN MARCIAL MONTHLY AVERAGE	Discharge (cfs)	Suspended Sediment Concentration (mg/L)	Suspended Sediment Load (tons/day)
JANUARY	606	2338	4292
FEBRUARY	647	2597	5354
MARCH	585	2002	5117
APRIL	943	1889	8473
MAY	1679	1955	11782
JUNE	1397	1402	9185
JULY	480	5810	10337
AUGUST	418	8861	17841
SEPTEMBER	252	7021	10957
OCTOBER	233	2727	3858
NOVEMBER	661	3557	7919
DECEMBER	672	2368	4700

The monthly average for the suspended sediment load does not have a normal distribution over the years, meaning that there may be outliers in the data set that skew the averages. Normal distribution is defined as having the median and mean values nearly the same. Box and whisker plots are used to show the maximum and minimum values, as well as the distribution of the upper (75^{th} percentile) and lower (25^{th} percentile) quartiles surrounding the median (50^{th} percentile) value. The monthly statistics for both gaps are visualized with box and whisker plots in Figure 16. Again, this data reflects field measurements conducted by the USGS at both the San Acacia (USGS 08354900) and San Marcial (USGS 08358400) gages that was collected at a frequency of about once a day for the period (1990-2013). The data over these years were separated into months for cross-annual analysis.

The suspended sediment concentration median during the non-irrigation seasons of November through February appears to be higher or about at the same level as the spring runoff months. This is not intuitive unless the flows are high enough that sands are increasingly mobile. MEI (2002) cited increased flows were high enough to mobilize fine to medium sands.

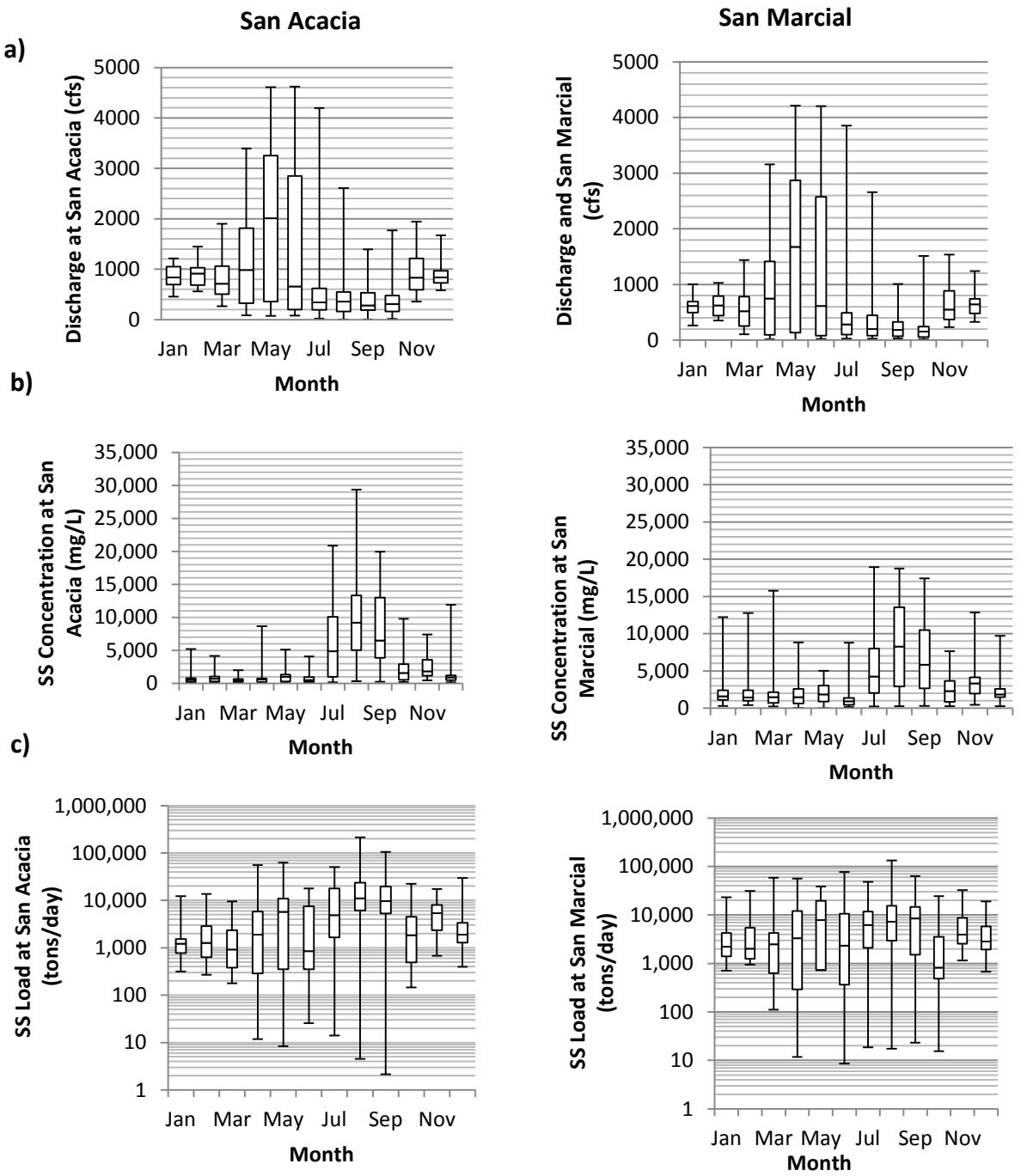

Figure 15 Box and whisker plots of the a) water discharge, b) suspended sediment concentration and c) suspended sediment load for San Acacia (USGS 08354900) and San Marcial (USGS 08358400) from 1990 to 2013.

Generally the seasonal variability of suspended sediment concentration and sediment load at both San Acacia and San Marcial had the similar trends and magnitude. Monthly plots for the discharge in Figure 15 indicate that the Rio Grande at both San Acacia and San Marcial has the highest magnitude of discharge during the snow-melt runoff, with peaks in the late spring. The suspended sediment concentration plots show that San Acacia is affected by monsoon events at a much greater extent than San Marcial. The peak for both gages is during the monsoonal season in July, August and September. The suspended sediment load shows an influence from both the

spring runoff and the monsoon events, with great variance in the median values. San Acacia appears to be more influenced than San Marcial by the monsoonal period as values of suspended sediment increase in the late summer. There is also less variance in the suspended sediment load values, as shown by the small range between quartiles. San Marcial, on the other hand, does not show as much fluctuation in the median of the suspended sediment load values, although there is less variance in the winter months. The median values for both gages are similar for discharge and suspended sediment concentration, though San Marcial (USGS 08358400) has slightly higher sediment concentration throughout the year and San Acacia (USGS 08354900) has slightly higher discharge values. Monthly median and mean values for these three parameters can be found in the appendix.

2.3.1.4 Difference in Mass: Net Sediment Gains or Losses in the Reach

In Figure 16, the difference between the suspended sediment load measured at USGS gages at San Acacia and San Marcial are shown. The figure demonstrates the net gain or loss of sediment in the reach by comparing the sediment load study reach outflow at San Marcial (USGS 08358400) to the inflow at San Acacia (USGS 08354900). Positive values indicate that the reach is losing suspended sediment (i.e. the transport rate is greater at San Marcial than San Acacia), while negative values indicate an accumulation (i.e. rate at San Marcial is less than San Acacia) of sediment in the reach.

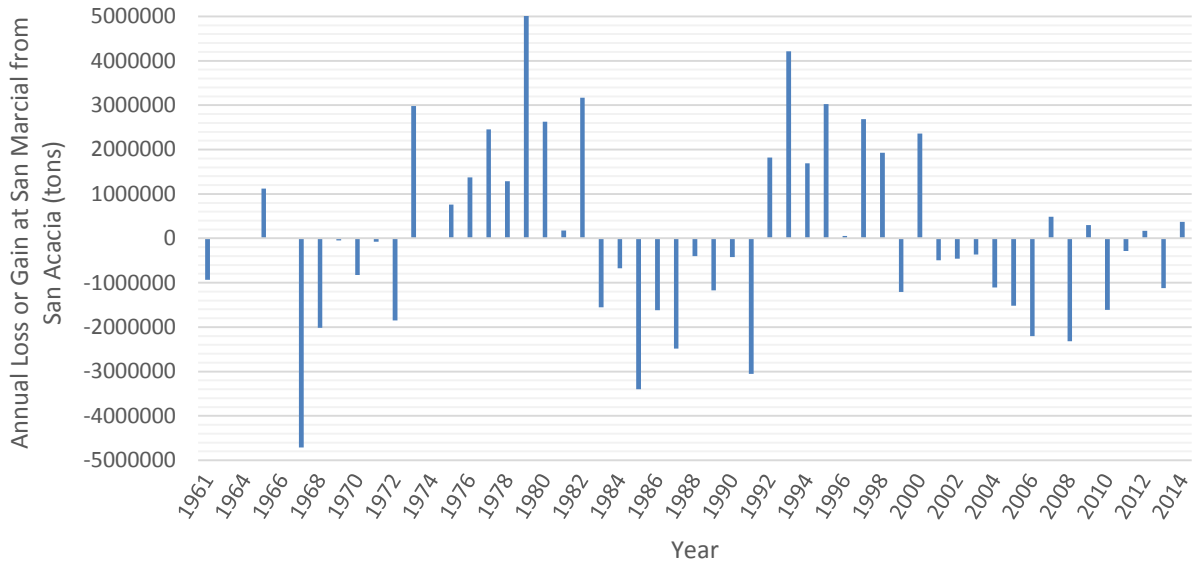

Figure 16 Annual net gain or loss of suspended sediment at San Marcial (USGS 08358400) when compared to San Acacia (USGS 08354900), from 1974 to 2014.

From Figure 16 it appears that the Rio Grande is generally losing sediment in this reach between 1974 and 2014, as indicated by mostly sediment gains, positive values, for the difference between San Marcial and San Acacia. It appears that the amount of sediment evacuation goes through increasing and decreasing phases, with eight to nine year phases between 1974-1982, 1982-1991, and 1991-2000. The current trend is sediment accumulation within the study reach, with occasional years where San Acacia has a little bit more sediment, this 14 year period is concurrent to the drought that started in 1999.

2.3.2 Suspended Sediment Load

2.3.2.1 Suspended Sediment Effective Discharge Curve

The effective discharge curve demonstrates the amount of sediment being moved at a particular discharge, its peak indicates the hydrologic situation where the most work is done on the alluvial boundary. Biedenharn and Copeland's (2000) method was applied for this analysis. The USGS field measurements of suspended sediment load at San Acacia (USGS 08354900) and San Marcial (USGS 08358400) were used in this reach analysis. The field sediment discharge measurements were acquired at a frequency of about once a month during this time period. The gages are triggered by an event sampler, and the samples do not represent a continuous record of the sediment discharge in the Rio Grande. Flow duration curves by Bui (2014) were used to complete the analysis. Bui (2014) had separated the year into four hydrologic seasons that reflect the life stages for the Rio Grande silvery minnow. These seasons are also unique hydrologically, for the sake of this study, pre-runoff and runoff season were combined to create three hydrologic seasons of equal duration: runoff (March through June), post-runoff or monsoon season (July through October) and winter (November through February).

The suspended sediment field-measured discharge was averaged for each discharge interval, for each hydrologic season. A suspended sediment discharge rating curve was created to estimate the sediment discharge per discharge interval, which was then multiplied by the annual frequency of these events, according to the Bui (2014) flow duration frequency analysis. For San Acacia (Figure 17) it was found that in the winter months, the effective discharge is 1,000 cfs. As shown in Figure 15, this time of year has a range of 500 to 2,000 cfs, with 1,000 cfs being nearly the median discharge. The run off is a season with a higher cumulative sediment transport, with a longer range of possible discharges than the winter months, the most effective discharge occurring at 4,000 cfs.

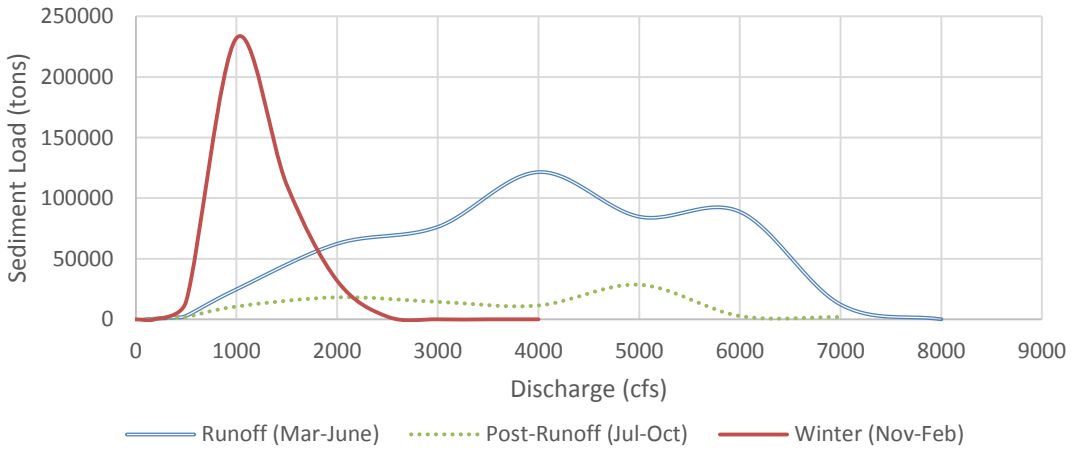

Figure 17 Effective sediment discharge for different discharge intervals for the Rio Grande at the USGS San Acacia (USGS 08354900) from 1993 to 2013.

For San Marcial, it was the post-run off season that transports the most sediment, as shown in Figure 18, with peak effective discharge at 2,000 cfs. Sediment discharge during the runoff time period is higher at San Marcial than San Acacia, confirming previous observations of higher sediment transport at the downstream gage. The effective discharge for winter months is at 1,000

cfs; similar to that of San Acacia, however the suspended sediment volume is slightly less significant than at the San Acacia station.

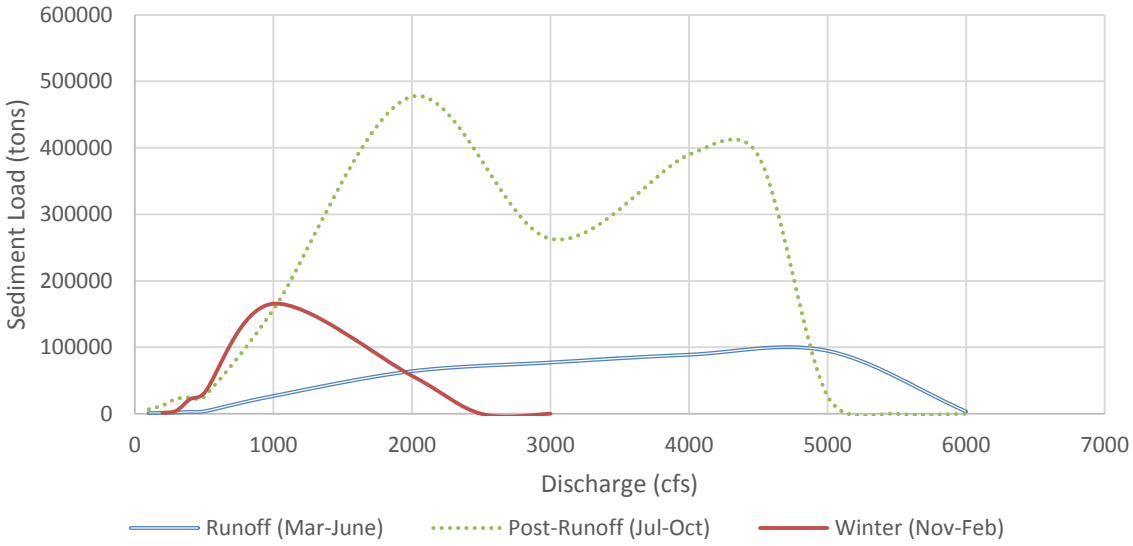

Figure 18 Effective sediment discharge for different discharge intervals for the Rio Grande at the USGS San Marcial gage (USGS 08358400) from 1993 to 2013.

2.3.2.2 Seasonal Suspended Sediment Load Curve

The four hydrologic seasons were plotted in Figure 19 to compare sediment load to discharge. These demonstrate the magnitude of sediment discharge at each USGS measured field event. Generally, post runoff discharge has a higher sediment load per discharge interval. The winter events generally have a smaller range of discharges throughout the season but with a sediment load similar or a littler greater than the runoff season.

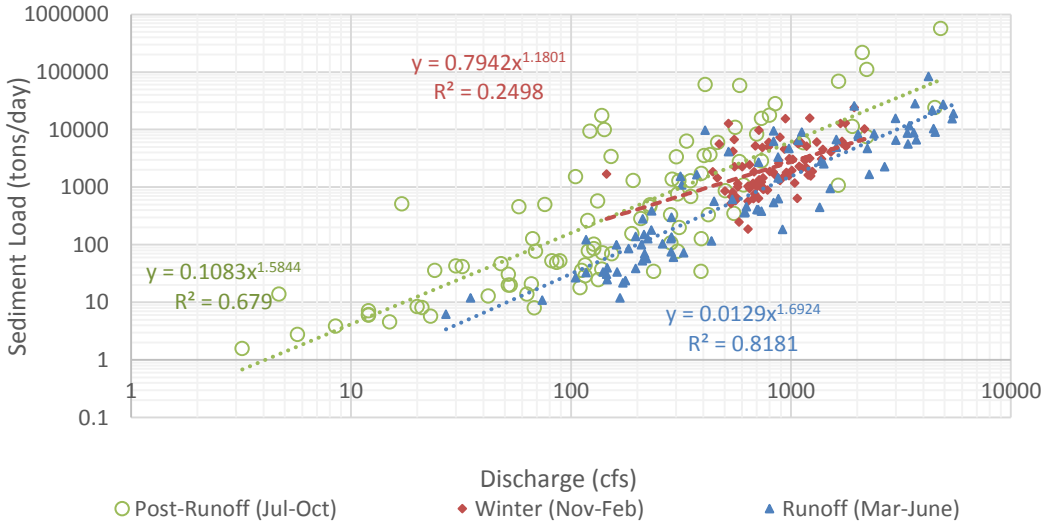

Figure 19 Field samples at San Acacia (USGS 08354900) separated by hydrologic season, instantaneous discharge. Sample dates from 1993 to 2013.

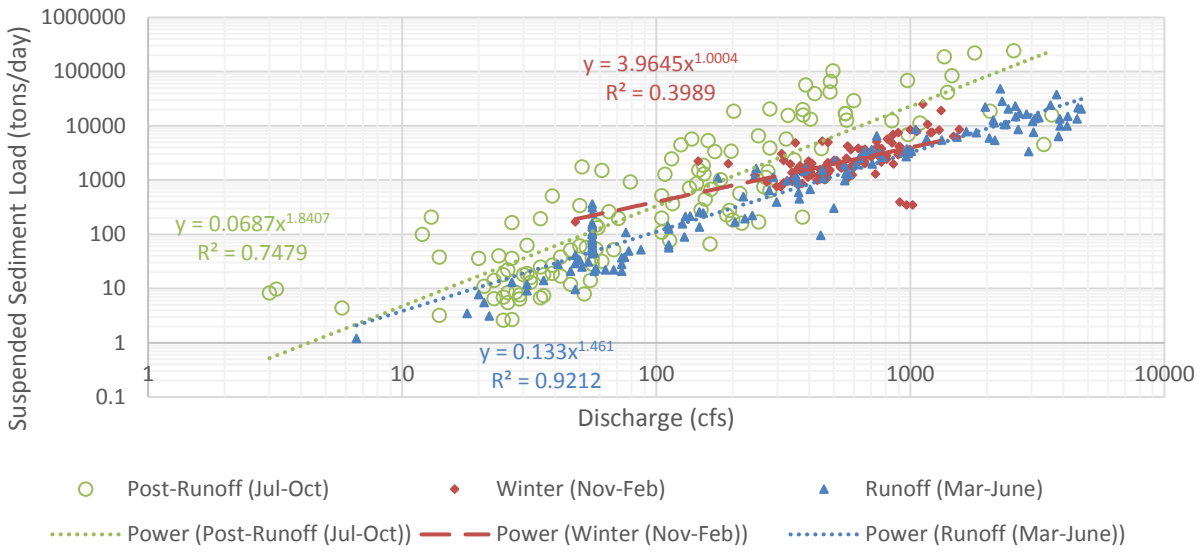

Figure 20 Field samples at San Marcial (USGS 08358400) separated by hydrologic season, instantaneous discharge. Sample dates from 1993 to 2013.

The distribution of sediment and discharge at the San Marcial gage (USGS 08358400) is more uniform across the seasons (Figure 20) than observed at the San Acacia gage (USGS 08354900) over the same time period as shown by a thinner distribution of points over time. Again, post run-off shows higher sediment load at a particular discharge. The range of discharges is less for winter months than of the other hydrologic seasons. The San Marcial gage shows lower discharges during the runoff season than San Acacia.

2.3.2.3 Suspended Sediment Load Curve Based on Particle Size

The grain size distribution was analyzed from the USGS field measurements to determine if a particular discharge is more likely to transport a certain sediment type. Sediment types were generalized into two main classes based on particle sizes to aid with visualizing the data. Figure 21through Figure 25 show the median grain size of the sample defined as:

- "Silt and Clays" (also known as "Fines"), where the median grain size in the suspended sediment sample is less than 0.0625 mm diameter in the measurement for the calculated USGS reported suspended sediment discharge load;
- "Sand", where the median grain size in the suspended sediment sample is between0.0625 mm and 2 mm diameter.

Sediment gradation is based on the standard USGS-accepted Wentworth grade scale (Wentworth 1922).These characterizations were applied in order to distinguish between a dominantly fine suspended sediment load and a dominant suspended sand load. The sediment type in the suspended load may indicate seasonal variations in the types of suspended sediment loads, different effective discharges for transporting varying sediment types, or increased seasonal sediment transport capacity. From the analysis at the San Acacia gage (Figure 21), it was found that discharge rates less than 100 cfs predominantly transport fines in the suspended sediment load. Also, for a particular discharge, when silt and clay is the predominant sediment type, the amount of suspended sediment transported is greater.

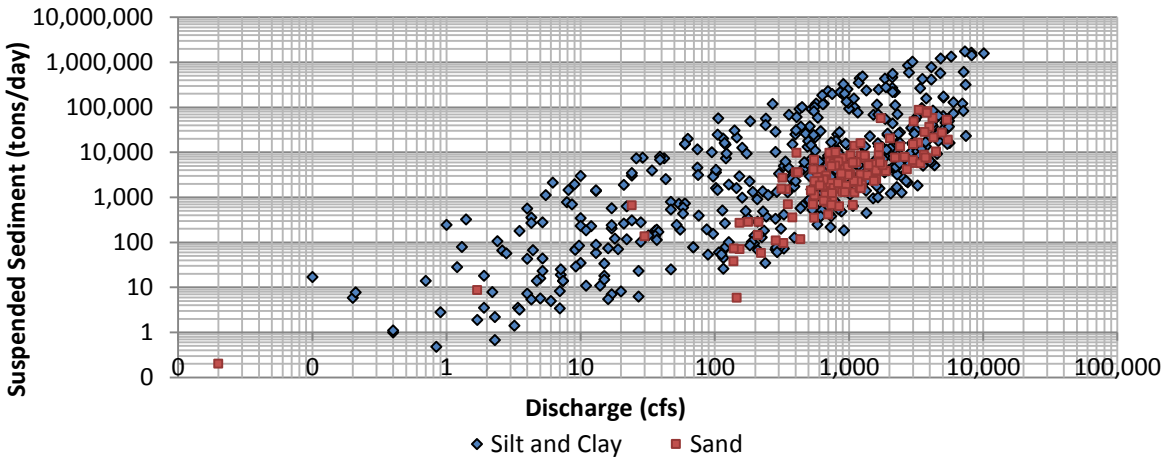

Figure 21 Suspended sediment discharge for different dominant sediment size ranges: sand dominate, silt and clay dominate. Data from San Acacia gage (USGS 08354900) field measurements by the USGS from 1960 to 2015.

For the San Marcial gage (USGS 08358400), silts and clays sized sediments dominate the suspended sediment load at flows less than 100 cfs. The occurrence of sand as the dominant material being transported becomes more prevalent at flows above 100 cfs. It is evident in Figure 22 that at particular discharges, more suspended sediment is transported when silts and clays are the predominant sediment grain size.

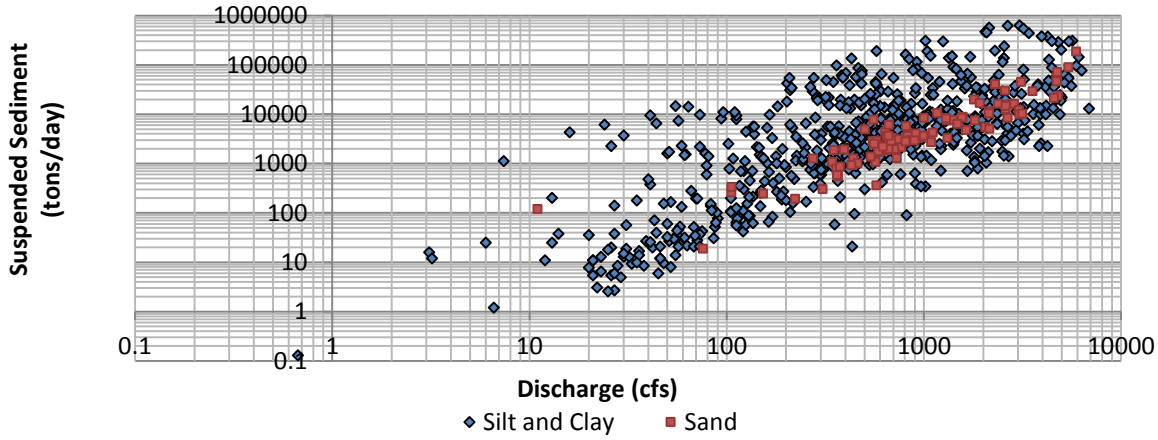

Figure 22 Suspended distribution of different sediment types: sand, clay, silt and loam. Data from San Marcial gage (USGS 08358400) field measurements from 1960 to 2015.

Generally, when sand was the dominant particle size, its transport at a particular discharge was similar for both gages (Figure 23). When silt and clay were the dominant sediment type, however, the San Acacia gage was shown to transport much more suspended sediment at a particular discharge than San Marcial. There were also more data points at higher discharges for San Acacia than San Marcial.

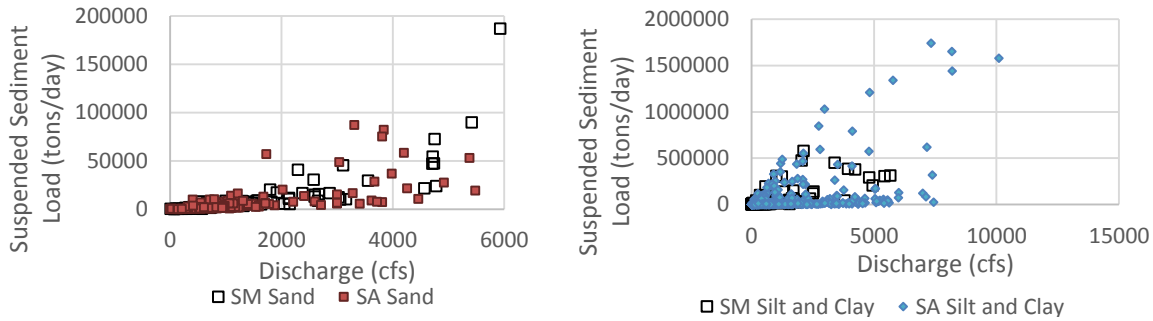

Figure 23 Comparison of the USGS field samples from the San Marcial (SM) gage (USGS 08358400) and the San Acacia (SA) gage (USGS 08354900), by suspended sediment type, field samples from 1960 to 2015.

The field measurements from USGS were then plotted chronologically to assess if there are temporal trends in sediment types. The USGS field measurements at San Acacia indicate that the suspended sediment load is temporally shifting to being predominantly sandy (Figure 24). At the same time, the suspended sediment concentration has been decreasing. For example, up until 1975 the suspended sediment was predominantly clay. In the late 1990s, the predominant grain size was sand.

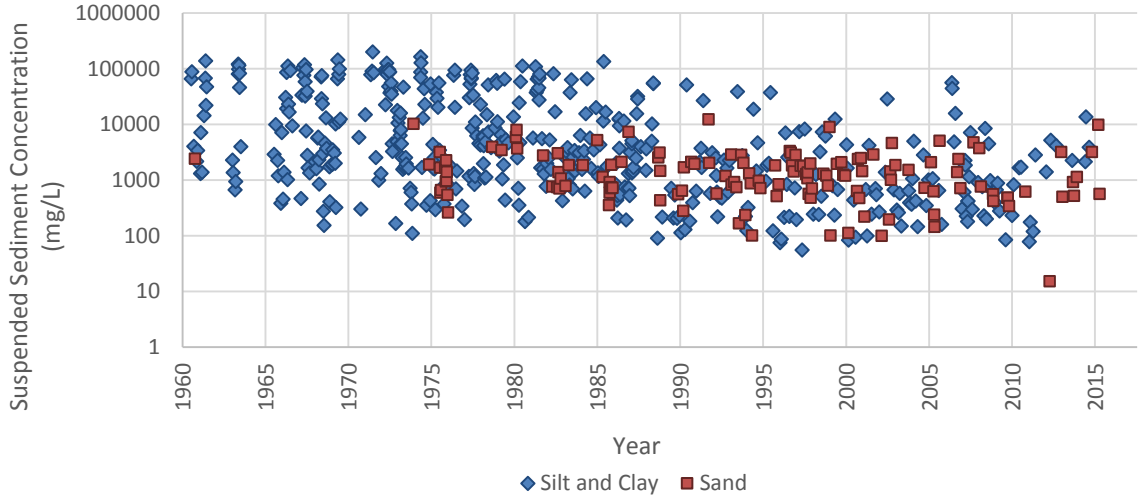

Figure 24 Suspended sediment concentration sorted by predominant grain size at the San Acacia gage (USGS 08354900) over time.

For San Marcial (USGS 08358400), the predominant suspended sediment type follows a similar pattern as San Marcial, in that predominant sand samples were not frequent until around 1976 (Figure 25), and the propensity for clay to be the dominant suspended sediments become less frequent around 1991.

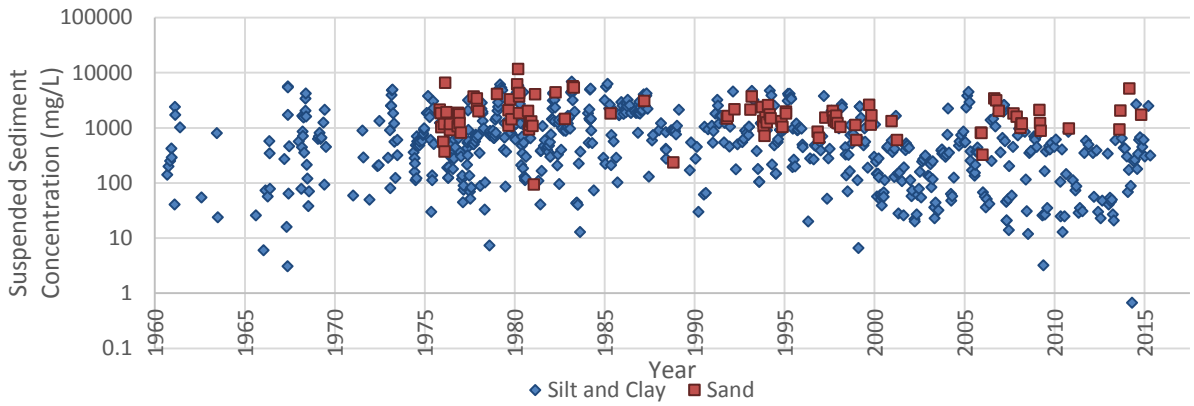

Figure 25 Suspended sediment concentration by predominant grain size at the San Marcial gage (USGS 08358400) over time.

2.3.2.4 Bed Material Data Based on Particle Size

Bed material samples are collected at the San Acacia (USGS 08354900) and San Marcial (USGS 08358400) gage sites at the time of field measurements. As with suspended sediment analysis, the bed material samples were characterized based on their median particle size. The objective was to identify underlying seasonal or long-term trends. Figure 26 and Figure 27 use the following definitions to provide better visualization of the collected data.:

- "Silt/Clay" (also known as "Fines") which is a sample that has a median grain size less 0.0625 mm diameter;
- "Sand" has its median grain size between 0.0625 mm and 2 mm diameter;
- "Gravel" has its median grain size larger than 2 mm diameter.

Because of the large number of sand samples, the sand field measurements were further defined as follows:

  - Sand with fine materials had a median grain size between 0.0625 mm and 2mm, with more than 10% of the composition being less than 0.0625 mm in diameter.
  - Sand with coarse materials was had a median grain size between 0.0625 mm and 2mm, with more than 15% of the composition being greater than 2 mm in diameter.

In San Acacia, the bed sediments (Figure 26) show evidence of the material coarsening over time. From the beginning of the period of record to November 1988, the bed material samples were silty or sandy. After that, there were bed materials with more than 15% gravel in several of the samples. Gravel became a predominant finding in the San Acacia bed samples starting in 2005.

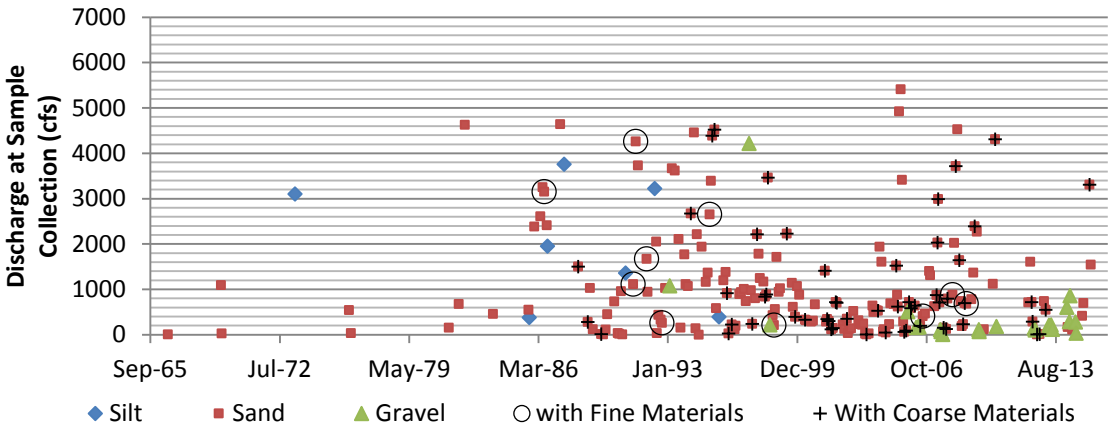

Figure 26 Bed sediment sizes from field measurements at San Acacia (USGS 08354900) from 1966 to 2015.

For San Marcial (USGS 08358400), Figure 27, the field measurements indicate primarily a sand bed substrate. The last record of silty bed sediment ended in June 1991. The period of bed sediment measurements ended in 1999 with one report in 2007.

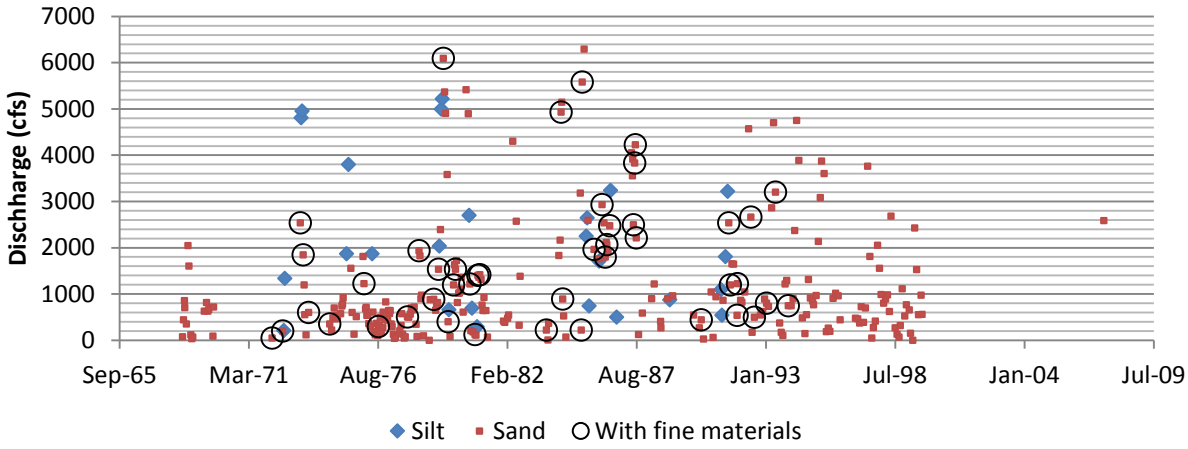

Figure 27 Bed sediment sizes from field measurements at San Marcial (USGS 08358400) from 1966 to 2015.

3.0 Geomorphic Parameters

After Makar and AuBuchon (2012), six geomorphology parameters are used to assess changes occurring on the Middle Rio Grande. These parameters involve the river width, slope, sinuosity, planform, channel depth and terrace elevations, as well as bed material size. The trends observed in geomorphic parameters are compared with trends observed in the drivers in order to analyze the influence of drivers on the geomorphology in the study area.

This report includes hydraulic modeling and analysis of the Reclamation and USGS hydrographic data collected within the Rio Grande. These include cross section and bed material collections. One-dimensional HEC-RAS modeling was also done in order to simulate the

channels' hydraulic properties and help identify river locations that are vulnerable to degradation or aggradation.

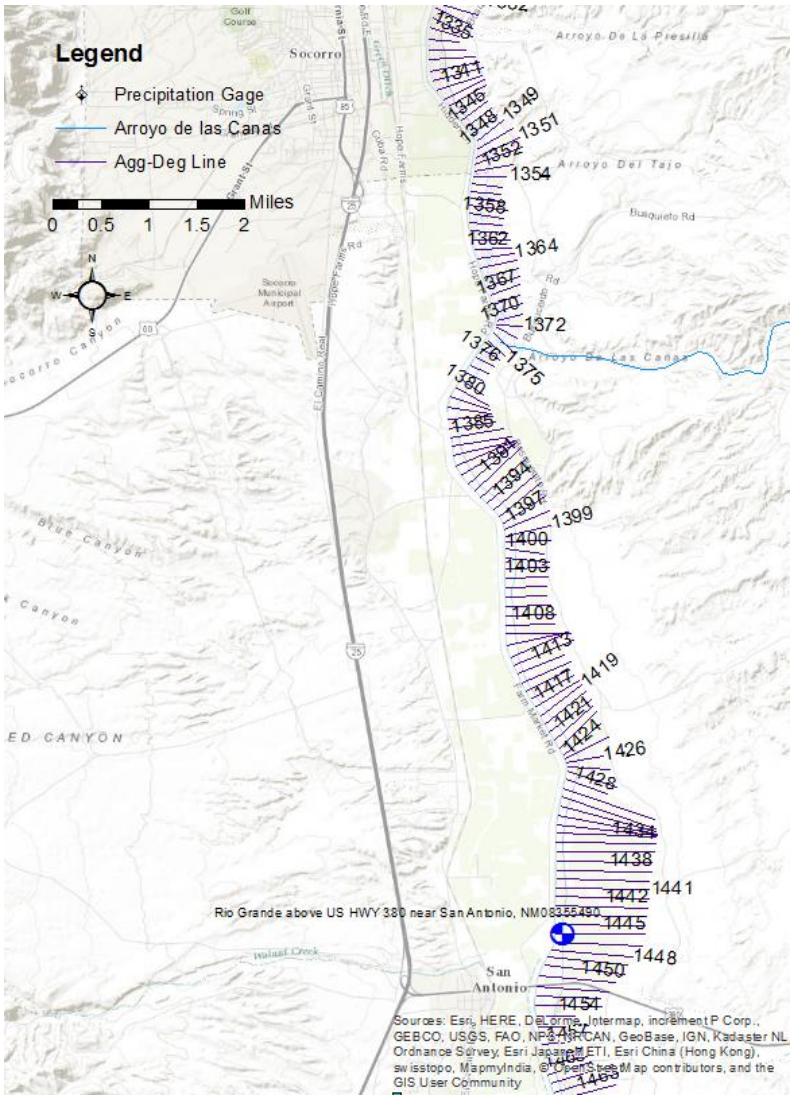

Figure 28 Map of the study reach, with agg-deg lines labeled.

For the geomorphic parameter assessment, the data was evaluated between agg-deg 1364 and agg-deg 1455 (see Figure 28). In river miles, this extent covers RM 101 to RM 89. The Arroyo de las Cañas' confluence is at agg-deg 1374 or RM 95.5. Geographically, the extent is below Arroyo de los Piños to about two miles above HWY 380.

A summary of the major findings in geomorphic parameter trends:

- The geomorphic trend indicates the stream is narrowing and degrading, with the channel becoming more incised upstream of the confluence.
- Based on hydraulic modeling of the river's geometry, the velocity has slightly decreased, this is most likely caused by the river's slope decreasing. Downstream of the confluence of the Arroyo de las Cañas the river is aggrading.

- The bend migration is more pronounced below agg-deg line 1355. The river is constrained the movement of the bends above this line, as evidenced by higher elevation terraces.
- The Arroyo de las Cañas contributes sediment that causes bed aggradation and the development of bars and islands near agg-deg 1394 and 1400. Particle stability is attributed to insufficient shear stresses; the particle size of materials contributed at the Arroyo de las Cañas is not mobile under Rio Grande channel hydraulics. This may be further aggravated in the future as the median bed size from samples within the study reach indicate particle sizes are increasing.
- Channel planform shifts (braided to meandering) suggest that the Rio Grande through this reach is moving from a bed load dominated system to a mixed load system, as indicated by the progression in Schumm's Qualitative model (Schumm, 1981) .
- The Arroyo de las Cañas has been widening and become more uniform in width. Also, the alluvial fan has become stable and vegetated, directing flow towards the opposite bank.
- The area of bars has generally decreased while the number of bars has stayed relatively constant.
- Vegetation extent in the Rio Grande for the study area has decreased between 1992 and 2008, with an increase in vegetation from 2008 to 2012. This corresponds to a period where sinuosity increased from 1992 to 2006, and then decreased at 2006 to 2012. Lateral migration and loss of vegetation may be related.
- Vegetation started growing on the Arroyo de las Cañas fan around 1992.
- Slope is generally decreasing in time, with exception of the Rio Grande below Arroyo de las Cañas between 1960 and 1992, here the slope was increasing.
- Slope transition occurs around Arroyo del Tajo from degradation to aggradation.
- Upstream of the Arroyo de las Cañas:
    - Slope is shifting, where areas that are steep are becoming flatter and vice versa (agg-deg 1340 to agg-deg 1370).
    - Downstream from agg-deg 1340, the slope profile is becoming less steep when compared from previous profiles.
    - The channel is more constrained due to the elevation of abandoned terraces, than downstream of the arroyo.
    - In the past 20 years, most bend migration to the west with some shifts alternating to the east.
    - Bar area has stayed relatively constant.
- Downstream of the Arroyo de las Cañas:
    - The bend migration has been to the east for the past 20 years (From agg-deg 1383 to agg-deg 1396); and the most extreme change occurs at agg-deg 1400 to agg-deg 1430. Alternating pattern of migration from east to west is more common in this section of the reach than upstream of Cañas.
    - From agg-deg 1400 and downstream, the thalweg has had the least stable elevation.
    - Island and bar formation is active here, with the most persistent islands being present. This is likely due to the stability of particles contributed by the arroyo.
    - Downstream of agg-deg 1380, the terraces have between zero and two feet of elevation on the east bank.

- Bed material has increased in size over time.
- Bed material decreases in size moving downstream; coarsening materials have been found around Arroyo de las Cañas.
- Bed material samples on the river indicate that the river bed is generally not stable when comparing particle stability to shear forces in the channel. Bed material samples from the Arroyo de las Cañas indicate a higher stability relative to Rio Grande bed material samples.
- Cross sections show that the channel has deepened and narrowed. The historic floodplain have become abandoned with new inset floodplains developing within the historic channel width.
- From 1962 to 2012 the following hydraulic characteristic trends were found for this study area:
    - Wetted area and perimeter has slightly increased.
    - Max depth has decreased.
    - Mean depth has stayed constant.
    - Average velocity has slowed.
    - Width to depth (W/D) ratio has slightly increased.
    - Froude number has slightly decreased.
    - Top width has decreased over time and become more uniform (less variation within the reach for a given discharge).

3.1 Channel Width

3.1.1 Average Channel Width

The channel width was determined by taking measurements of the active channel planform, or the riverine area that likely conveys flow (Figure 29). The agg-deg lines were overlaid on river planform polygons, and the length of the agg-deg line across the polygon was measured using ESRI's ArcGIS Geometry Calculator (version 10.1). In general, the active channel width in the study area has decreased since 1918. After the closure of Cochiti Dam in 1973, the Rio Grande experienced a widening in the 1980s, but the width again decreased until present day. The box and whisker plots in Figure 29 demonstrate the maximum and minimum measured channel widths; the bottom of the box identifies the 25th percentile, the middle line the median, and the top of the box the 75th percentile of the width measurements for the Rio Grande.

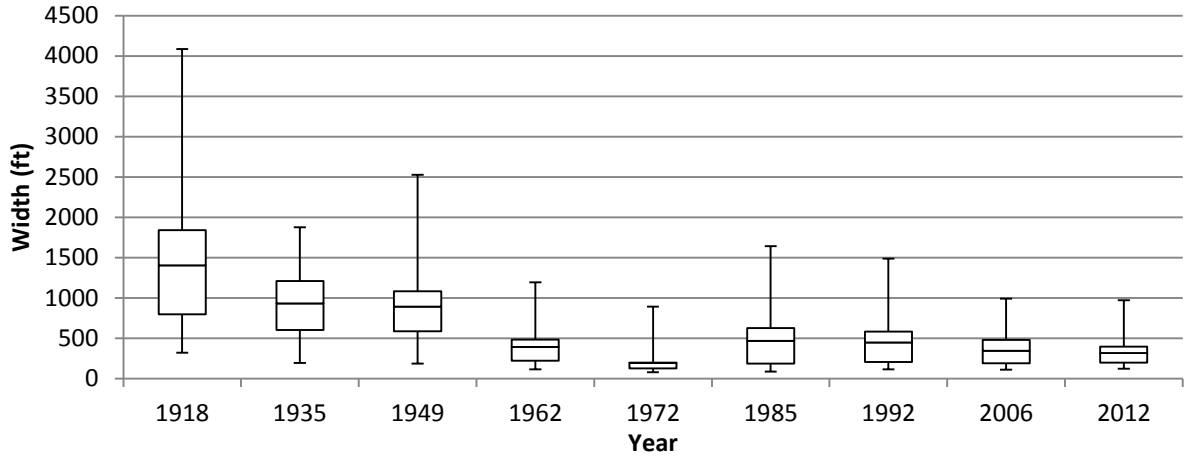

Figure 29 Average width of the Rio Grande from agg-deg1364 to agg-deg1455; Box and whisker boxes enclose the 25th and 75th percentile, with the line across it indicating the median.

From Figure 29, it is apparent that the median channel width has generally been decreasing over time, with exception between 1972 and 1985, where the channel became wider again. This period correlates with a period of high flow and floodway mowing activities. The high flow and lack of vegetation would have made it more possible for the banks to erode which may have facilitated the widening trend. The range of widths for the channel (demonstrated by the length of the 'box') also experiences narrowing over time. This time corresponds with the beginning of the operation of the Cochiti Dam, as well as the end of LFCC operation. The narrowing period between 1949 and 1962 would have been especially affected by the installation of rip rap and jetty jacks in the 1950s which was to improve channelization of the Rio Grande.

3.1.2 Longitudinal Channel Planform Width

Leading up to 1972, the channel widths of the Rio Grande within the study area experienced narrowing from agg-deg 1422 (RM 93) to the end of the study area at agg-deg 1455. The channel has persisted being narrow to this day. From agg-deg 1376 to 1397 (RM 97.5 to RM 95.5) the channel generally narrowed and had a uniform width less than 500 ft wide. This area corresponds with the confluence of Arroyo del Tajo at the upstream side and the Arroyo de las Cañas on the downstream side. After the closure for Cochiti Dam the channel widened again (see Figure 30), in regions that had been wide in 1918: agg-deg 1361 and 1400 (RM 99 and RM 95). These agg-deg lines are below the Arroyo de Presilla and the Arroyo de las Cañas. The channel did not widen though to the extent observed in 1948 and before, barely exceeding 1000 ft wide. From 1985 onward, the channel generally narrowed.

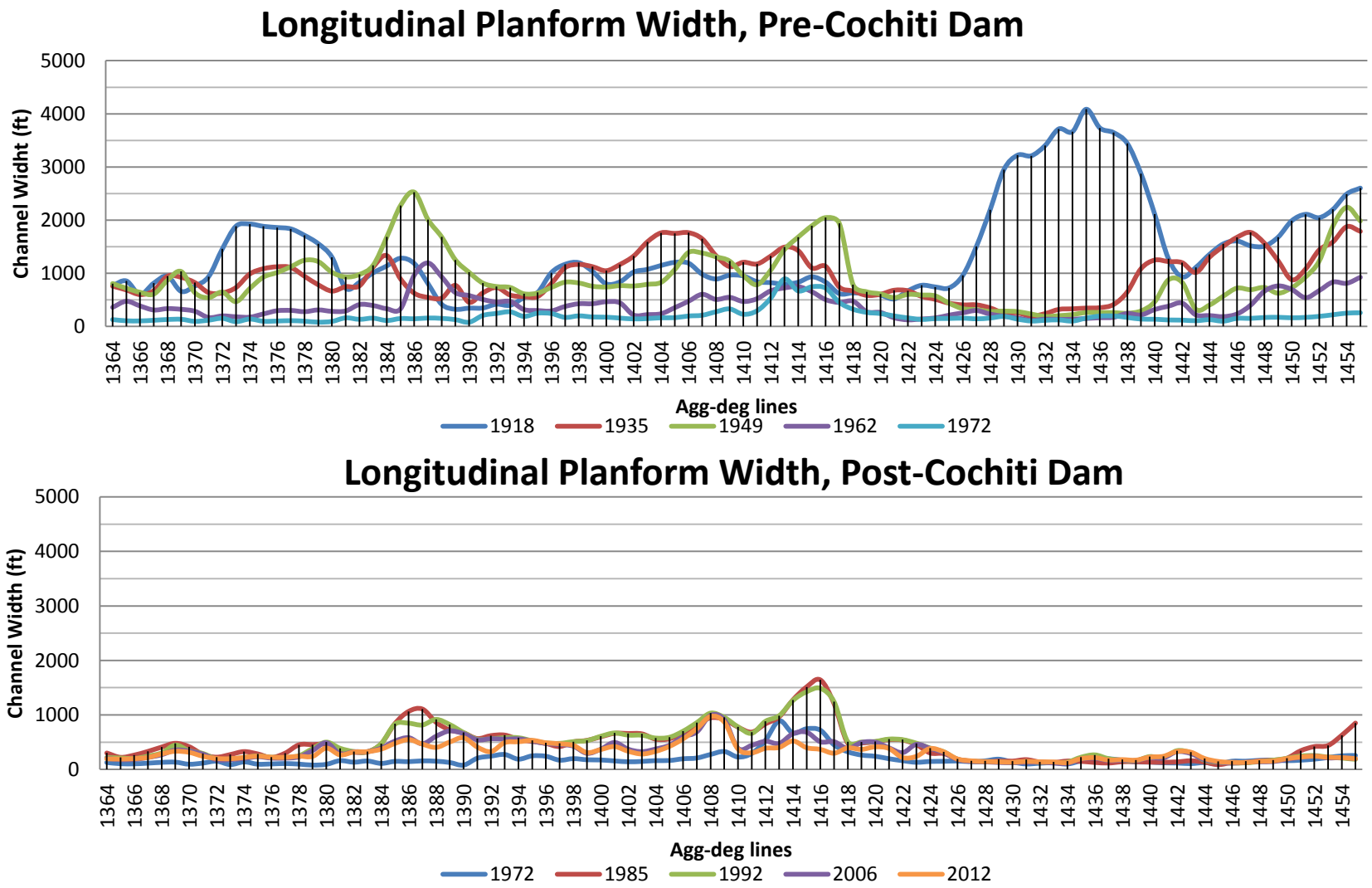

Figure 30 The channel planform width within the study area, from 1918 to 2012.

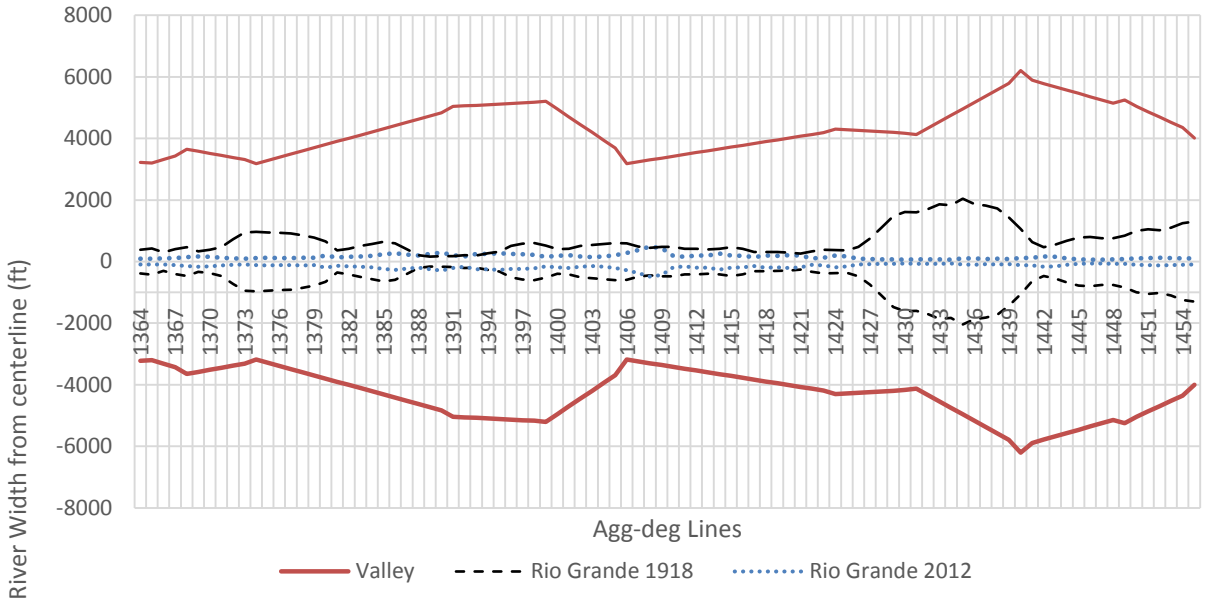

Figure 31 A plot of the 1918 and 2012 river width relative to changes in valley width, centerline is zero.

A sketch of the valley width after Brierley and Fryirs (2005), along with the active channel width in 1918 and 2012 was plotted in Figure 31 to evaluate valley and channel changes. From this figure the valley geology does not appear to confine the width of the river planform. There are a couple of locations where the channel widens just before the valley widens at agg-deg 1427 and 1370. Generally the width of the river has decreased and has a more uniform width in 2012 than in 1918.

The change at each agg-deg line is visualized in Figure 32. From year to year, at every agg-deg line, it was calculated whether the channel width was decreasing or increasing. The net change is represented by the solid bar that points either in the positive or negative direction. The net trend has been channel narrowing, with exceptions to widening in 1985. The area around the confluence of the Arroyo de las Cañas (agg-deg 1374) has been narrowing throughout the study period. 1985 and 1992 represent major shifts in observed widths, with channel widening by 1985 and then narrowing by almost the same magnitude in 1992. The former corresponds to the operation and closure of the LFCC (Reclamation, 1985; Reclamation, 2000), and the latter corresponds to a period at which Elephant Butte was filling or essentially full. The most dramatic shifts in recent years are channel narrowing at agg-deg 1368 and at the Arroyo de las Cañas at agg-deg 1374. Downstream of agg-deg 1401, the stream has shifted to a general trend of widening in the past 40 years.

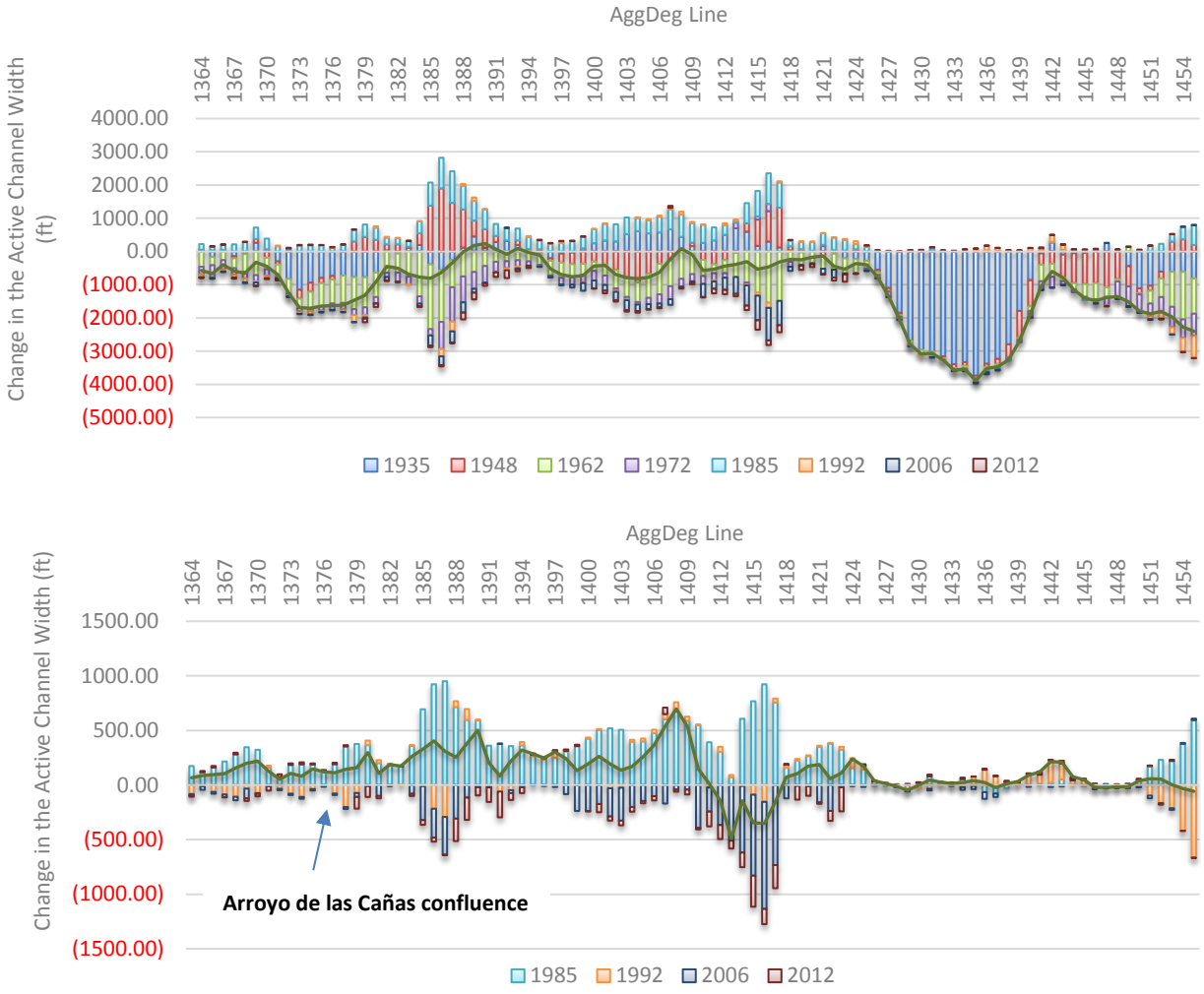

Figure 32 Active channel planform width loss or gains in width from 1918 to 2012, by agg-deg line a) for the period of record from 1935 to 2012 and b) for post-Cochiti Dam, from 1985 to 2012. Solid line shows net loss or gain for each time period.

3.2 Channel Location and Planform

The location of the channel and its planform is an indication of the geomorphic trends in the study area. The migration of the channel is affected by the effective transport of sediment, and long term trends may be helpful indications of future bend migration or channel movement. Channel planforms for the study are presented in Figure 33 and were used in the following analysis.

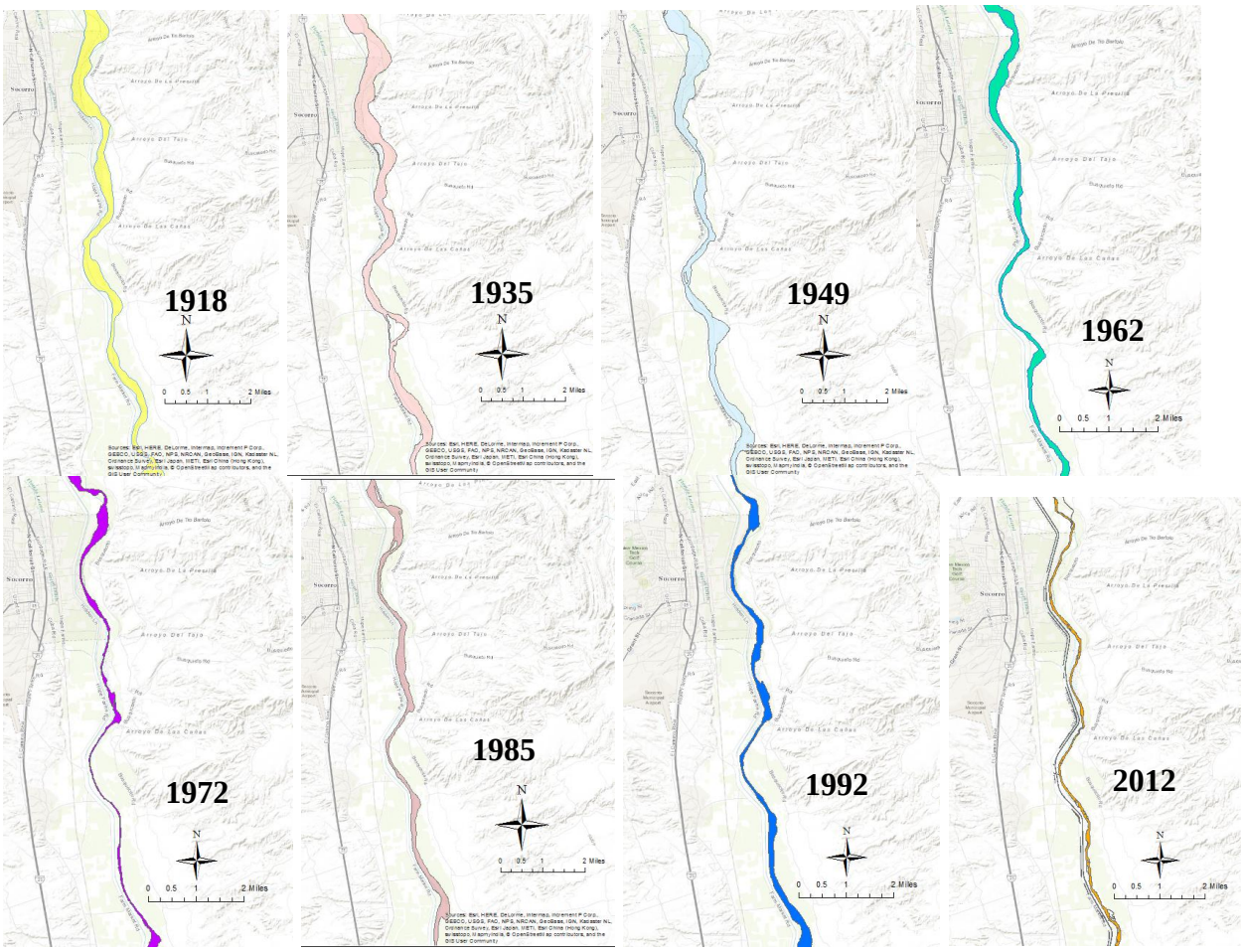

Figure 33 The Rio Grande planform near the Arroyo de las Cañas confluence, set over a current (2012) topography map.

3.2.1 Planform Classification

The general shape of the channel was assessed for available aerial photographs between 1918 and 2012. Schumm (1981) and Massong et al. (2010) have classified the formation of meandering bends or new dominant channels as indications of the relative transport capacity of the river. If the river is transporting more sediment than its transport capacity, the sediment may deposit and force the river to redirect its flow to a lower elevation. If the transport capacity in the channel exceeds the incoming sediment supply, then the channel may erode vertically and increase the channel size (Massong et al., 2010).

It was found that the study reach has progressed into a migrating planform pattern (Table 6), but has not progressed to the higher levels of rapid bend movement, according to Massong et al.'s planform stage classification. The results from the Schumm analysis shows that the sediment transport was generally via bed load (stages 1-5) or of a mixed load (stages 6 – 10), with the period of mixed load sediment transport occurring since 1962.

Table 7 Channel Classification for the Arroyo de las Cañas study area

Years	Massong et al. (2010)	Schumm (1977, 1981)
1918	1	3
1935	1	4
1949	2	5
1962	3	7
1972	M4	7
1992	M4	7
2002	M5	8
2012	M5	8

As for Massong et al.'s planform evolution, stage M4 coincides with periods at which the transport capacity in the channel exceeds the incoming sediment. This confirms the sediment losses within the reach from 1972-1982 and 1992-2000 (Figure 16). The channel is vertically eroding over this time to increase the channel side. Side channels are abandoned, and vegetation encroaches (Massong et al, 2010). Stage M5 is a progression from stage M4, and channels often find stability in this planform evolution stage.

3.2.2 Vegetation and River Bar Trends

River bars (both point bars and mid-channel bars) are an indication of sediment deposition, typically in areas where the energy of the river is dropping. As bars become stable for an extended period of time, the bar surfaces become colonized by woody vegetation that can lead to increased sediment deposition during larger flow events. Vegetation trends for this analysis were determined by drawing a polygon in ArcGIS that encompasses a study area. The study area included the river channel and the surrounding floodplain. Each aerial photography year was then analyzed by the author in ArcGIS, with islands and river bars being demarcated by polygons. The acreages encompassed in the polygon was then calculated using ESRI's ArcGIS Geometry Calculator (version 10.1) for each aerial photography year to determine the total vegetated area for that year. This areal sum was then divided by the total study area to obtain a percent vegetated.

Results for this analysis between 1992 and 2012 are shown in Table 7. As can be seen from this table the vegetation within the study area has been fairly consistent for the past 20 years. The vegetation along the banks immediately alongside the active channel of the river was also assessed for percent vegetation per length of bank. Actively eroding or new bank areas may have less vegetation, so a decrease in vegetation may indicate channel movement.

Bar trends were assessed in a similar manner, with all bar deposits (bare earth and vegetated) identified within the active channel boundaries. Polygons were created in ArcGIS to map these bars. These features may be transient or semi-permanent, and are used to identify the depositional and reworked areas of the river. This evaluation may be limited by the discharge in the Rio Grande at the time when the aerial photographs are taken, as river discharge may obscure observations. Generally, the number and area of bars decreased. The area of bars greatly decreased between 2005 and 2008, corresponding with significant discharge events which may have broken up the islands and transported the sediment downstream. From 2008 to 2012, the number of river bars and the area of the river bars have increased. The increase in the number of

bars may have to do with the absence of discharge events greater than 3,000 cfs within the reach (Figure 10). The presence of these bars and their vegetation aligns with the evolution of planforms described by Massong et al., 2010. The stabilization of bars with woody vegetation change the morphology of the river over time. Bar area may apparently decrease, especially on the side of channel banks, as the bars are incorporated into the active channel planform.

Table 8 Vegetation and bar trends within the study area from agg-deg1364 to agg-deg1455.

Year	Vegetation (%)	Non-vegetated Banks (%)	Number of Bars	Bar Area (acre)
1992	50.8	17.6	54	187
2002	53.3	13.3	92	143
2005	56.1	16.0	23	118
2008	46.3	8.3	26	49
2012	49.1	15.7	52	71

The locations of the island formation and river bar erosion were evaluated by dividing the Rio Grande at agg-deg lines that encompassed bends (agg-deg 1371, 1382, 1391, and 1430) and straight reaches of the river (agg-deg 1364, 1377, and 1410). It was found that the agg-deg lines below the Arroyo de las Cañas showed the greatest amount of formation and erosional loss of bars and islands from 1973 to present day. The range lines below the Arroyo de las Cañas (agg-deg 1374) from agg-deg 1391 to 1429 experienced the most flux in the creation and erosion of islands (Figure 34).

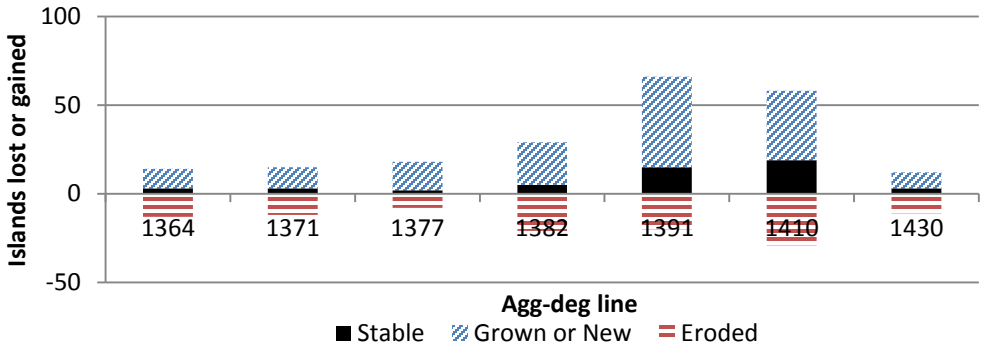

Figure 34 Number of islands lost or gained from 1973 to 2012 between agg-deg1364 and agg-deg1455.

3.2.3 Lateral Bend Migration

Bend migration was measured by identifying the apex of the bend and corresponding Aggradation/Degradation range line in aerial photographs and measuring the distance between its coordinate location and later aerial photographs. The bend movement was designated as "east" or "west" in Figure 35, notwithstanding various degrees of northern or southern migration. The greatest magnitude of bend migration occurred from 1962 to 1972 downstream of the arroyo at agg-deg 1400. Generally the period of 1972 to 1992 saw bends migrating to the West. After 1992, the bends downstream of the Arroyo de las Cañas confluence (agg-deg 1374) generally migrated east for the rest of the study period.

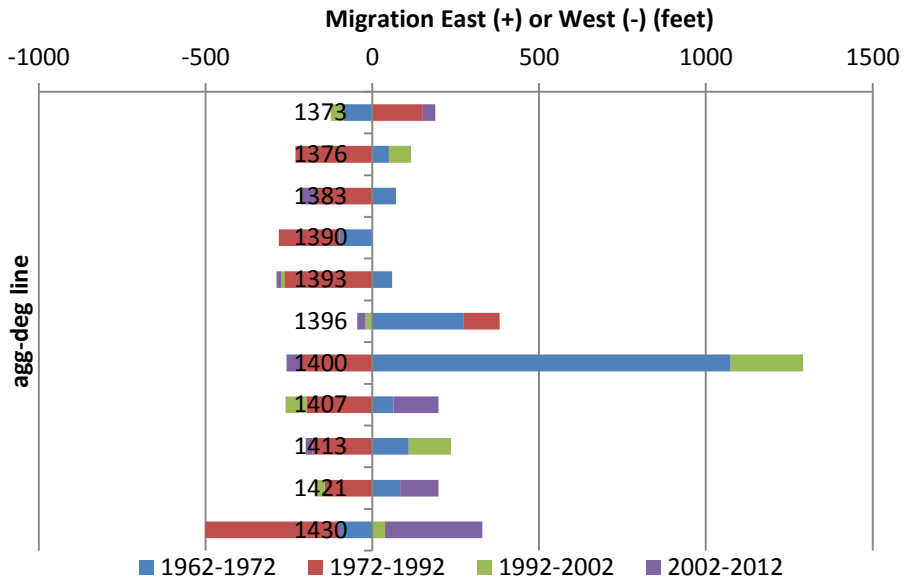

Figure 35 Lateral Bend migration at agg-deg lines within the study area.

Results from this analysis is tabulated in Table 8. It was found that from 1972 to 1992, the bends migrated along the entire reach, most toward the West, nearer to the LFCC spoil levee. Since then, there has been migration south of agg-deg 1400 towards the east.

Table 9 Bend migration analysis for the Arroyo de las Cañas study reach in feet (+ is West, - is East)

Agg-Deg Line	1962-1972	1972-1992	1992-2002	2002-2012
1373	-87	151	-38	38
1376	50	-231	66	0
1383	71	-167	0	-46
1390	-98	-182	0	0
1393	59	-264	-10	-13
1396	274	108	-20	-25
1400	1074	-217	217	-40
1407	63	-198	-62	135
1413	109	-179	127	-21
1421	83	-143	-30	115
1430	-100	-401	38	292

3.2.4 Narrative on Arroyo de las Cañas Planform Changes

A polygon was drawn over the Arroyo de las Cañas and Rio Grande confluence from an aerial photograph in 1962. Changes in the planform of the arroyo and observations of the confluence area were evaluated for available aerial photography from 1962 to 2012 within this polygon. The length of the observed section of the arroyo to the Rio Grande confluence was approximately 2,200 ft in 1962. The average width of the arroyo channel through this section at this time was 386 ft, with its alluvial fan extending 352 feet beyond the left Rio Grande river bank, looking downstream. There is sparse vegetation on the south bank of the arroyo. The arroyo channel is braided, with some apparent incision appearing on the left arroyo bank.

In 1972, the arroyo is wider (average width is approximately 440 feet), due to the right bank expanding north. It appears as if the arroyo channel has shifted from a braided planform to a single channel planform within the study area. The Rio Grande has shifted to the East into the arroyo's alluvial fan, which shortened the length of the arroyo within the study area. The arroyo appears to be relatively uniform in width, although there are wider areas extending 66 to 90 ft wider in some places. Vegetation has started to cover some of the alluvial fan.

In 1992, the arroyo planform is the same width as in 1972 (440 ft). The aerial photography from 1992 has better resolution than in 1972, and it is visible that the dry arroyo channel is braided with sparse vegetation. The shifting of the Rio Grande has eroded the arroyo's alluvial fan near the confluence in some areas up to ninety feet. The arroyo fan appears to be established with vegetation. The fan extension is now about 551 feet long but has been reduced in width.

In 2002 the arroyo is braided and appears to be widening. Larger vegetation is evident on the alluvial fan. The Rio Grande has shifted to the West, increasing the arroyo length in the study polygon. The right arroyo bank appears incised, and the fan appears to cover the same amount of area. The width of the arroyo is about 663 ft.

In 2012 the fan has extended past previous fan terminus about 260 feet, and the stream paths that meander within the arroyo channel have extended in width. The width of the arroyo has not changed.

3.3 Channel Slope

The agg-deg lines were used to quantify the channel slope and the mean bed elevation for years spanning from 1962 to 2012. The agg-deg data is derived from photogrammetry techniques and does not capture the underwater portion. The Technical Services Center (TSC) in Denver, CO has developed a program that adjusts the bed to create a best match for the underwater prism (Varyu 2013). The agg-deg geometry is processed through an executable program called bedelevation.exe which determines the mean bed elevation between main channel points in a HEC-RAS data-file. The mean bed file is an extraction of the HEC-RAS data compared to known water surface elevations and top width. The depth is iterated upon in order to conserve energy between cross sections by assuming a trapezoidal shape for the river topography under the water. This is called a mean bed because it is believed to represent the average bed condition.

The data provided by the bedelevation.exe is organized by agg-deg number, cumulative distance downstream of Cochiti Dam, and the mean bed elevation (Reclamation 2015a). These cumulative distances from Cochiti are not accurate from these files, because they were not measured every year, but assumed to be constant in the bedelevation.exe (Reclamation 2015a). Instead, the length between agg-deg lines for the following figures was referenced from a previously compiled database (Reclamation 2015b).

In Figure 36 the river's length from 2002 to 2012 within the study reach (Arroyo de los Piños to ~ 2 miles upstream of the 380 Bridge near San Antonio, NM) has only increased in length by approximately 160 feet. The cumulative change from 1992 to 2002 was of a similar magnitude,

but this due to lengthening and shortening near agg-deg 1375 and 1448 respectively. It is evident in Figure 36 that changes in river length were more dramatic from 1962 to 1992.

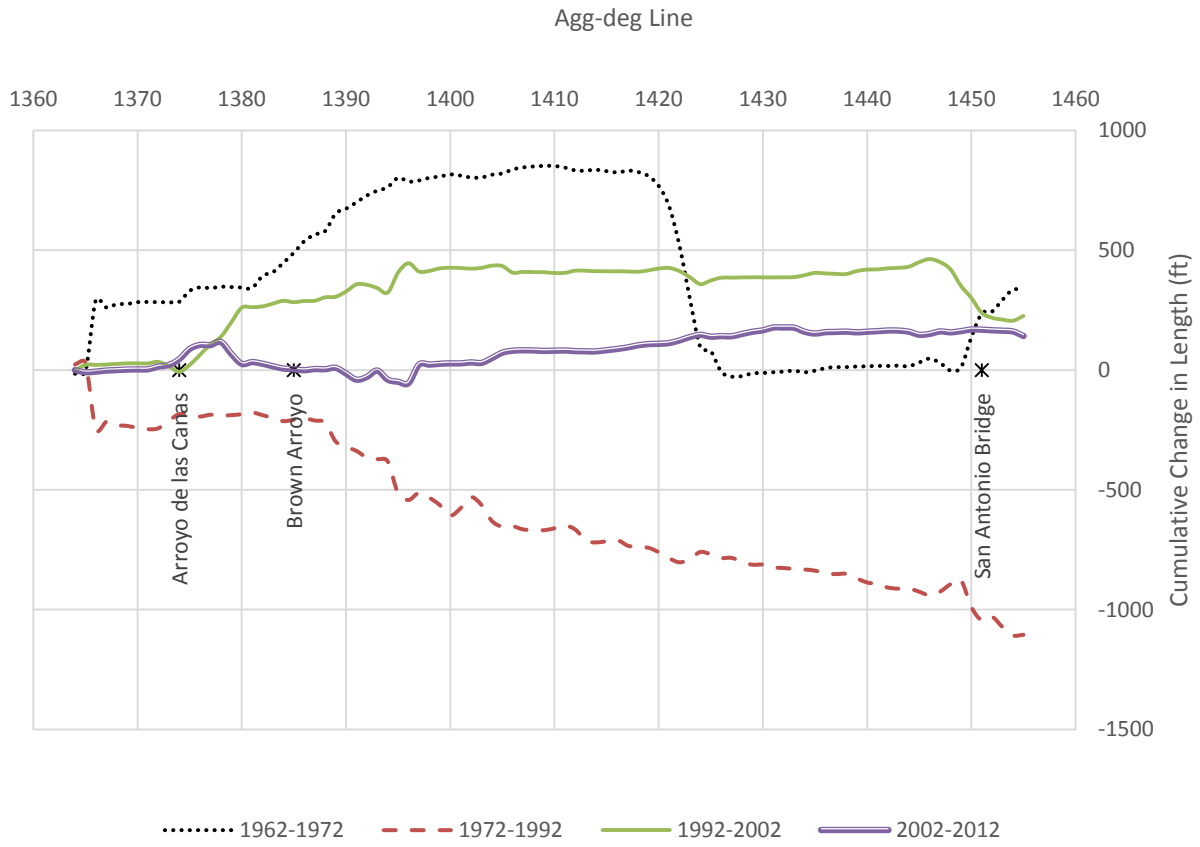

Figure 36 Cumulative change in length from San Acacia Diversion Dam to San Antonio Bridge from data in Reclamation (2015).

A change in channel length may indicate that the river is moving and slope may be affected by this change. The combination of data from the mean bed elevation calculations (Reclamation 2015a) and river channel lengths (Reclamation 2015b) were used to determine the slope of the study reach over various years (Figure 37).

Because the change in slope data is gradual and varies from location to location, cumulative change in slope was calculated to amplify reach-wide trends. The slope in Figure 37 indicates the magnitude of change as one progresses downstream. The slope was calculated for each agg-deg location by dividing the change of elevation from one agg-deg and its downstream agg-deg line by the length between the two lines. Change was determined by subtracting the slope from each agg-deg line from its corresponding agg-deg location from a later year. Cumulative change was then determined by the slope from each agg-deg line added to each other as one progresses downstream.

The figure was simplified by updating data only where agg-deg change in slope was greater than 0.002 feet/feet than the previous agg-deg line, though the magnitude of change may not appear

as much because it is plotted at the actual cumulative change. The result was a smoothing of the data, but the magnitude of change may be off by as much as 0.002 ft/ft.

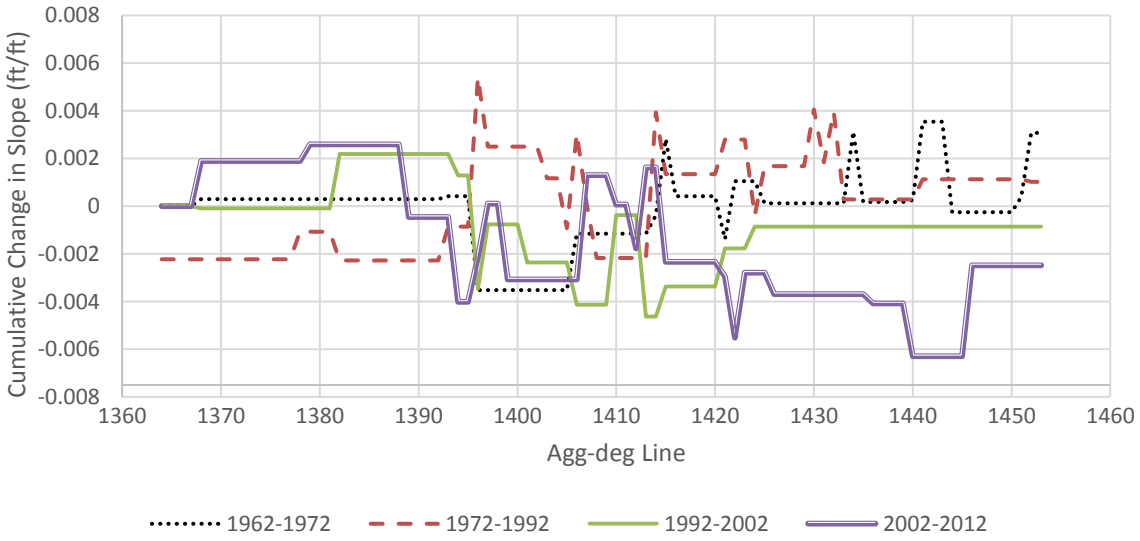

Figure 37 Change in slope at each Agg-deg line from the study area.

When the line is above zero, it indicates that the cumulative slope has become steeper. If the line has a slope that is increasing above zero, this part of the reach has become steeper. If the line is below zero, the reach has become flatter up to this point. Straight lines indicate less than 0.002 ft/ft of change. The unabridged data for change in slope is available in the appendix. More figures that indicate the slope trends, that is, reach average slope and mean bed elevation, are shown in the following section, in Figures 38 and 39 respectively.

The most change in slope has occurred between agg-deg lines 1390 and 1425, as indicated by increasing and decreasing cumulative values within this section of the reach. In more recent years, change of slope has occurred above agg-deg 1390, while in 1962 to 1992 there was not much cumulative change in this area. Alternatively, downstream of agg-deg 1420 has not seen very much change since 1992, as indicated by a relatively flat line for cumulative change (besides the shift from agg-deg 1440 to 1445 from 2002 to 2012); while from 1962 to 1992 the slope showed more instances of varying.

Since 1992 the slope has generally been decreasing, though at agg-deg 1380 (below Arroyo de las Cañas) and at agg-deg 1420, there are indications that the slope has increased locally, as shown by positive or near-zero (rising from more negative) cumulative values. Figure 37 indicates that between agg-deg lines there's more varied change occurring than what is indicated by reach average slope (next section).

3.3.1 Reach Average Slope

The reach average slope was calculated based on the results of the mean bed elevation calculations and the channel lengths. The study reach was divided from San Acacia Diversion Dam to the Arroyo de las Cañas confluence and from the Arroyo de las Cañas confluence to the San Antonio Bridge. Generally the slope of the Rio Grande above the Arroyo de las Cañas has

been decreasing from 1962 to 2012, except in 2002, where there was a slight increase in the slope (Figure 38). For downstream of the Arroyo de las Cañas, the slope was generally increasing from 1962 to 1992. Since 1992 there has been a decreasing trend of slope for both upstream and downstream of the Arroyo de las Cañas confluence, as if both river reaches have conformed to similar geomorphic influences.

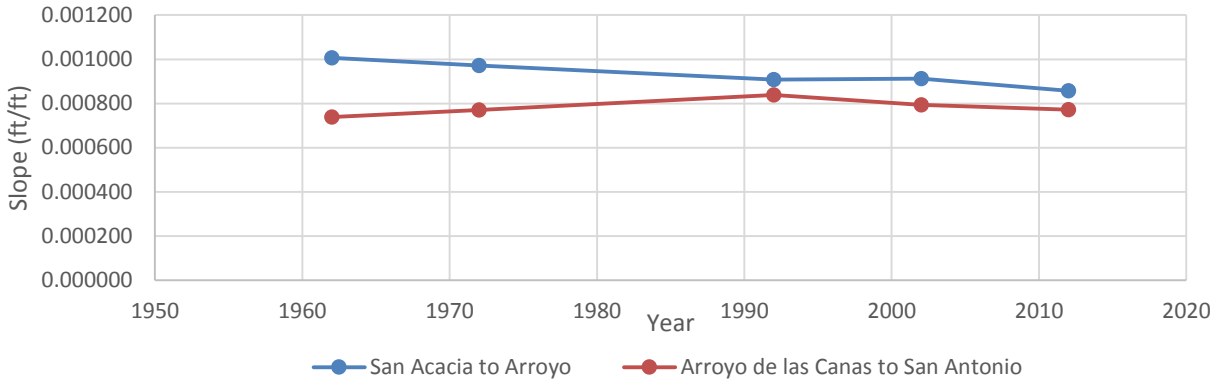

Figure 38 Average slope within the study area from San Acacia to Arroyo de las Cañas and Arroyo de las Cañas to San Antonio Bridge at HWY 380 from 1962 to 2012.

Table 10 Reach average slope by year

Reach Average Slope (ft/ft)	1962	1972	1992	2002	2012
San Acacia to Arroyo	0.001006	0.000972 (-3% change)	0.000909 (-6% change)	0.000912 (+0.3% change)	0.000857 (-6% change)
Arroyo de las Cañas to San Antonio	0.000739	0.000771 (+4% change)	0.000838 (+8% change)	0.000794 (-5% change)	0.000772 (-2% change)

3.3.2 Mean Bed River Profiles over Time

As shown in Figure 39 below, the mean bed elevation was graphed to compare various years. In 1962 and 1972 the mean elevation above agg-deg 1350 (below Arroyo de Tío Bartolo) was generally greater than the following years. The bed elevation here continues to decrease, with 2012 having the lowest elevation. Downstream of agg-deg 1350, and most apparently below agg-deg line 1420, the mean bed elevation of the Rio Grande is greater than previous years in 2012.

The upper reach of the study area, to Arroyo de Presilla has degraded over time, while the lower reach from agg-deg 1400 downstream has aggraded. There is no relative change is bed elevation from the Arroyo de Presilla to just downstream of the Arroyo de las Cañas.

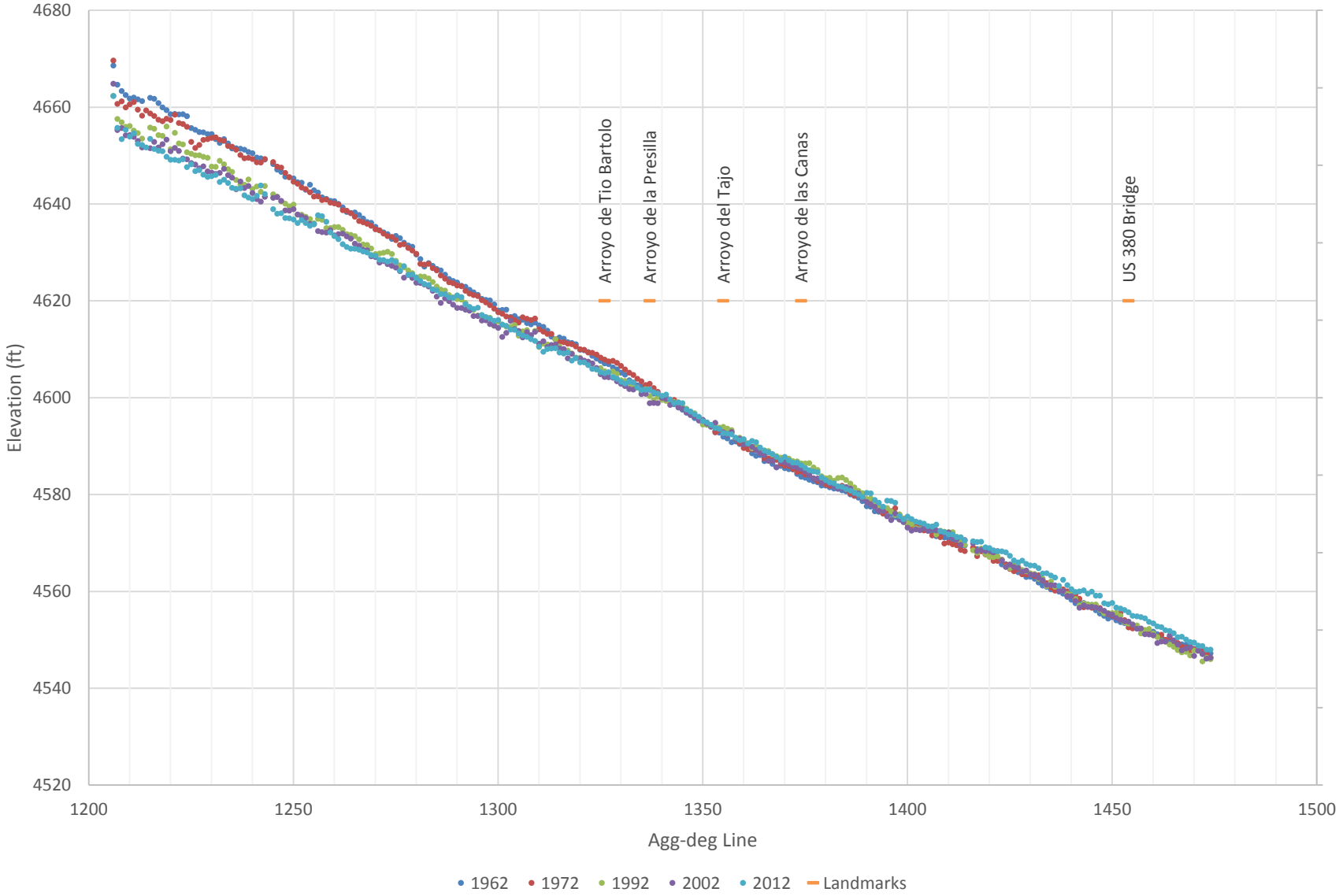

Figure 39 Longitudinal elevation of the Rio Grande from agg-deg 1206 to agg-deg 1473 in various years.

3.3.3 Thalweg Elevations over Time

The thalweg data was plotted to see temporal changes (Figure 40) at different SO lines within the study area. The data had previously been compiled by Larsen et al. (2011). The SO lines are established range lines and represent hydrographic data collected on the ground by surveyors. These differ from agg-deg lines in that the agg-deg data is collected from aerial photogrammetry and typically does not capture the underwater section. The hydrographic data also tends to be more accurate than the photogrammetry data. Anything prior to 2001 had data collected in NGVD29, and anything after 2004 had data collected in NAVD88. Cross-sections prior to 2004 was adjusted to the NAVD88 datum based on range-line location.

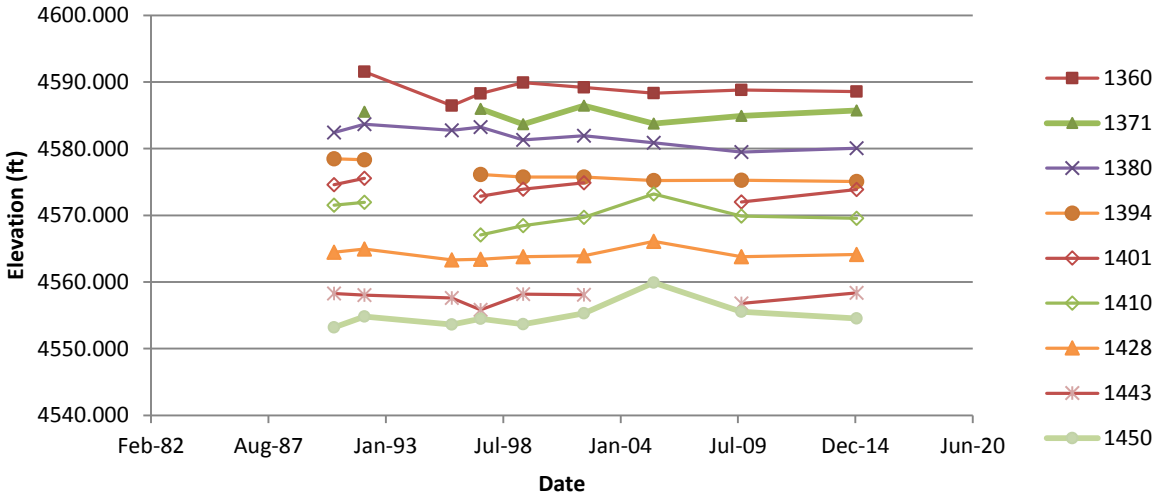

Figure 40 Elevations at different SO lines for the Rio Grande between 1989 and 2015.

In the data it appears there was a degradation period between 1992 and 1997, which is a period when the Elephant Butte Reservoir was initially filling and then experienced a drought from 1995 onward. There also appears to be aggradation in 2005, downstream of the Arroyo de las Cañas (around SO-1395). This was a wet water year. A contributor would be the sediment from arroyos within the reach, being mobilized and deposited.

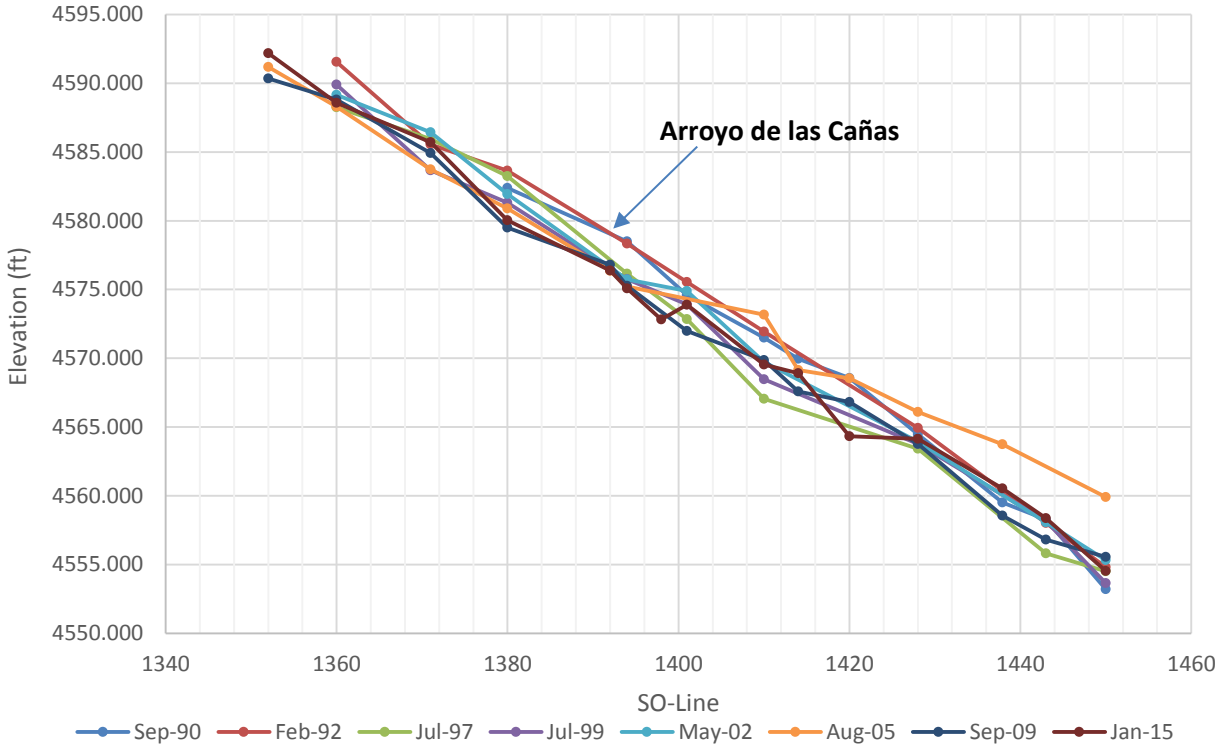

Figure 41 Thalweg elevation for SO lines within the study area. Elevations collected by cross section measurement.

The deepest part of each SO line can be plotted to create a downstream bed profile, as graphically shown in Figure 41 and 42. What is apparent in both Figure 41 and 42 is that the channel is still undergoing bed elevation change below Arroyo de las Cañas. Especially below SO-1394, where the most variation occurs across the years. At this location aggradation and degradation events affect the thalweg elevation by up to 3 feet over the course of five years. In another representation (Figure 42) it is apparent that the Rio Grande has aggraded below the Arroyo de las Cañas, when compared to an aggrading period between 1990 and 2005.

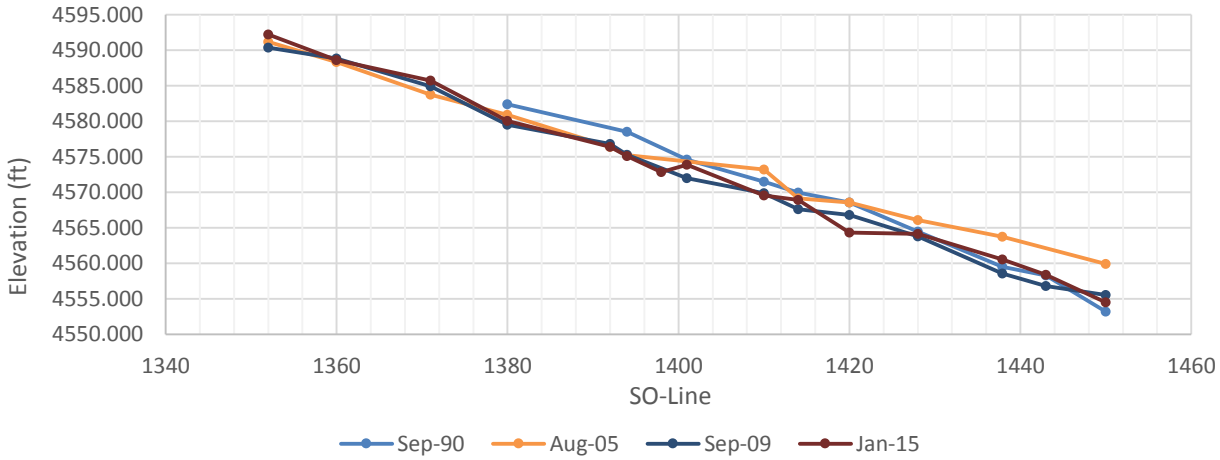

Figure 42 Thalweg elevation of SO lines within the study area in 1990, 2005, 2009 and 2015.

3.4 Channel Sinuosity

There are several river maintenance figures covering the valley length and river length within the study area. Combined in Figure 43 are two lines from Reclamation River maintenance figures: San Acacia Diversion Dam (agg-deg 1206) to below Arroyo de la Cañas (agg-deg 1397); Below Arroyo de las Cañas to San Antonio (agg-deg 1474); and one line from hydraulic modeling analysis conducted by Larsen et al. in 2011. Sub reach 2 in this report covers the Rio Grande from agg-deg 1364 to agg-deg 1454. The data was updated to include observations in 2012. The channel sinuosity was measured by observing aerial photography and using the ArcGIS measure tool. The valley length for all of these was based on the lengths river maintenance figure. It was found that the sinuosity of the channel has generally been decreasing over the period of record, though there was an increase from 1985 to around 2006 (Figure 43). This period coincides with Elephant Butte being full (1985-2000) and the period after clearing and mowing in the flood plain (1955-1985); the period of increasing sinuosity coincides with the end of the wet period in 2006.

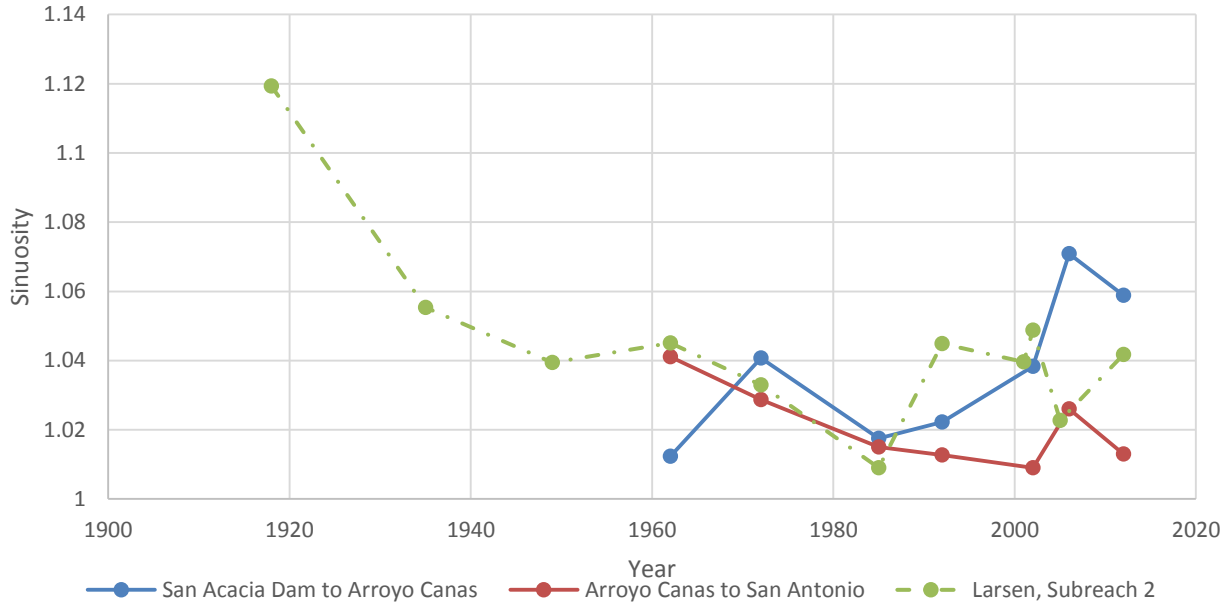

Figure 43 Reach Average Channel Sinuosity, modified from Larsen et al. 2011

Table 11 Profiles evaluated for Sinuosity analysis.

	Agg-deg	Valley Length
San Acacia Dam to Arroyo Cañas	1206 to 1397	Average 501 ft between each agg-deg
Arroyo Cañas to San Antonio	1398 to 1474	Average 490 ft between each agg-deg
Sub reach 2 (Larsen et al. 2011)	1364 to 1454	Average 480 ft between each agg-deg

3.5 Bed Material Size and Type

3.5.1 Median Bed Sizes over Time

Bed material size was addressed briefly in the suspended sediment section. Here the data at USGS gages in San Acacia (USGS 08354900) and San Marcial (USGS 08358400) was combined with field measurements conducted by Reclamation (MEI 2002, Massong 2006).

From 2002 onward, the grain size of the bed material from San Acacia was greater than that at San Marcial. The trend was generally decreasing grain size for downstream bed sediment samples. Before 2002, the grain sizes were similar between San Acacia and San Marcial. Data shows that the median grain size above the confluence of the Arroyo de las Cañas (agg-deg 1374) was greater than at San Acacia. From intermediate measurements of cross sections between the two USGS gages, median grain size generally decrease in the downstream direction. Reclamation field measurements may not fully characterize the bed material size as they were not taken as frequently as the USGS gages at San Acacia and San Marcial.

Table 12 Median grain sizes (mm) for bed material on the Rio Grande within the study area. ND. Refers to no data. USGS was not evaluated for 2016, as the year is incomplete at the time of this writing.

Location (Data Source)	*1992*	*1996*	*1999*	*2002*	*2006*	*2009*	*2014*	*2016*
San Acacia (near SO-1187)	0.2*	0.3*	0.31*	0.38*	0.36*	0.45*	0.52*	--
SO-1371	ND.	0.33†	0.34†	ND.	ND.	ND.	ND.	0.35
SO-1374	ND.	ND.	ND.	0.3⁞	ND.	ND.	ND.	ND.
SO-1390 to 98	ND.	ND.	ND.	ND.	0.27†	0.4†	0.3†	0.40
SO-1414	0.25†	0.23†	0.25†	0.3†	ND.	ND.	ND.	0.39
San Marcial near SO-1701)	0.19*	0.28*	0.31*	0.24*	0.22*	0.23*	0.25*	--

** USGS data; † Massong 2006;⁞ MEI 2002; 2016 data was collected for this report, refer to the appendix.*

The grain size measurements within the reach were averaged and plotted in Figure 44 below against San Marcial and San Acacia measurements. Generally the median grain size through the study reach is greater than San Marcial since 2002. The median San Acacia grain size has increased over time. The median grain size was fairly uniform among the samples up to 1999.

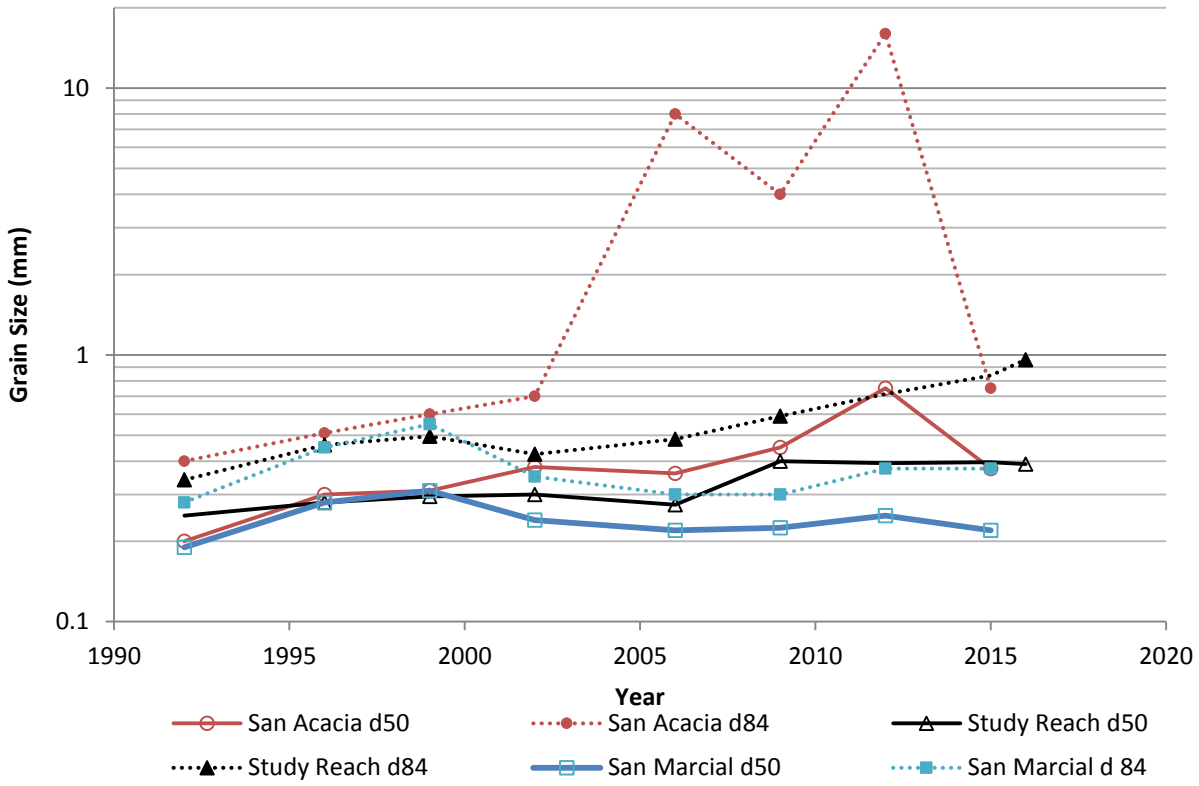

Figure 44 Bed material grain sizes for the Rio Grande study reach.

For the 84th percentile, the grain size at San Acacia was consistently larger than that at San Marcial. The D_{84} size range has been steadily increasing until present, with an exception for agg-degs below Arroyo de las Cañas in 1999. The SO-1371 grain sizes are slightly larger than that of San Acacia for the two data points that are available, but the data collection in 2016 indicated that the median grain size is smaller than previously measured. The study reach showed that San Acacia has experienced a larger gain in grain size than in locations downstream in the study reach..

Table 13 The 84 percentile grain size (mm) for bed material on the Rio Grande within the study area. ND. indicates no data. Asterisk indicates that the diameter was greater than the sieve size measured. USGS was not evaluated for 2016, as the year is incomplete at the time of this writing.

Location (Data Source)	*1992*	*1995*	*1996*	*1999*	*2002*	*2006*	*2009*	*2014*	*2016*
San Acacia (USGS, near SO-1187)	0.4	0.4	0.51	0.6	0.7	8	4	16*	--
SO-1371 (Reclamation)	ND.	ND.	0.53	0.64	ND.	ND.	ND.	ND.	0.49
SO-1374 (MEI 2002)	ND.	ND.	ND.	ND.	0.4	ND.	ND.	ND.	ND.
SO-1390 to 98 (Reclamation)	ND.	ND.	ND.	ND.	ND.	0.48	0.59	ND.	10.58
SO-1414 (Reclamation)	0.34	0.38	0.39	0.35	0.45	ND.	ND.	ND.	0.96
San Marcial (USGS, near SO-1701)	0.28	0.38	0.45	0.55	0.35	0.3	0.3	0.4	--

There were bed samples taken from the Arroyo de las Cañas in two locations in 2015, and the confluence grain size was measured in 2016. The grain size analysis showed a coarsening of bed material from the headwaters of the arroyo to the confluence. Grain sizes were much larger than those identified at San Marcial (USGS 08358400) and San Acacia (USGS 08354900) gages that year.

Table 14 Grain sizes from field measurements on the Arroyo de las Cañas in 2015 (AuBuchon). Asterisk indicates that the diameter was greater than the sieve size measured.

	Arr. de las Cañas, Near Bosquecito Road 4/3/2015	*Arr. de las Cañas, near the Rio Grande Confluence 4/3/2015*	*Arr. De las Cañas, near the Rio Grande Confluence 6/30/2016*
D_{50}	5.2	11.3	13.59
D_{84}	29.7	50.80*	53

3.5.2 Bed Particle Stability

HEC-RAS was used to estimate the normal shear stresses at different discharges by 1,000 cfs increments up to 10,000 cfs. The hydraulic radius and the reach slope were used to estimate that normal shear stress at each cross section and discharge using Equation 1.

$$\tau_o = \gamma R s \quad (1)$$

Where τ_o = normal shear stress, γ is the specific gravity, R is the hydraulic radius, s is slope.

The critical shear for incipient motion was estimated for the d50 and d84 particle sizes in the study reach using Yang's approach (1996), where a minimum stable particle size was calculated based on an empirical equation that incorporates the HEC-RAS estimation of shear stress at a particular discharge and cross-section, the bed material type, the weight of sediment and the moving fluid (Equation 2).

$$d = \frac{\tau_o}{C(\gamma_s - \gamma_f)} \quad (2)$$

Where d = critical particle diameter; τ_o = normal shear stress at Q_i; C = an empirical constant related to bed material type (0.03 was used, representing sandy bed material); γ_s, γ_f = specific weights of sediment and fluid, respectively. It was assumed that the sediment specific gravity was 2.65.

The results from critical shear stress calculations are shown in Figure 45; these were based on particle sizes of 1 mm, 5 mm, and 10 mm. It was found that the critical shear for 0.25 mm and 0.5 mm diameter particles would not be stable at any cross section. These two sizes correspond to the d50 and d84 found at bed material samples within the reach. The larger sizes represent the mean bed particle size found at the Arroyo de las Cañas confluence.

At 1 mm particle size, there were four instances within the study reach that the material could withstand the shear stress calculated from HEC-RAS hydraulic radius and slope at 100 cfs and for all other discharges would exceed the critical shear stress for particle stability. These cross-sections are located in straight regions of the study area, before bends. At 5 mm, or what would be the median grain size that would be contributed from the arroyo, it was found to be stable at

flows up to 1,000 cfs in some locations (agg-deg 1444 and 1454). The 5 mm particle size was stable at 100 cfs at most agg-deg locations,

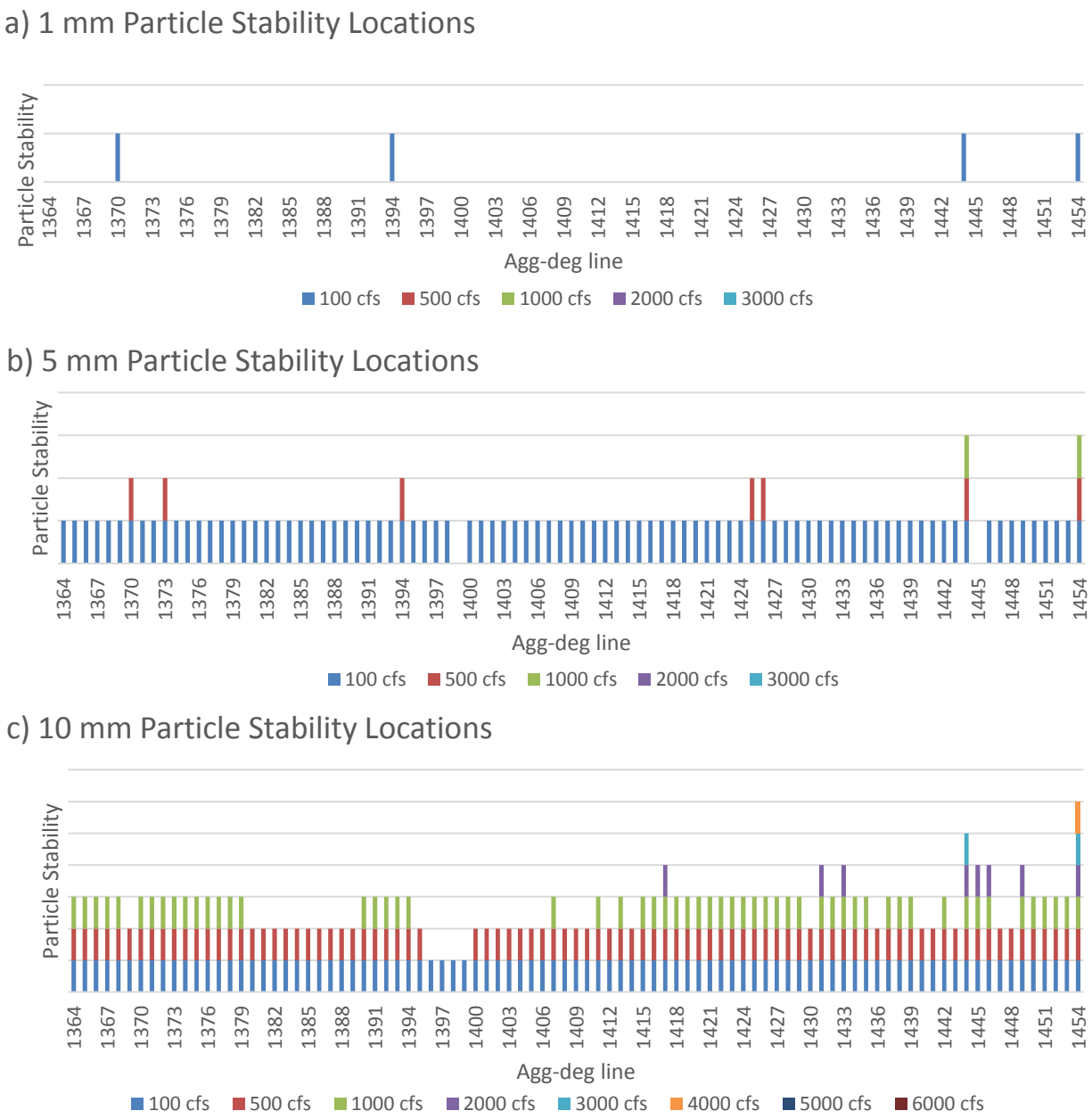

Figure 45 Particle stability for agg-deg lines in the study reach, per discharge at a) 1 mm particle size, b) 5 mm, c) 10 mm particle size.

Figure 45 shows a tick-mark for discharges at which the particle size indicated will be stable. The particle sizes used are based on bed material sizes found within the bed of the Arroyo de las Cañas. If sediment is transported into the Rio Grande, it is evident that the particles may be stable at the arroyo's confluence at low flows. For example, at agg-deg 1394, the 1 mm particle would be stable at 100 cfs, but not at 500 cfs; the 5 mm particle would be stable at 100 and 500 cfs, but not at 1,000 cfs; the 10mm particle would be stable at 100, 500 and 1,000 cfs, but not at

greater discharge rates. The stability of particles at agg-deg 1454 may not be accurate, because this is the boundary location of the HEC-RAS model, and may not accurately represent shear forces in the river at this location.

3.6 Channel Floodplain Topography

3.6.1 Hydrographic Cross Section Comparison

Data from field cross-section measurements were compared at SO-lines 1360, 1380, 1394, 1414, and 1443 (see Figure 46 for location information). The years 1992, 2005 and 2013 were generally available for all of these cross sections. Left end point (LEP), when provided, was used as the origin (X=0) station location. In one instance, the LEP had a different Northing and Easting than other years. If Northing and Easting were not available to confirm the location of the LEP, then the data was phase shifted so that levees or higher elevation points, assumed to be fixed, were aligned. For data from 1992, the elevation was changed so that it conformed to the NADV88 datum. Plots of the available data are shown in Figure 47.

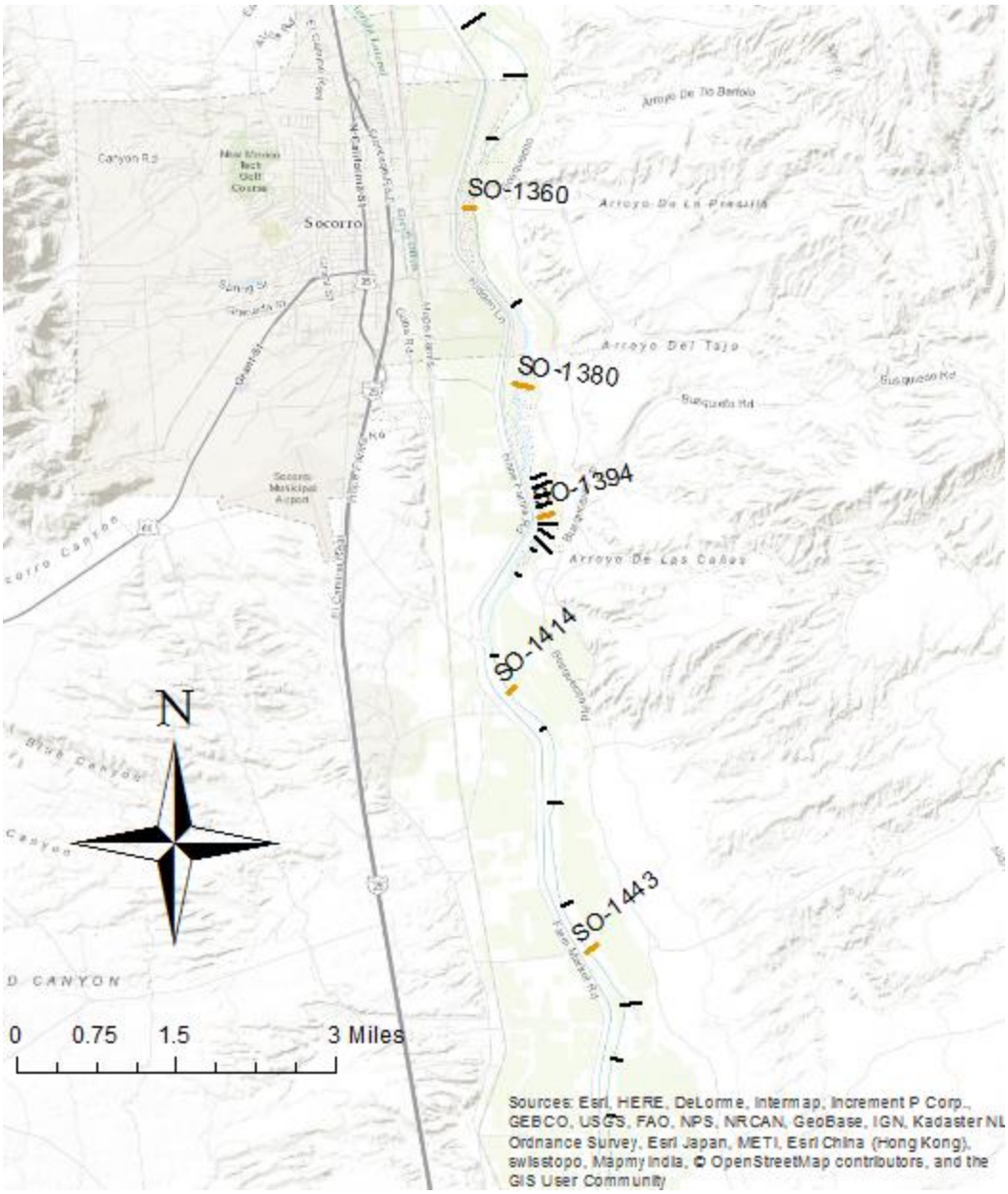

Figure 46 Range lines included in the cross section analysis.

At SO-1360 and SO-1443, it is apparent that the thalweg has shifted to opposite banks, as visualized by the aggradation where the previous channel had been and the degradation to indicate the new channel. The other channels indicate degradation since 1992, with the channel narrowing and becoming more incised by 2 to 4 feet between 1992 and 2013. A description of the changes in the cross section over time can be found in Table 14.

Table 15 Narrative of Cross-section survey comparisons within the study area in 1992, 2005 and 2013.

	1992	*2005*	*2013*
SO-1360	~ 150 foot channel with a low floodplain, 2-3 feet above channel bottom.	Channel narrowing (now about 100 feet) and deepening (~ 3 feet deeper than 1992), Channel moved to river right. Bar is forming on river left, filling in 2-3 feet over old channel bottom.	Channel widened back out to around 150 feet. Channel depth has not changed since 2005. Bar on river left has accreted around 1-2 feet more.
SO-1380	~200 foot channel with low floodplain (~1 foot from channel bottom). Channel is not well defined.	Channel shifted to river right. Channel is defined and about ~250 feet wide. Channel has deepened~ 3 feet from 1992 with a floodplain that is now 4-5 feet above the channel bottom.	Channel has filled in on river left and right, decreasing the channel width to about 125 feet. Bar on river left is about 3 feet above the river bottom. Channel depth has not changed significantly since 2005.
SO-1394	~260 foot channel with low floodplain (~2 foot from channel bottom). Channel is not well defined.	Formation of a side channel on river right. Side channel is 2.5 feet deeper than the channel in 1992 and is narrowed to ~100 feet.	Channel is ~300 feet wide, shifted further to the river right by about 40 feet. As deep as in 2005, more uniform channel bottom.
SO-1414	Channel is 2-3 feet deep, ~220 feet wide, and more defined than upstream cross sections.	Channel depth has become more uniform and deeper, about 3 to 4 feet in depth. Channel is about 6 feet narrower, from the river right side.	Channel thalweg has shifted about 90 feet to the right, the channel is 3 to 6 feet deep. Channel banks have narrowed by 10 feet on the river right side.
SO-1443	Channel is not well defined. Floodplain is 3 feet above the channel thalweg.	Channel thalweg shifts river right, and becomes defined from the flood plain. Channel is 3 feet deep, and has a uniform bottom ~200 feet wide.	Channel shifts further to the river right. Thalweg is defined from the channel bottom. Main channel has narrowed ~50 ft.

a) SO-1360

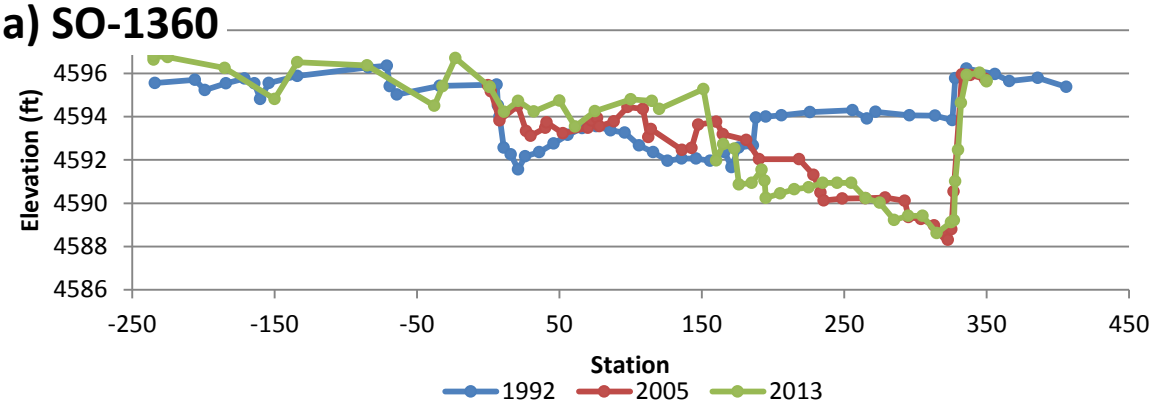

b) SO-1380

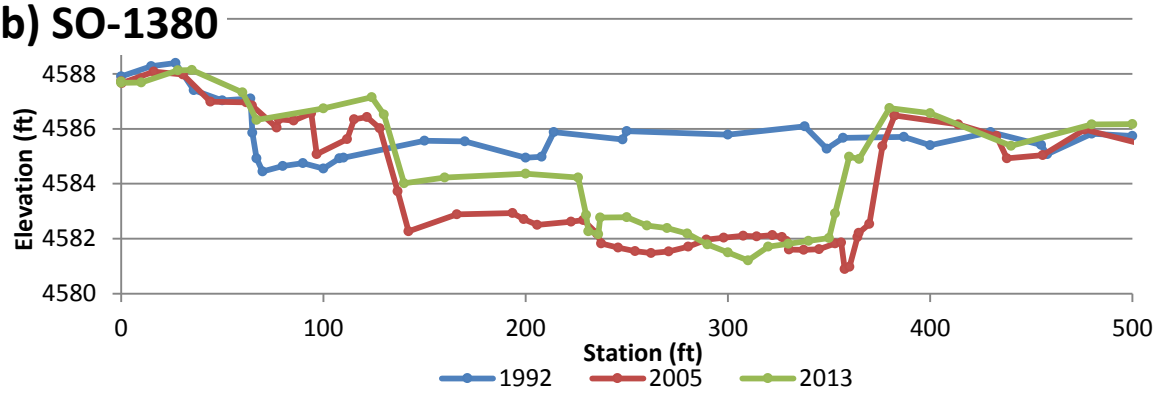

c) SO-1394

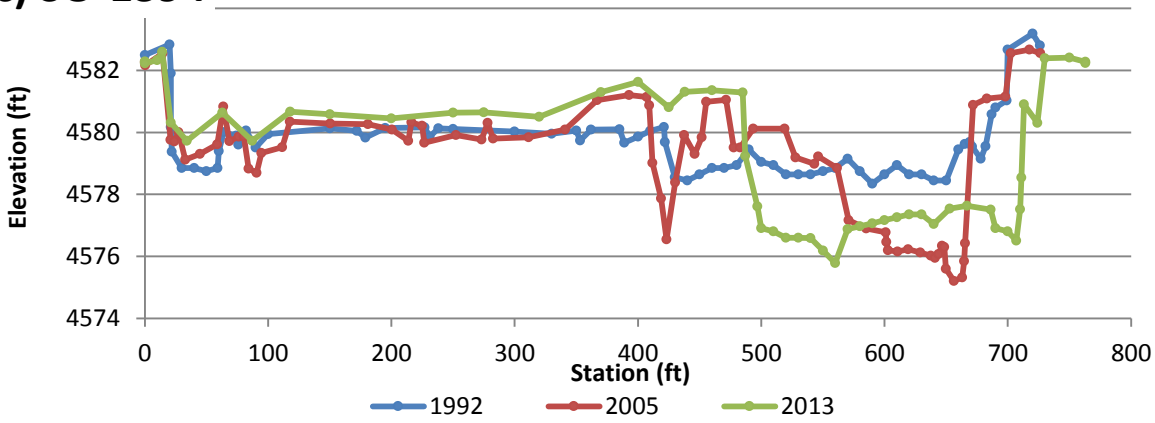

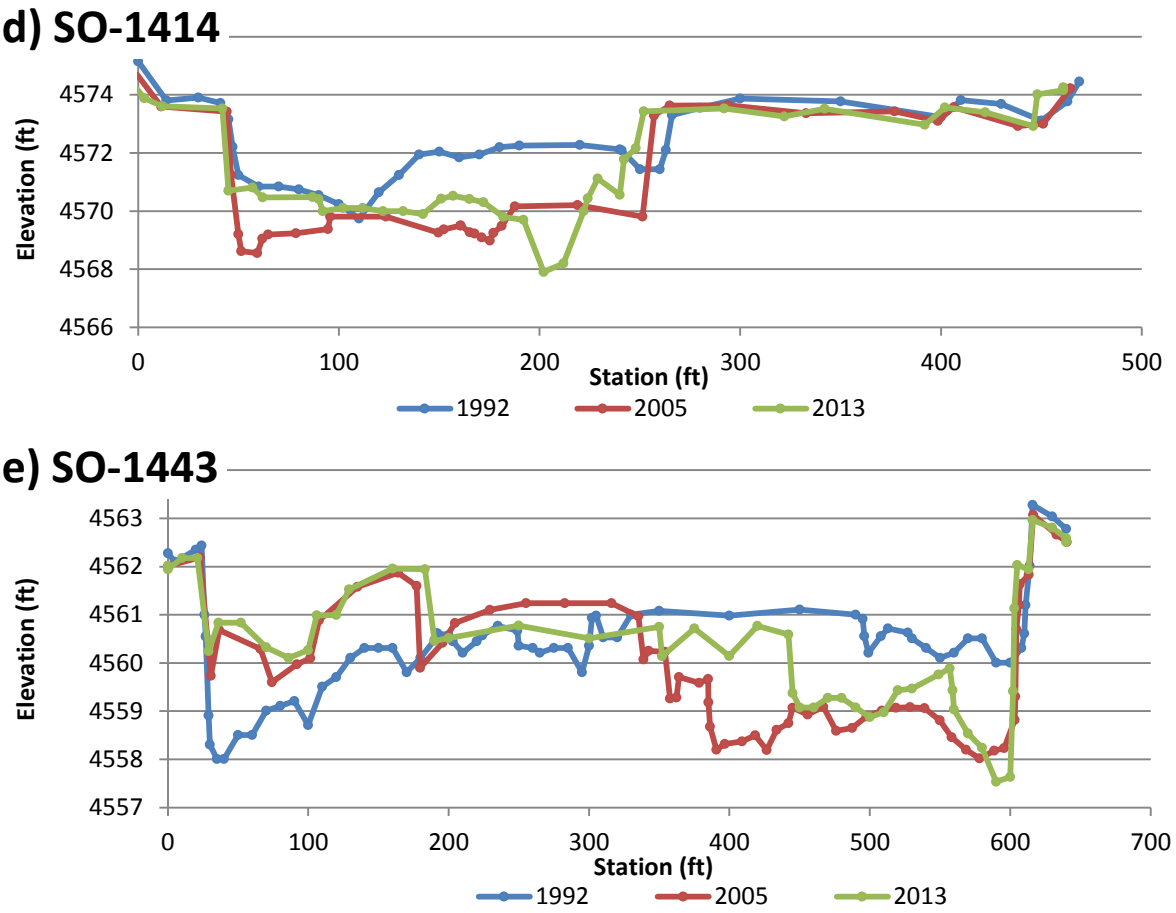

Figure 47 Cross section survey for 1992, 2005 and 2013 within the study area at a) SO-1360, b) SO-1380, c) SO-1394, d) SO-1414, and e) SO-1443.

3.6.2 Reach-Average Channel Geometry

Overall channel characteristics were estimated using HEC-RAS models. The HEC-RAS models were run at a steady state 5,000 cfs discharge for each agg-deg collection year. Channel geometry parameters were collected for each year at the agg-deg line, with results weighted by channel length between the lines for a reach average. Again, a limitation in this analysis is that for these years the distances between the agg-deg lines were the same in the HEC-RAS model which may not reflect reality. The results for each year are presented in a box-and-whisker plot, demonstrating the distribution of the cross sections. The whiskers represent the maximum and minimum values; edges of the boxes indicate the first 25th percentile, the median, and the 75th percentile from top to bottom (Figure 48).

The wetted area and the wetted perimeter generally increased over the years, though the maximum was still significantly larger than the median. The wetted perimeter decreased between 2002 and 2012. The most variance occurred in 1972 for these two parameters. Alternatively, the hydraulic radius, which is the area over perimeter, generally stayed the same. Maximum depth generally decreases, with an exception between 1962 to 1972 and 2002 to 2012, where the depth

increased. This confirms that the channel is becoming more uniform in depth, as wetted area increases and the maximum depth decreases. The average velocity has been decreasing slightly since 1972, and the variance is decreasing as well. The width to depth ratio has been increasing and has had increasing variance and extremes of the maximum ratio outliers. This trend did not continue in 2012, with a decreasing width to depth ratio. The Froude number is generally decreasing indicating that channel flow is increasingly subcritical, where flow is slow and stable.

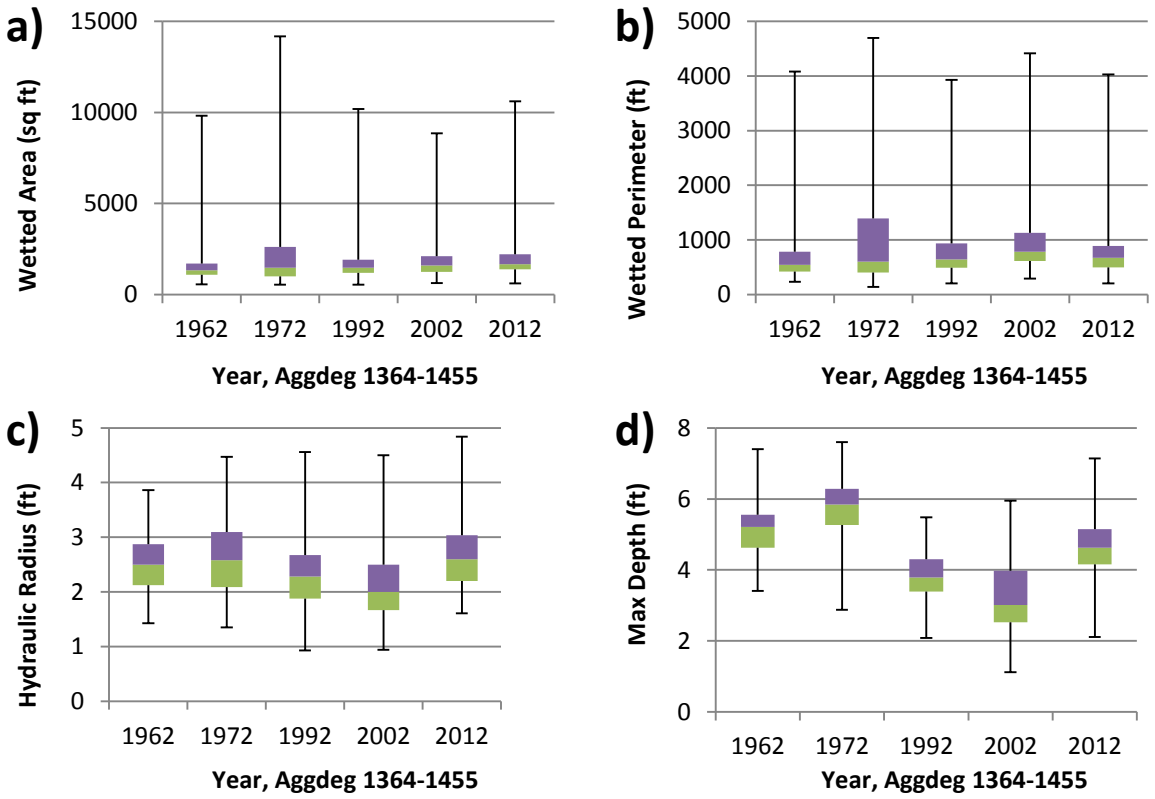

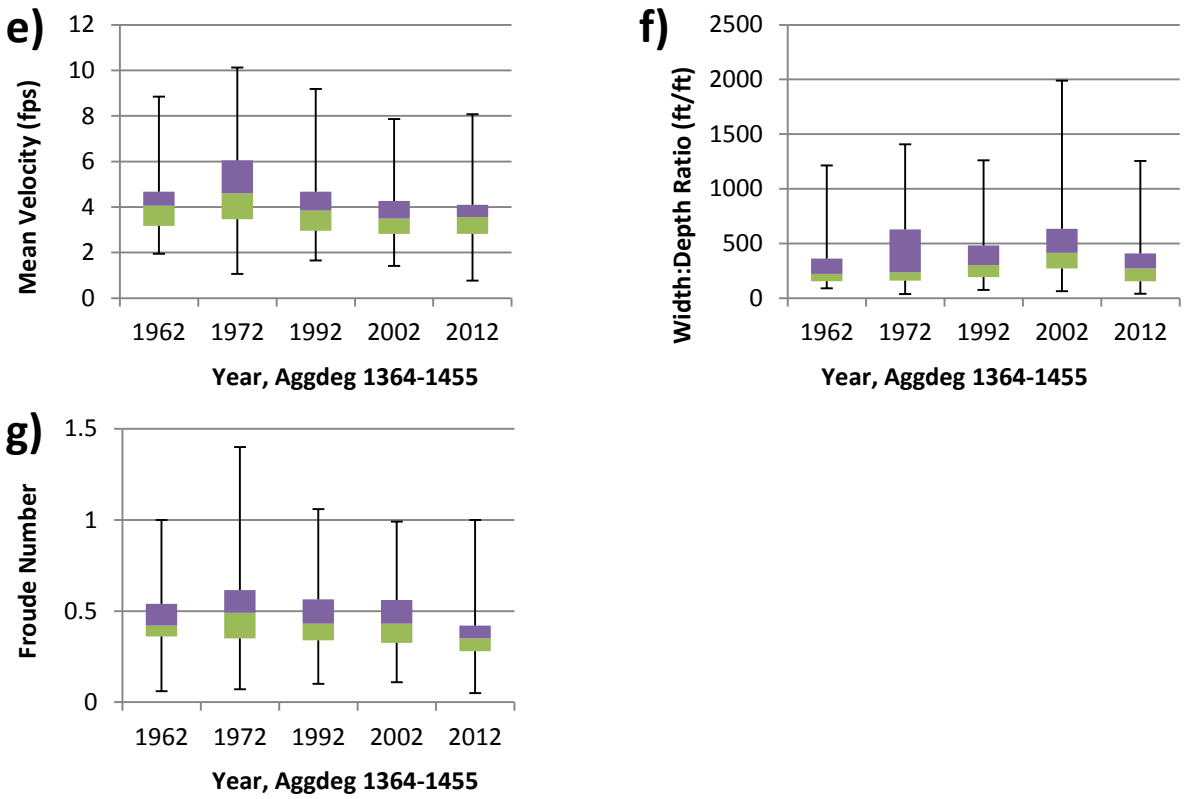

Figure 48 Channel geometry parameters which are weight-distance -averaged for HEC-RAS models of the study area from 1962 to 2012.

Table 16 Distance weighted average of channel geometry parameters based on HEC-RAS models of the study area from 1962 to 2012.

	1962	*1972*	*1992*	*2002*	*2012*
Wetted area (ft^2)	1700	2600	1700	2000	2000
Wetted perimeter (ft)	690	970	760	950	800
Hydraulic radius (ft)	2.5	2.7	2.4	2.2	2.7
Max depth (ft)	5.1	5.8	3.9	3.3	4.7
Mean velocity (ft/s)	4.1	4.8	4.0	3.7	3.5
Width/Depth (ft/ft)	300	390	360	500	330
Froude number	0.5	0.5	0.5	0.4	0.4

3.6.3 Terrace Mapping

Terraces are low-lying, flat areas of abandoned active channels and floodplains. At times, these prove to be optimal areas for habitat restoration and flood control. A raster was created from 2012 LiDAR elevation data. HEC-GeoRAS was used to generate a raster of the water surface elevation from a 500 cfs discharge simulation on the HEC-RAS model. The two rasters were subtracted using ArcGIS Raster Math tool to create a height differential raster. Then, general terraces or flat areas, where the slope was less than 0.5 degrees, were identified from the ArcGIS Slope 3D Analysis tool. Flat areas and the height differential layer were combined to identify the terraces as shown in Figures 49 and 50. The data was validated by extracting certain agg-deg lines, and comparing the height differential to the HEC-RAS results.

It was found that above the Arroyo de las Cañas, the terraces are generally greater than two feet above the water surface elevation, while below Cañas there are wide floodplain areas on the eastern side of the Rio Grande that are two feet or less.

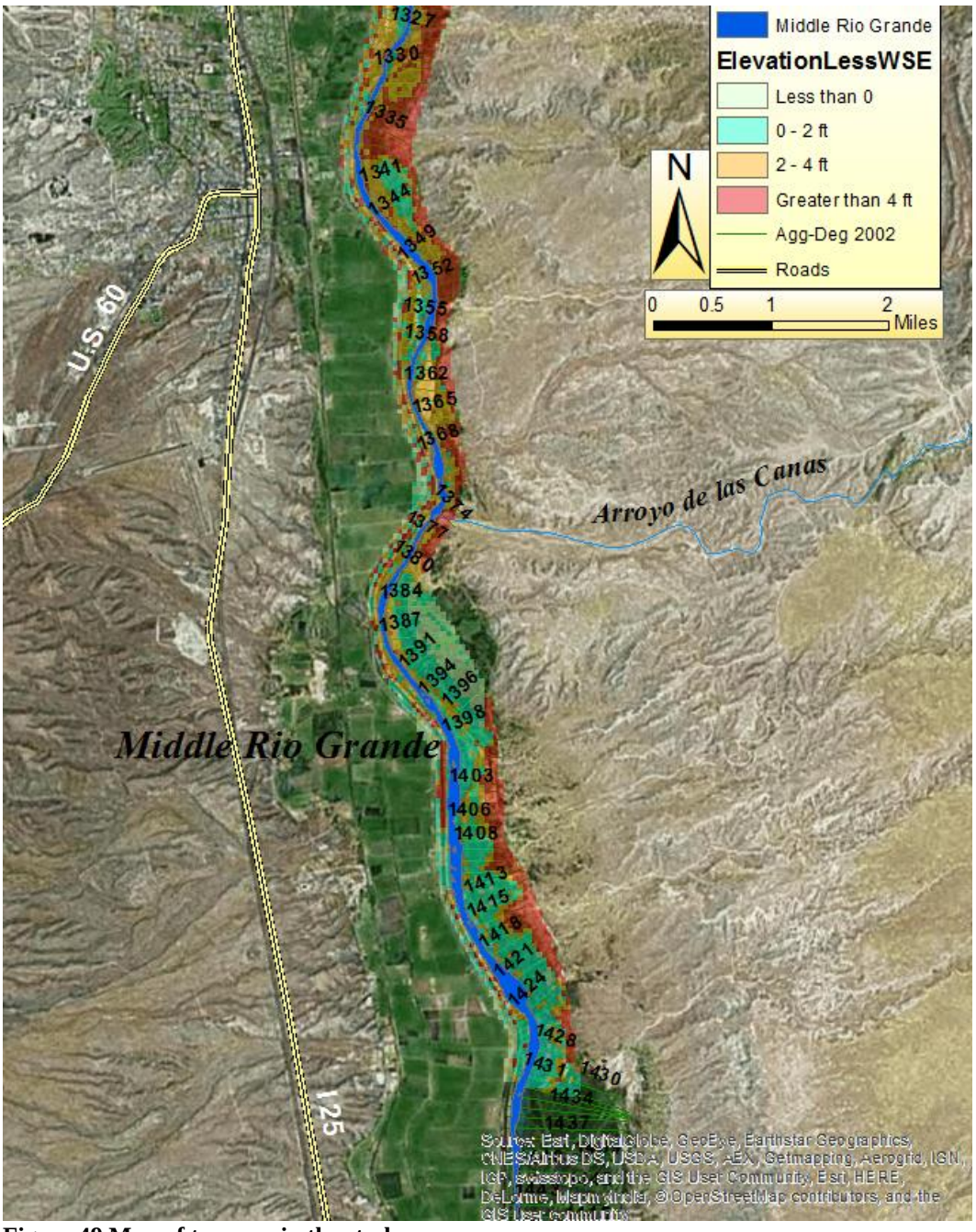

Figure 49 Map of terraces in the study area.

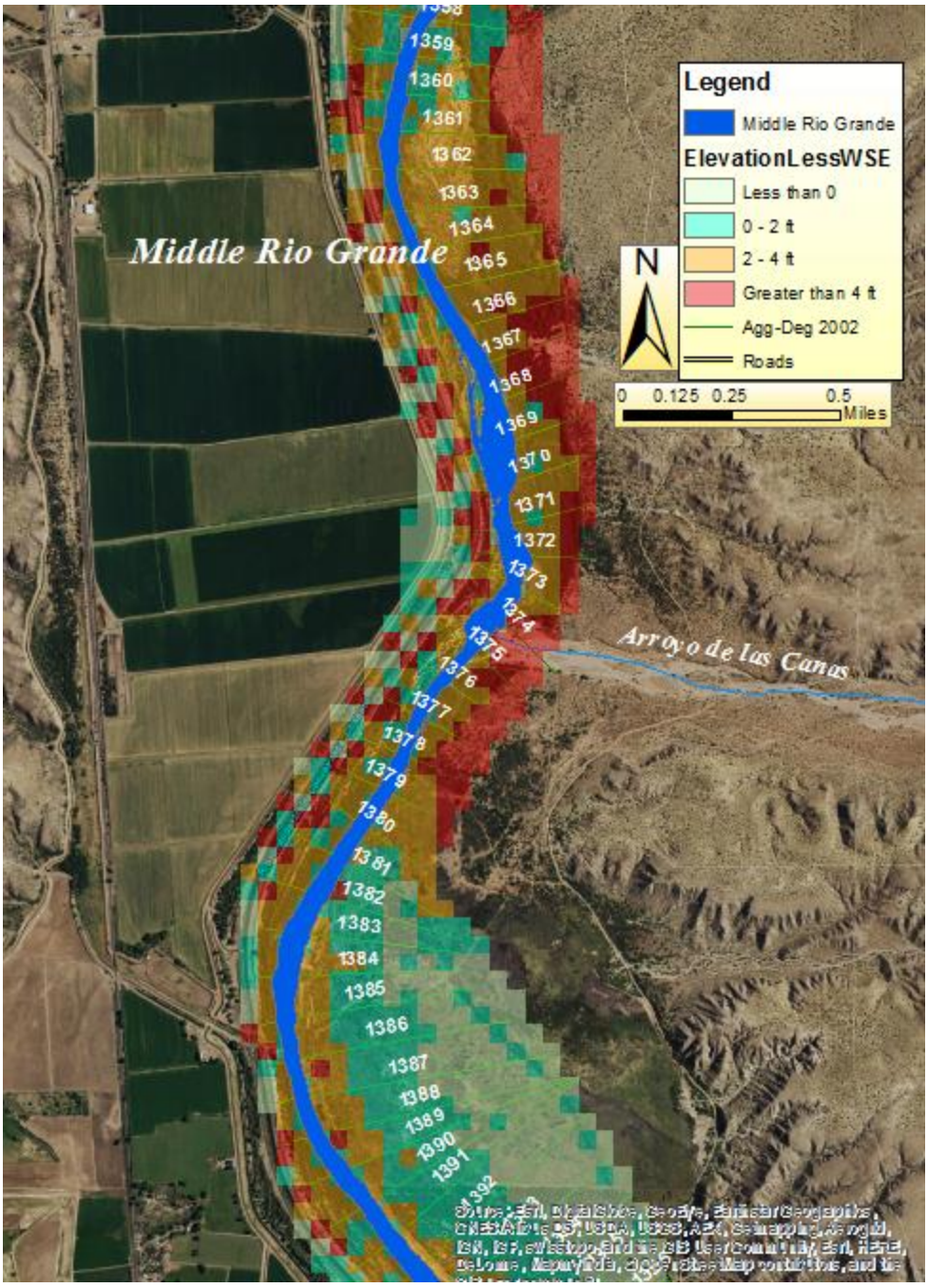

Figure 50 Terraces surrounding the Arroyo de las Cañas confluence.

3.6.4 Top Width Variation

The top width of the agg-deg lines within the study reach was recorded for various river discharges and then compared over time (Figure 51). It was found that the river width upstream of the Arroyo de las Cañas does not overbank at higher flows as much as it had in previous years, possibly because of the terraces identified in the previous section. Downstream from the Arroyo de las Cañas confluence, around agg-deg 1403 to 1420 and agg-deg 1427 to agg-deg 1450, 1972 and 2012 showed a greater number of instances of overbanking at around 5000 cfs. The extent of overbanking at very high flows (17,800 cfs) has not changed greatly over the study period.

a)1962

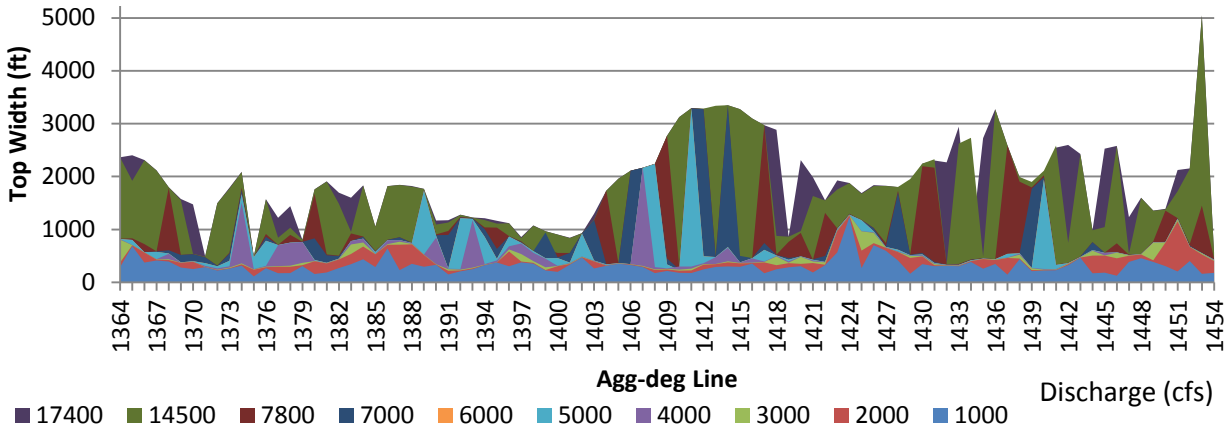

b)1972

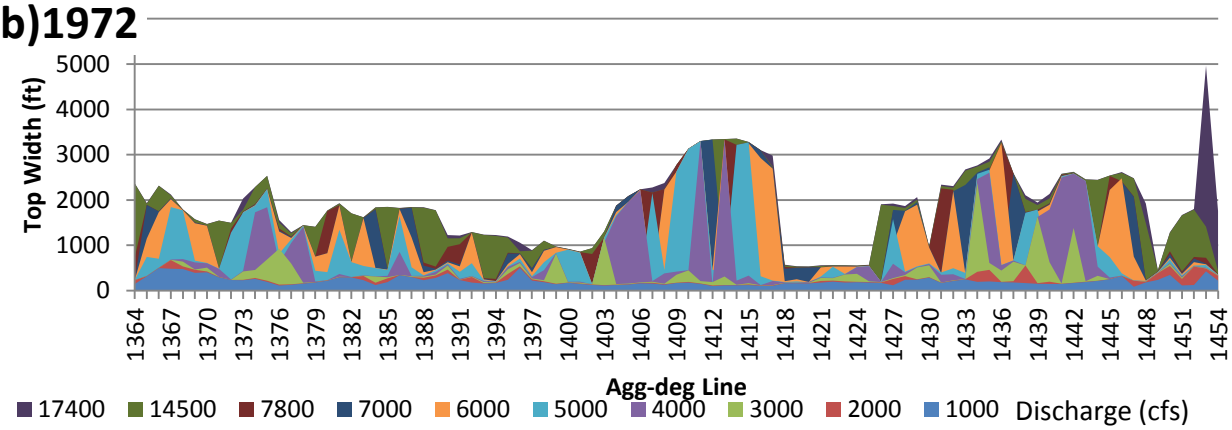

c)1992

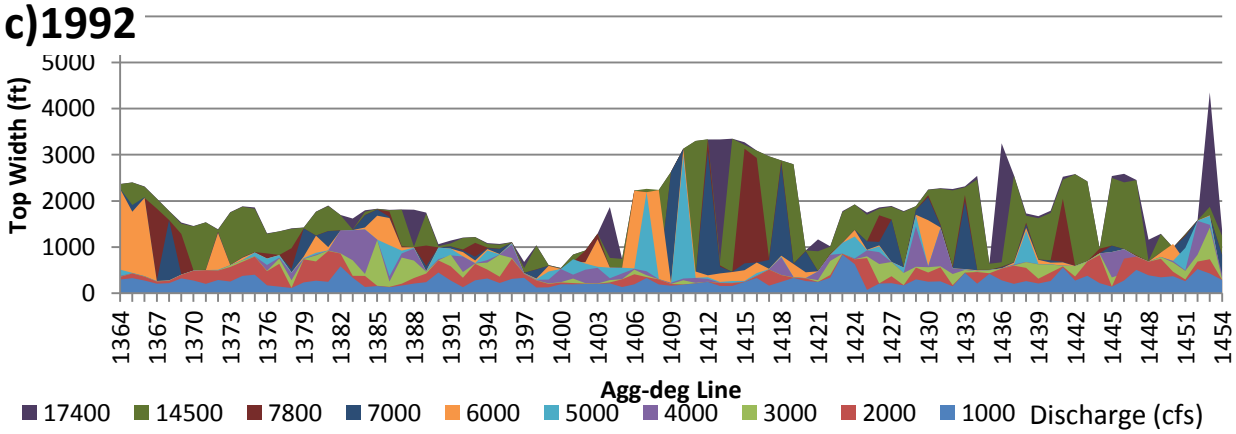

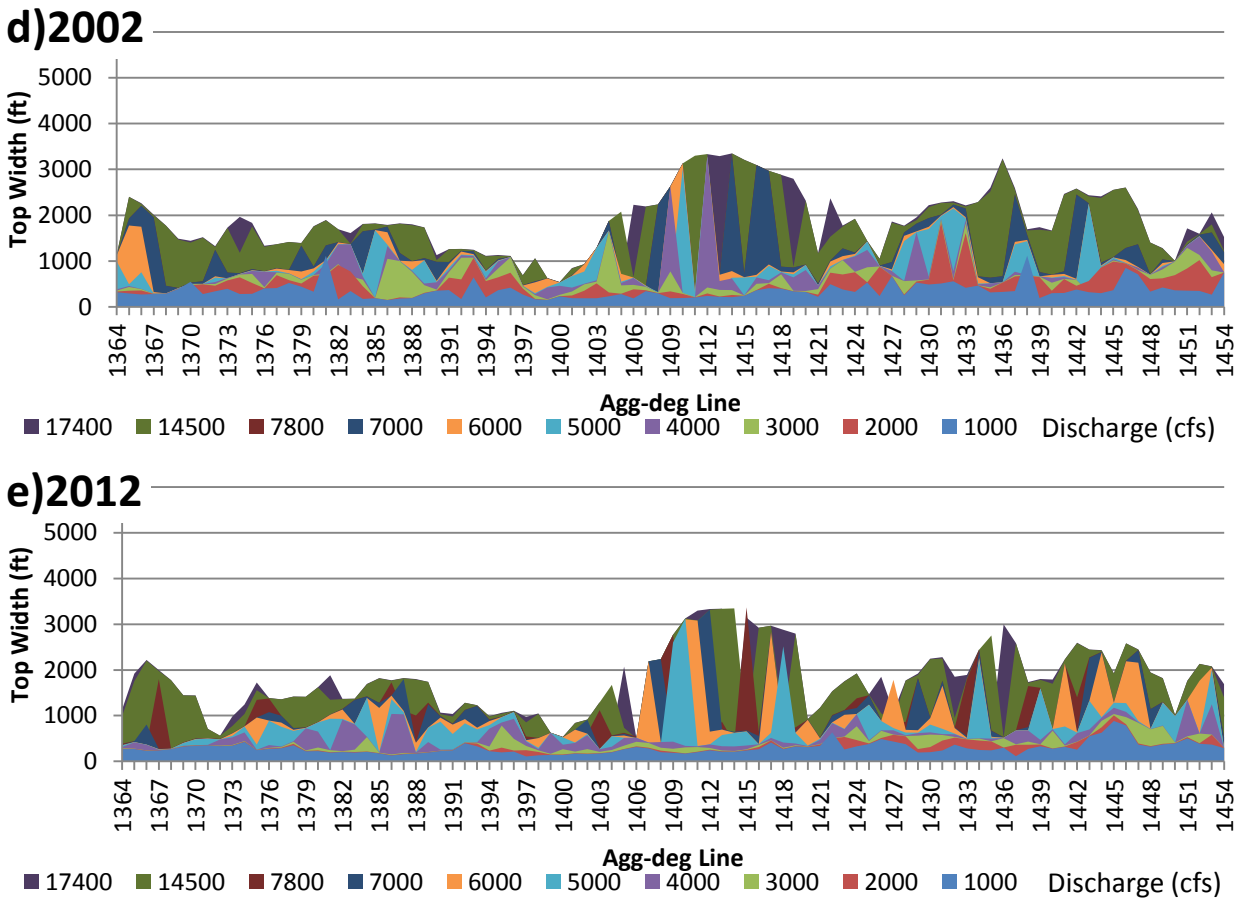

Figure 51 Channel top widths within the study area over various discharges in a) 1962, b) 1972, c) 1992, d) 2002 and e) 2012.

As indicated before, within this study reach: 1,000 cfs increments were used up to 7,000 cfs; 4,000 cfs corresponds nearly to the annual flood rate (Bui, 2014); 7,800 cfs most nearly corresponds to a 2 year flood frequency according to Wright (2010), or a 10 year return frequency according to data analyzed in MEI (2002); 17,400 corresponds with the frequency of ten year floods according to Wright (2010).

A distance-weighted top width was calculated based on the HEC-RAS geometry results. The levees were drawn in HEC-RAS to constrain flow to the channel or any higher elevation regions that would constrain flow in reality. The flow would be split into two channels if the two thalwegs were at similar depth, otherwise the higher elevation channel would be simulated to have no flow when the water surface elevation was less than the channel bank elevation. HEC-RAS has a table tool that records the wetted top width at every cross section. The average was weighted based on the length of the channel between HEC-RAS cross sections. The simulation results are summarized in Figure 52.

In 1972, inundation exceeded all other years starting at 4,000 cfs. In 2002, the channel top width was generally greater than in preceding years and 2012. In 2012, the channel top width was less than all other modeled years. This indicates that the channel is increasing in its capacity, but not by a great magnitude

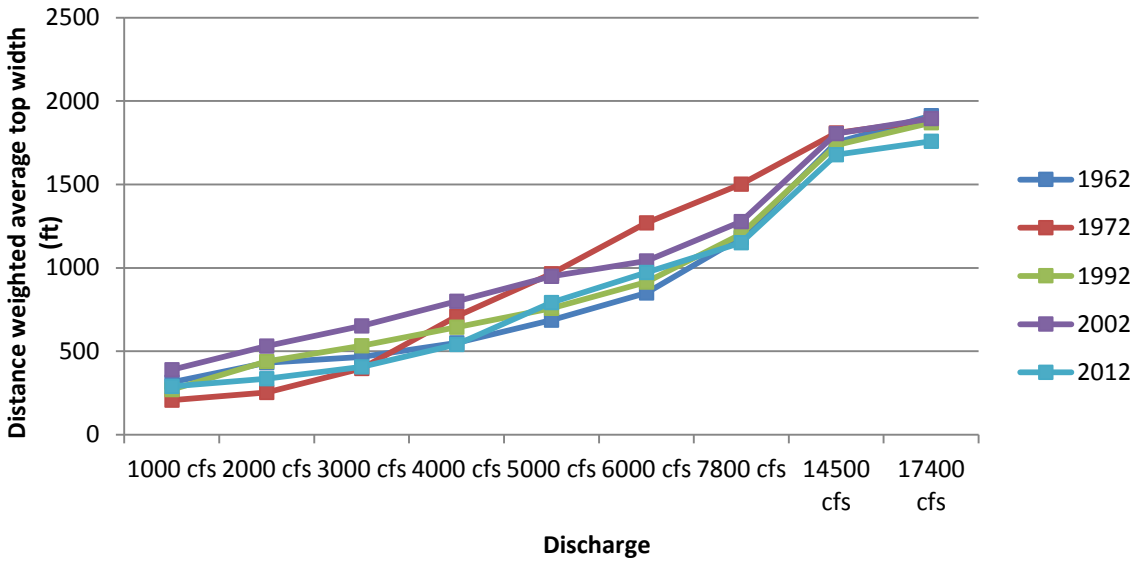

Figure 52 Average top width for the study areas under different discharge rates.

The increase in duration of flow in the Rio Grande and general narrowing of the channel confirms that the channel form will have a propensity to be sinuous. The ratio of the mean discharge and the peak discharge has decreased, so peak discharges are less likely to widen the channel (Knighton, 1998). Instead it would be expected that high flows would cause channel migration, with erosion where the channel meanders.

4.0 Future Channel Response

Using these observations of channel geometry, sediment transport patterns, and hydrologic drivers in the Rio Grande surrounding the Arroyo de las Cañas, several predictions can be made related to expected future channel response, given changes to system drivers. Lane (1954) outlines a general relationship with the sediment and water discharge loads on fluvial geomorphology. Assuming that a system gravitates towards equilibrium, one can make assumptions on the effects of the river system if one of the four variables below are adjusted:

$$Q_s d_{50} \propto Q_w S$$

Where Q_s is the quantity of sediment, d_{50} is the particle diameter, Q_w is the water discharge, and S is slope.

Schumm (1977) also discusses the metamorphosis of river morphology based on changing sediment and discharge loads. Treating sediment discharge and water discharge separately, Schumm identified riverine geometry characteristics that are affected by each.

$$Q_w \approx \frac{b,d,\lambda}{S} \quad \text{and} \quad Q_s \approx \frac{b,\lambda,S}{d,P}$$

Where b is width, d is depth, λ is meander wavelength, S is slope, and P is sinuosity.

Both Schumm's and Lane's relationships are applied in predicting general trends for a river system, and explaining future channel responses due to current trends observed on the Middle Rio Grande, as discussed previously in this paper and shown graphically in Figure 53 and Figure 54.

$$Q_s \downarrow \quad S \downarrow \quad d_{50} \uparrow \quad Q_w(low) \uparrow \quad Q_w(high) \downarrow \quad b \downarrow \quad d \uparrow \quad \lambda \downarrow \quad P \uparrow$$

Figure 53. Current trends in geomorphic drivers and parameters upstream of the Arroyo de las Cañas

$$Q_s \downarrow \quad S \uparrow \quad d_{50} \uparrow \quad Q_w(low) \uparrow \quad Q_w(high) \downarrow \quad \boldsymbol{b} \downarrow \quad \boldsymbol{d} \downarrow \quad \lambda \downarrow \quad \boldsymbol{P} \downarrow$$

Figure 54. Current trends in geomorphic drivers and parameters changes downstream of the Arroyo de las Cañas

General riverine trends suggested by these relationships for a channel in equilibrium can be made for both the cases of a reduction in the sediment and water discharge loads, as observed on the Middle Rio Grande. Given a reduction in the sediment discharge load (and constant water discharge load) the relationship proposed by Lane and Schumm would suggest the following: channel width decrease, meander wavelength decrease, slope decrease, depth increase, sinuosity increase, and bed material increase. A reduction in the water discharge load (with constant sediment discharge load) would indicate the following changes: channel width decrease, meander wavelength decrease, slope increase, and bed material decrease.

In comparing these theoretical river responses to observations of the Middle Rio Grande (as shown in Figure 53 and Figure 54) it can be seen that that observed geomorphic parameter trends reflect components of both a reduction in the water and sediment discharge loads. For example, the width (b) and meander wavelength (λ) were observed to decrease through the entire Cañas reach of the Rio Grande, an observation that meshes well with both the theoretical trends of a reduction in water and sediment discharge load. The decrease in the high flows and increase in the low flows also indicates that the ratio of peak flow to mean flow is decreasing. Knighton (1998) observed that the larger the ratio of peak flow to mean flow, the larger variation in active channel width. This observation of more uniformity of channel width has also been observed within this reach of the Rio Grande.

Changes in the depth (d), sinuosity (P), and slope (S) are different upstream and downstream of the Arroyo de las Cañas. Upstream the observed trends mesh well with the theoretical trend of a reduction in the sediment discharge load. The opposite trends for depth, sinuosity, and slope are observed downstream of the Arroyo de las Cañas, which may indicate more of an effect from the water discharge load reduction or an increase in the sediment discharge load. Observations that the suspended sediment load is greater at San Acacia (USGS 08354900) than San Marcial (USGS 08358400) suggest an accumulation of sediment between the two gaging stations, which may create a local increase in the sediment discharge load.

Another strong trend observed on the Rio Grande through this reach is the coarsening of the bed material. This trend is observed both upstream and downstream of the Arroyo de las Cañas and is similar to the theoretical trend expected from a reduction in the sediment discharge load or an increase in the water discharge load. At first, the observations of a decrease in the flow discharge

would seem to contradict this trend, since it would be expected that bed material should be fining from the theoretical trend for a reduction in water discharge load. If the relationships stated by Lane (1954) and Schumm (1977) are valid, then this contradiction suggests that either the sediment discharge load reduction is a considerably stronger trend than the water discharge load reduction or there is an increase in the water discharge load that can transport the available bed material.

Without some mechanical resetting of historic processes, it is estimated that the observed trends on the Middle Rio Grande will continue through this reach. If fluvial processes are able to remove established vegetation, sinuosity will also increase. As bed material coarsens the main channel may become stabilized, limiting the amount of channel widening that would occur if a large flow were to occur. Mechanical intervention could reset the connection of the channel to the floodplain through terrace lowering or streambed raising, with the latter more representative of the sediment reworking from a large flood event. A natural very large flood event is unlikely given current water operations on the Rio Grande. The reset would cause the active channel width to be temporarily increased, with a corresponding decrease in unit discharge per width. This may results in local fining of sediment and a decrease in the sediment load further downstream. The depth of the channel may also decrease as the potential for the river to return to a braided planform increases. These effects, however, would not be sustainable unless longer term changes in the sediment and water discharge loads were experienced. If eastern arroyos in the vicinity of the Arroyo de las Cañas are cleared of vegetation, allowing for a more direct route for floods entering the Rio Grande, sediment discharge loads may increase. If the load was of sufficient volume and frequency the Rio Grande planform may widen, become shallower, and potentially result in a braided channel planform.

References

AuBuchon, J. 2015. *Arroyo de las Canas April 2015 Site Visit – Trip Report*. U.S. Department of the Interior, Bureau of Reclamation, Upper Colorado Region, Albuquerque, NM. 48 pp.

Biedenharn, D.S. and Copeland, R.R.. 2000. *Effective Discharge Calculation. Technical Note,* US Army Corps of Engineers. Vicksburg, MS. 10 pp.

Brierley, G. and Fryirs, K., 2005. *Geomorphology and River Management: Applications of the River Styles Framework.* Blackwell Publications, Oxford, UK. 398 pp.

Bui, Chi, 2014. *Flow Duration Curve Analysis from Cochiti Dam to Elephant Butte Reservoir*, September 2014, Bureau of Reclamation , Albuquerque Area Office, Technical Services Division, Albuquerque, NM, 51p.

Bullard, K. and Lane, W., 1993. *Middle Rio Grande Peak Flow Frequency Study*, November 1993, Bureau of Reclamation, Technical Service Center, Flood Hydrology Group, Denver, CO, 235p.

Bullard, K., 2004. *Derivation of Middle Rio Grande Tributary Hydrographs*, U.S. Department of the Interior, Bureau of reclamation, Technical Services Center, Flood Hydrology Group. Denver, CO. 5p.

Knighton, D., 1998. *Fluvial Forms and Processes, a New Perspective.* Adjustment of Channel Form, p. 174.Oxford University Press.

Lane, E.W. 1954. *The Importance of Fluvial Morphology in Hydraulic Engineering*. Hydraulic Laboratory Report No. 372. Department of the Interior, Bureau of Reclamation, Engineering Laboratories, Denver, CO. 108 19 pp.

Larsen, A.K., Shah-Fairbank, S.C., and Julien, P. 2011. *Escondida Reach: Escondida to San Antonio Hydraulic Modeling Analysis 1962-2006.* Colorado State University, Fort Collins, CO. 188 pp.

Maestas, J., Padilla, R., Nemeth, M., AuBuchon, J., Casuga, J., Makar, P., and Varyu, D. 2014. *Determination of River Maintenance Need at Individual Sites and Reaches on the Middle Rio Grande, NM.* U.S. Department of the Interior, Bureau of Reclamation, Upper Colorado Region, Albuquerque, NM. 32 pp

Makar, P. and AuBuchon, J. 2012. *Channel Conditions and Dynamics of the Middle Rio Grande.* U.S. Department of the Interior, Bureau of Reclamation, Upper Colorado Region, Albuquerque, NM. 108 pp.

Massong, T., 2006. *River Maintenance Priority Sites near Arroyo de las Cañas*, Geomorphic Trends Assessment, Bureau of Reclamation, Albuquerque Area Office, Albuquerque, NM, 14p.

Massong, T., Makar, P., and Bauer, T. 2010. *Planform Evolution Model for the Middle Rio Grande, NM.* 2nd Joint Federal Interagency Conference, 12 pp. Las Vegas, NV. June 27-July 1, 2010.

MEI, 2002. *Geomorphic and Sedimentologic Investigations of the Middle Rio Grande between Cochiti Dam and Elephant Butte Reservoir*. Mussetter Engineering Inc., for New Mexico Interstate Stream Commission, Albuquerque, NM. 229p.

Nemeth, M. 2008. *Arroyo de las Cañas Explanation of Downgrade to Monitored Sites.* U.S. Department of the Interior, Bureau of Reclamation, Upper Colorado Region, Albuquerque, NM. 2 pp.

Owen, T., Anderson, K., Shah-Fairbank, S., Julien, P., 2012. *Elephant Butte Reach Report South Boundary of Bosque del Apache NWR to Elephant Butte Reservoir, Hydraulic Modeling Analysis 1962-2010*. Colorado State University for the Bureau of Reclamation. Fort Collins, CO.

Reclamation. 1985. *Volume XXXV Annual Project History: Calendar Year 1985*. Bureau of Reclamation, Upper Colorado Region, Albuquerque Area Office, Albuquerque, New Mexico. 161 pp.

Reclamation, 2000. *Rio Grande and Low Flow Conveyance Channel Modifications Draft Environmental Impact Statement*. Bureau of Reclamation, Albuquerque Area Office, Albuquerque, NM.

Reclamation, 2015a. Historical mean_bed.xlsm Microsoft Excel File, Sheet OriginalData. Unpublished bed generation data from photogrammetry along aggradation-degradation lines. Bureau of Reclamation, Technical Service Center, Denver, CO.

Reclamation, 2015b. lengths.xlsm Microsoft Excel file, Sheet lengths(2). . Unpublished distance downstream between aggradation-degradation lines. Bureau of Reclamation, Technical Service Center, Denver, CO.

Schumm, S., 1977. *The Fluvial System*, The Blackburn Press. Breinigsville, PA.

Schumm, S., 1981. *Evolution and response of the fluvial system, sedimentologic implications'*, Society of Economic Paleontologists and Mineralogists. Pp. 19-29, 31. Tulsa, OK.

Varyu, D. 2013. *Aggradation/Degradation Volume Calculations: 2002-2012*. U.S. Department of the Interior, Bureau of Reclamation, Technical Service Center, Denver, CO. 455 pp.
Wentworth, C.K., 1922, A scale of grade and class terms for clastic sediments: Journal of Geology, v. 30, p. 377-392.

Wright, J. 2010. *Middle Rio Grande Peak Discharge Frequency Study*. U.S. Department of the Interior, Bureau of Reclamation, Technical Service Center, Denver, CO. 151 pp.

Yang, C. T., 1996. *Sediment Transport Theory and Practice*. Ch 2. Incipient Motion Criteria and Applications. Pp 20-2. McGraw-Hill.

Appendix A: Geomorphic and Hydrologic Analysis

Table 17 Duration, in days, of the Rio Grande at San Acacia (USGS 08354900) at different ranges of discharges from 1959 to 2014. Ranges are represented by the minimum, and are the summation of days until the next step, i.e. 500 – 999 cfs, 1000 cfs – 1999 cfs, etc.

	1 cfs	100 cfs	500 cfs	1000 cfs	2000 cfs	3000 cfs	4000 cfs	5000 cfs	6000 cfs
1959	121	63	72	1	0	0	0	0	0
1960	125	23	59	50	18	11	1	0	0
1961	200	17	65	28	7	3	0	0	0
1962	255	14	11	8	11	15	6	2	0
1963	249	6	3	0	0	0	0	0	0
1964	134	6	0	0	0	0	0	0	0
1965	185	33	7	40	35	8	2	1	0
1966	285	8	4	0	0	0	0	0	0
1967	269	12	3	2	1	2	0	0	5
1968	234	26	27	32	10	6	2	1	2
1969	239	45	18	32	21	4	0	1	1
1970	308	13	31	0	0	0	0	0	0
1971	289	6	1	1	0	0	0	0	0
1972	287	10	7	6	2	0	1	0	0
1973	238	17	22	32	17	9	6	16	7
1974	353	9	1	0	0	0	0	0	0
1975	169	69	22	27	45	25	4	3	0
1976	186	63	52	10	1	0	0	0	0
1977	238	10	3	1	0	1	0	0	0
1978	175	27	8	7	1	0	0	0	0
1979	156	37	5	10	15	56	18	9	0
1980	206	10	2	17	9	15	28	12	0
1981	152	86	66	3	0	0	0	0	0
1982	9	23	147	103	40	32	10	1	0
1983	56	81	43	9	10	8	36	39	0
1984	249	21	8	28	7	15	7	19	1
1985	69	52	50	47	33	45	17	17	0
1986			3	53	169	107	27	6	0
1987	19	59	9	92	68	67	47	4	0
1988	20	55	67	169	36	17	2	0	0
1989	128	101	63	28	29	16	0	0	0
1990	48	114	125	70	3	0	0	0	0
1991	9	51	39	149	71	39	7	0	0
1992	17	82	105	88	14	32	18	10	0
1993	3	63	28	157	38	36	18	19	3
1994	16	68	71	120	23	21	31	13	2
1995	2	48	70	124	31	22	59	8	1
1996	97	97	100	71	0	0	0	1	0

1997	0	42	119	130	37	20	16	1	0
1998	5	104	100	142	12	2	0	0	0
1999	0	78	124	116	26	14	7	0	0
2000	0	178	153	35	0	0	0	0	0
2001	0	161	185	17	2	0	0	0	0
2002	53	184	122	6	0	0	0	0	0
2003	113	130	113	1	1	0	0	0	0
2004	71	90	146	32	15	2	0	0	0
2005	46	66	136	43	5	22	24	24	0
2006	6	165	79	92	14	5	4	0	0
2007	50	90	146	57	19	3	0	0	0
2008	0	91	130	54	44	42	5	0	0
2009	33	117	146	26	24	18	1	0	0
2010	54	73	172	20	42	4	0	0	0
2011	74	151	136	4	0	0	0	0	0
2012	125	92	139	9	1	0	0	0	0
2013	63	175	91	30	2	1	1	0	2
2014	39	157	161	8.00	0	0	0	0	0

Table 18 Duration, in days, of the Rio Grande at San Marcial (USGS 08358400) at different ranges of discharges from 1995 to 2014. Ranges are represented by the minimum, and are the summation of days until the next step, i.e. 500 – 999 cfs, 1000 cfs – 1999 cfs, etc.

	1 cfs	**100 cfs**	**500 cfs**	**1000 cfs**	**2000 cfs**	**3000 cfs**	**4000 cfs**	**5000 cfs**	**6000 cfs**
1959	36	80	2	0	0	0	0	0	0
1960	29	51	29	32	21	4	0	0	0
1961	39	69	16	18	5	0	0	0	0
1962	25	10	7	5	23	9	1		0
1963	16	2	0	0	0	0	0	0	0
1964	7	2	1	0	0	0	0	0	0
1965	34	12	11	55	18	3			0
1966	26	5	0	0	0	0	0	0	0
1967	46	13	1	3	1	0	2	2	0
1968	53	46	23	26	9	4	1	0	0
1969	33	40	19	34	5	1	2	0	0
1970	18	28	9	0	0	0	0	0	0
1971	20	3	0	0	0	0	0	0	0
1972	30	14	2	7	0	0	0	0	0
1973	22	18	34	21	14	8	13	10	0
1974	28	63	55	0	0	0	0	0	0
1975	17	36	70	68	33	12	4	0	0
1976	6	173	129	51	7	0	0	0	0
1977	88	133	84	8	3	0	0	0	0
1978	41	49	132	48	12	0	0	0	0
1979	3	59	78	109	14	12	42	41	7
1980	16	72	63	133	14	9	18	36	4
1981	72	100	100	14	0	0	0	0	0

1982	9	102	97	70	46	26	4	0	0
1983	76	30	46	84	11	13	49	9	0
1984	27	2	17	16	11	18	11	9	0
1985	24	62	35	40	46	28	7	16	25
1986	0	6	11	152	129	67	0	0	0
1987	23	29	67	60	88	48	27	0	0
1988	52	49	112	116	19	7	1	0	0
1989	38	60	87	26	34	2	0	0	0
1990	59	114	86	24	2	0	0	0	0
1991	29	39	102	90	42	20	2	1	2
1992	20	55	129	34	27	15	25	8	0
1993	16	55	75	103	42	24	14	16	0
1994	14	52	140	43	23	34	19	3	0
1995	9	64	110	73	16	44	41	0	0
1996	15	90	84	40	0	0	0	0	0
1997	13	62	102	137	12	17	18	0	0
1998	39	55	171	43	29	0	0	0	0
1999	37	87	145	61	18	11	6	0	0
2000	99	159	103	5	0	0	0	0	0
2001	96	169	77	21	2	0	0	0	0
2002	191	157	15	2	0	0	0	0	0
2003	179	182	3	1	0	0	0	0	0
2004	130	138	67	21	10	0	0	0	0
2005	22	100	110	19	9	24	37	0	0
2006	139	68	72	61	18	3	3	1	0
2007	103	100	125	28	9	0	0	0	0
2008	33	103	106	46	59	17	2	0	0
2009	57	100	135	27	17	19	0	0	0
2010	92	129	90	40	12	2	0	0	0
2011	155	109	101	0	0	0	0	0	0
2012	165	111	81	9	0	0	0	0	0
2013	170	129	47	14	3	1	1	0	0
2014	138	137	86	4	0	0	0	0	0

Table 19 Monthly mean and median values for discharge for the San Acacia (USGS 08354900) and San Marcial (USGS 08358400) gages from 1990 to 2013.

Discharge (cfs)	San Acacia		San Marcial	
	Mean	Median	Mean	Median
January	860	840	610	610
February	890	910	650	620
March	840	710	590	520
April	1200	990	940	740
May	2000	2000	1700	1700
June	1600	660	1400	610
July	590	340	480	280

August	580	360	420	200
September	430	280	250	190
October	400	310	230	150
November	930	830	660	550
December	910	840	670	640

Table 20 Monthly mean and median values for suspended sediment concentration for the San Acacia (USGS 08354900) and San Marcial (USGS 08358400) gages from 1990 to 2013.

Suspended Sediment Concentration (mg/L)	San Acacia		San Marcial	
	Mean	Median	Mean	Median
January	890	570	2338	1600
February	1000	710	2600	1400
March	580	450	2000	1500
April	1100	570	1900	1500
May	1200	980	2000	1900
June	790	510	1400	930
July	6400	4900	5800	4300
August	9500	9200	8900	8300
September	8200	6500	7000	5800
October	2300	1600	2700	2300
November	2500	1800	3600	3300
December	1400	910	2400	1900

Table 21 Monthly mean and median values for suspended sediment load for the San Acacia (USGS 08354900) and San Marcial (USGS 08358400) gages from 1990 to 2013.

Suspended Sediment Load (tons/day)	San Acacia		San Marcial	
	Mean	Median	Mean	Median
January	2200	1200	4300	2200
February	2900	1300	5400	2000
March	1700	900	5100	2500
April	6100	1900	8500	3300
May	9000	5700	12000	7800
June	4100	850	9200	2300
July	12000	4900	10000	6200
August	28000	11000	18000	7300
September	16000	9600	11000	8500
October	3800	1900	3900	810
November	6000	5300	7900	3900
December	3500	1900	4700	2800

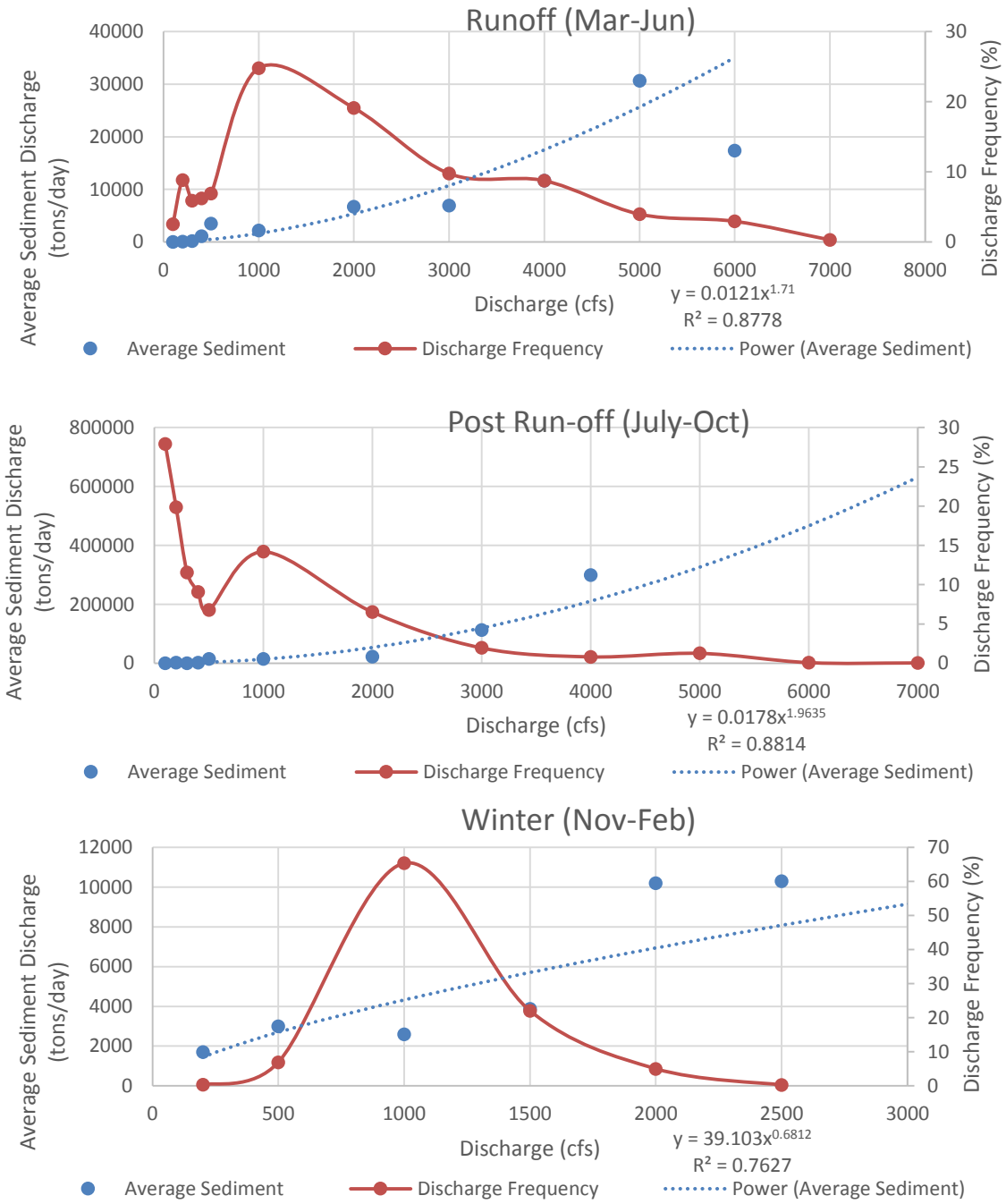

Figure 55 Discharge frequency and sediment discharge rating curve for the San Acacia gage (USGS 08354900) for three hydrologic seasons; data from 1993 to 2013. Discharge frequency modified from Bui 2014.

Table 22 Results of discharge frequency analysis for runoff hydrologic season for San Acacia gage (USGS 08354900) USGS data coincides with Bui's report, 1993 to 2013.

Discharge interval (cfs)	0-100	100-200	200-300	300-400	400-500	500-1000	1000-2000	2000-3000	3000-4000	4000-5000	5000-6000	6000-7000
Frequency % (Bui 2014)	2.5	8.8	5.9	6.2	6.9	24.8	19.1	9.75	8.73	3.96	2.94	0.3
Average Sediment per event (tons/day)	9.76	51.5	148	1100	3500	2160	6680	6930	11.7k	30.7k	17.4k	No data
Effective Discharge (tons)	24.7	563	899	1680	2880	24.8k	62.4k	78.3k	122k	84.7k	88.8k	12.2k

Table 23 Results of discharge frequency analysis for post-runoff hydrologic season for San Acacia gage (USGS 08354900). USGS data coincides with Bui's report, 1993 to 2013.

Discharge interval (cfs)	0-100	100-200	200-300	300-400	400-500	500-1000	1000-2000	2000-3000	3000-4000	4000-5000
Frequency % (Bui 2014)	27.9	19.8	11.5	9.06	6.79	14.2	6.50	1.95	0.81	1.26
Average Sediment per event (tons/day)	73.6	2250	445	1450	15.0k	14.7k	22.1k	112.9k	299k	No data
Effective Discharge (tons)	119	688	1060	1580	1910	10.6k	18.2k	14.4k	11.4k	28.6k

Discharge interval (cfs)	5000-6000	6000-7000	7000-8500
Frequency % (Bui 2014)	0.08	0.04	0.04
Average Sediment per event (tons/day)	No data	No data	No data
Effective Discharge (tons)	2700	1860	2600

Table 24 Results of discharge frequency analysis for winter hydrologic season for San Acacia gage (USGS 08354900). USGS data coincides with Bui's report, 1993 to 2013.

Discharge interval (cfs)	0-200	200-500	500-1000	1000-1500	1500-2000	2000-2500
Frequency % (Bui 2014)	0.37	6.94	65.3	22.0	5.03	0.29
Average Sediment per event (tons/day)	1700	2990	2590	3870	10.2k	10.3k
Effective Discharge (tons)	337	14.7k	232k	111k	31.8k	2190

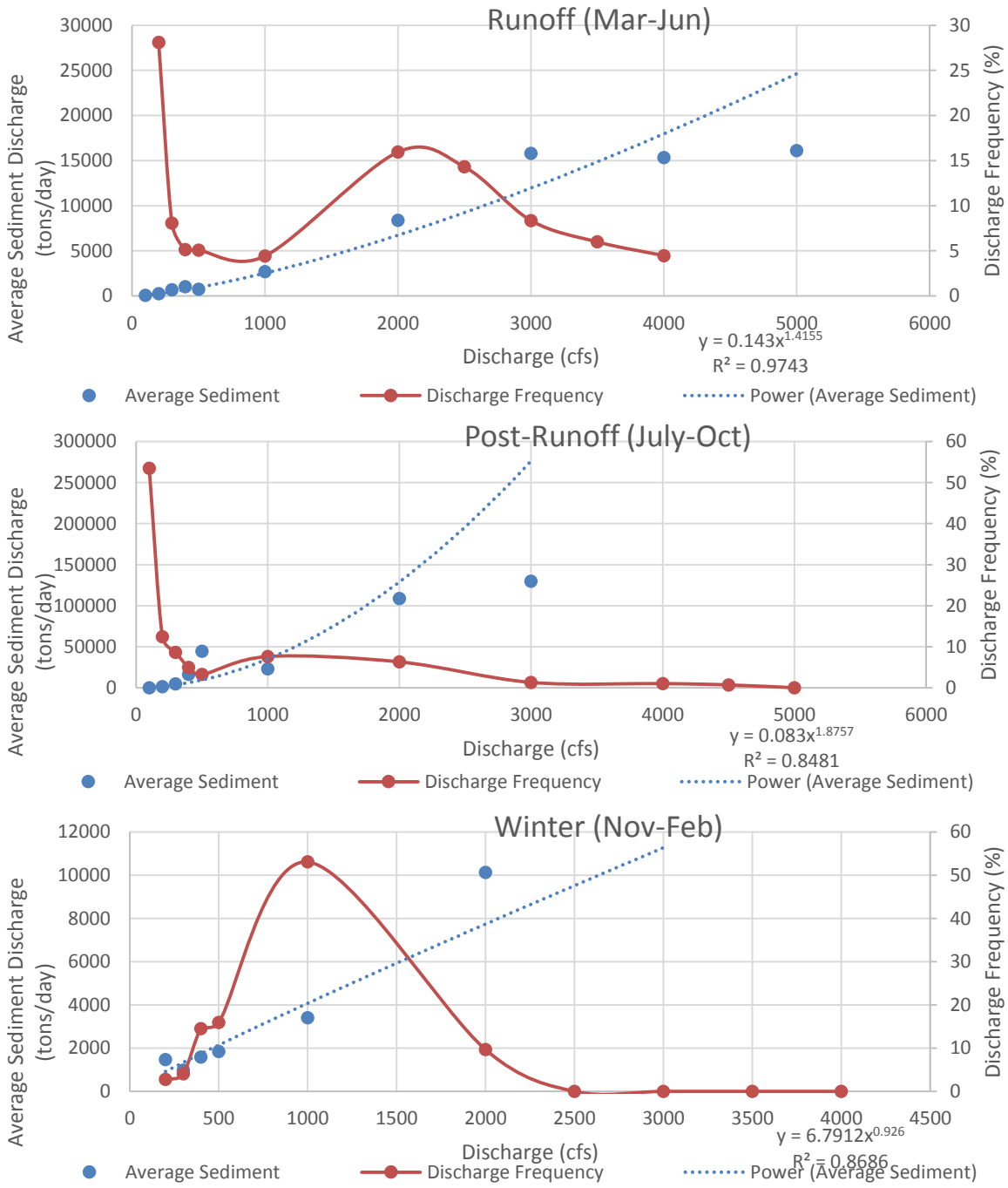

Figure 56 Discharge frequency and sediment discharge rating curve for the San Marcial gage (USGS 08358400) for three hydrologic seasons; data from 1993 to 2013. Discharge frequency modified from Bui 2014.

Table 25 Results of discharge frequency analysis for run-off hydrologic season for San Marcial gage (USGS 08358400) USGS data coincides with Bui's report, 1993 to 2013.

Discharge interval (cfs)	0-100	100-200	200-300	300-400	400-500	500-1000	1000-2000	2000-3000	3000-4000	4000-5000	5000-6000
Frequency % (Bui 2014)	28.1	8.1	5.1	5.1	4.4	15.9	14.3	8.4	6.0	4.5	0.1
Average Sediment per event (tons/day)	64.9	233	667	1030	735	2700	8370	15.8k	15.3k	16.1k	No data
Effective Discharge (tons)	1020	1390	1820	2900	3600	26.8k	64.0k	77.2k	88.9k	94.7k	3460

Table 26 Results of discharge frequency analysis for post runoff hydrologic season for San Marcial gage (USGS 08358400) USGS data coincides with Bui's report, 1993 to 2013.

Discharge interval (cfs)	0-100	100-200	200-300	300-400	400-500	500-1000	1000-2000	2000-3000	3000-4000	4000-5000	5000-6000
Frequency % (Bui 2014)	53.5	12.4	8.66	5.00	3.25	7.64	6.34	1.34	1.06	0.73	0.04
Average Sediment per event (tons/day)	127	1470	4940	16.6k	44.5k	23.3k	109k	130k	10.1k	No data	No data
Effective Discharge (tons)	6830	12.5k	22.6k	24.5k	25.6k	157k	477k	263k	390k	388k	26.6k

Table 27 Results of discharge frequency analysis for winter hydrologic season for San Marcial gage (USGS 08358400) USGS data coincides with Bui's report, 1993 to 2013.

Discharge interval (cfs)	0-200	200-300	300-400	400-500	500-1000	100-2000
Frequency % (Bui 2014)	2.79	4.07	14.5	15.9	53.1	9.64
Average Sediment per event (tons/day)	1470	975	1580	1850	3410	10.1k
Effective Discharge (tons)	1350	4600	22.4k	31.0k	166k	57.2k

Table 28 Cumulative change in slope in the study reach, based on agg-deg lines.

	CUMULATIVE CHANGE IN SLOPE (FT/FT)			
AGG-DEG LINE	1962-1972	1972-1992	1992-2002	2002-2012
1364	0.000145	-0.00222	0.000465	0.000447
1365	0.000562	-0.00186	0.002452	-0.00108
1366	-0.00086	-0.00071	0.001214	-0.00054
1367	-0.00207	-0.00039	0.003	-0.00179
1368	0.000307	-0.00137	-8.5E-05	0.001903
1369	9.2E-05	-0.00215	0.000171	0.000354
1370	-0.00019	-0.00185	0.000722	0.000903
1371	0.001049	-0.00208	0.000477	0.001058
1372	0.000418	-0.00319	0.000922	0.000497
1373	-0.00111	-0.00205	0.000472	0.001123

1374	-0.00028	-0.00343	0.001639	0.00117
1375	-0.00084	-0.00372	0.002985	0.000697
1376	-0.00013	-0.00334	0.002662	-0.0002
1377	0.000541	-0.00348	0.001691	0.000138
1378	-0.00023	-0.00107	0.000511	0.000347
1379	0.000396	-0.0008	-0.00143	0.002601
1380	0.000425	-0.00196	1.92E-05	0.002552
1381	-0.00058	-0.00013	-9.2E-05	0.001742
1382	0.000321	-0.00227	0.002193	0.002075
1383	-0.00104	-0.00201	0.002001	0.002648
1384	6.68E-05	-0.0025	0.000535	0.004045
1385	0.000274	-0.00259	-0.00015	0.003992
1386	0.000591	-0.00199	0.00025	0.002756
1387	-0.00057	-0.00023	-0.00116	0.003549
1388	-0.00169	0.000393	-0.00012	0.002466
1389	-0.00221	0.001256	-0.00112	-0.00045
1390	-0.00199	0.000563	0.000202	-0.00132
1391	-0.00225	0.000439	-0.00042	0.000483
1392	-0.00241	0.002117	-0.00042	-0.00021
1393	0.000419	-0.00086	-0.0009	0.001387
1394	9.7E-05	0.000806	0.001293	-0.00401
1395	-0.00118	0.002574	0.001003	-0.00579
1396	-0.00351	0.005421	-0.00346	-0.00212
1397	-0.00176	0.002509	-0.00076	0.000111
1398	-0.00024	0.001457	-0.00135	0.000495
1399	0.000701	0.002397	-0.00102	-0.00306
1400	0.000366	0.00246	-0.00026	-0.00319
1401	-0.00075	0.003349	-0.00236	-0.00171
1402	0.00099	0.003185	-0.00249	-0.00156
1403	0.000451	0.001175	-0.00232	-0.0002
1404	4.75E-05	0.001406	-0.00102	-0.00052
1405	0.001274	-0.00092	-0.002	0.000814
1406	-0.00115	0.003064	-0.00413	-0.00094
1407	0.000816	8.6E-05	-0.00237	0.00131
1408	0.002457	-0.00217	-0.00199	0.000974
1409	0.001821	-0.00159	-0.00252	0.00225
1410	0.000833	-0.00232	-0.00037	7.65E-05
1411	0.000159	-0.00089	-0.0014	0.000292
1412	0.001126	-0.00075	-0.00116	-0.00177
1413	0.002131	0.000228	-0.00462	0.001631
1414	-0.00039	0.003942	-0.00554	0.000564
1416	0.002821	0.00135	-0.00336	-0.00233
1417	0.000417	0.001553	-0.00206	-0.00192
1418	0.000986	0.002442	-0.00366	-0.00027
1419	0.001304	0.002909	-0.00555	0.000688

1420	0.00226	0.001187	-0.00452	0.000521
1421	0.001193	0.000665	-0.00459	0.001392
1422	-0.00138	0.002804	-0.00177	-0.00295
1423	0.001052	0.003644	-0.00195	-0.00552
1424	0.00272	0.002321	-0.0037	-0.00279
1425	0.002914	-0.0004	-0.00085	-0.00194
1426	0.000132	0.001679	-0.00162	-0.00148
1427	0.001417	0.000955	-0.00152	-0.00369
1428	0.000472	0.001386	-0.00251	-0.00195
1429	0.00021	0.002635	-0.00182	-0.00295
1430	0.000381	0.001804	-0.0019	-0.00302
1431	-0.00139	0.004055	-0.0026	-0.00324
1432	-0.00041	0.001844	-0.00152	-0.00214
1433	1.55E-05	0.00396	-0.00271	-0.0041
1434	0.000928	0.000293	-0.00081	-0.00332
1435	0.003128	0.001196	-0.00277	-0.0026
1436	0.000178	0.002754	-0.00129	-0.00153
1437	-6.2E-05	0.00329	-0.00226	-0.00407
1438	-0.00055	0.003665	-0.0015	-0.00393
1439	-0.00171	0.003973	-0.00163	-0.00243
1440	-0.00179	0.004427	-0.00149	-0.00328
1441	0.000268	0.00557	-0.00146	-0.00629
1442	0.003548	0.00113	-0.00163	-0.00556
1443	0.00178	0.0024	-0.00124	-0.00493
1444	0.002718	0.001582	-0.00153	-0.00567
1445	-0.00024	0.002236	-0.00121	-0.00425
1446	-0.00082	0.003531	-0.00274	-0.00488
1447	-0.00012	0.003418	-0.00342	-0.00248
1448	-0.00035	0.002309	-0.00204	-0.00326
1449	0.001001	0.001626	-0.00157	-0.00424
1450	-0.00098	0.00203	0.00021	-0.0038
1451	-0.00229	0.003756	-0.00011	-0.0042
1452	0.000398	0.003298	-0.0021	-0.00423
1453	0.003075	0.001029	-0.00259	-0.0033
1454	0.001826	0.000916	-0.00159	-0.00306

Table 29 Shear stress calculations from the HEC-RAS 1-D model at various flows.

	1000 cfs	**2000 cfs**	**3000 cfs**	**4000 cfs**	**5000 cfs**	**6000 cfs**	**7000 cfs**	**8000 cfs**	**9000 cfs**	**10k cfs**
Agg-deg Line	Shear (lb/ft^2)	Shear (lb/ft^2)	Shear (lb/ft^2)	Shear (lb/ft^2)	Shear (lb/ft^2)	Shear (lb/ft^2)	Shear (lb/ft^2)	Shear (lb/ft^2)	Shear (lb/ft^2)	Shear (lb/ft^2)
1364	0.1	0.14	0.17	0.20	0.22	0.24	0.27	0.03	0.58	0.22
1365	0.09	0.13	0.17	0.15	0.17	0.19	0.21	0.25	0.08	0.07
1366	0.12	0.18	0.23	0.20	0.22	0.25	0.13	0.20	0.05	0.25
1367	0.09	0.15	0.20	0.24	0.28	0.33	0.38	0.04	0.05	0.06
1368	0.08	0.13	0.17	0.21	0.25	0.30	0.35	0.40	0.33	0.07
1369	0.03	0.06	0.09	0.12	0.13	0.15	0.18	0.20	0.06	0.07
1370	0.12	0.15	0.18	0.20	0.19	0.22	0.24	0.26	0.28	0.23
1371	0.07	0.10	0.13	0.15	0.14	0.17	0.19	0.22	0.24	0.20
1372	0.06	0.09	0.12	0.11	0.13	0.16	0.19	0.22	0.22	0.25
1373	0.11	0.14	0.15	0.14	0.15	0.18	0.21	0.24	0.27	0.26
1374	0.05	0.07	0.08	0.07	0.08	0.10	0.12	0.14	0.16	0.15
1375	0.11	0.17	0.20	0.27	0.27	0.13	0.16	0.11	0.12	0.14
1376	0.08	0.12	0.15	0.17	0.10	0.11	0.11	0.09	0.09	0.12
1377	0.08	0.12	0.13	0.17	0.10	0.10	0.10	0.11	0.12	0.11
1378	0.11	0.11	0.10	0.13	0.11	0.13	0.14	0.16	0.18	0.12
1379	0.12	0.15	0.17	0.09	0.12	0.14	0.16	0.18	0.19	0.15
1380	0.08	0.11	0.11	0.08	0.09	0.11	0.13	0.15	0.16	0.10
1381	0.11	0.16	0.17	0.26	0.09	0.11	0.12	0.14	0.16	0.13
1382	0.1	0.13	0.16	0.06	0.07	0.08	0.09	0.09	0.11	0.12
1383	0.08	0.12	0.13	0.06	0.08	0.11	0.08	0.09	0.10	0.11
1384	0.09	0.12	0.07	0.10	0.04	0.07	0.07	0.09	0.10	0.11
1385	0.09	0.14	0.18	0.30	0.40	0.08	0.08	0.10	0.11	0.08
1386	0.19	0.30	0.39	0.07	0.06	0.06	0.07	0.07	0.08	0.09
1387	0.12	0.20	0.25	0.06	0.06	0.07	0.05	0.12	0.07	0.08
1388	0.14	0.22	0.28	0.35	0.46	0.30	0.37	0.14	0.14	0.15
1389	0.12	0.19	0.24	0.16	0.12	0.14	0.10	0.10	0.09	0.09
1390	0.11	0.17	0.21	0.25	0.10	0.11	0.12	0.12	0.13	0.14
1391	0.14	0.17	0.20	0.25	0.15	0.13	0.14	0.15	0.15	0.16
1392	0.05	0.05	0.06	0.08	0.05	0.06	0.05	0.06	0.06	0.07
1393	0.06	0.06	0.07	0.09	0.06	0.07	0.06	0.06	0.06	0.07
1394	0.11	0.12	0.12	0.07	0.07	0.08	0.08	0.09	0.09	0.10
1395	0.05	0.06	0.04	0.04	0.04	0.05	0.06	0.06	0.07	0.08
1396	0.05	0.08	0.06	0.04	0.04	0.05	0.05	0.06	0.06	0.07
1397	0.27	0.20	0.20	0.18	0.20	0.25	0.27	0.29	0.30	0.27
1398	0.11	0.13	0.15	0.20	0.23	0.17	0.19	0.23	0.24	0.23
1399	0.08	0.14	0.20	0.08	0.11	0.13	0.15	0.17	0.20	0.22

1400	0.16	0.25	0.19	0.17	0.15	0.18	0.21	0.26	0.31	0.35
1401	0.13	0.18	0.19	0.15	0.18	0.12	0.14	0.18	0.23	0.21
1402	0.11	0.18	0.16	0.11	0.12	0.14	0.10	0.29	0.19	0.21
1403	0.12	0.19	0.24	0.24	0.33	0.43	0.49	0.08	0.09	0.08
1404	0.1	0.16	0.18	0.19	0.15	0.21	0.24	0.28	0.30	0.36
1405	0.06	0.09	0.10	0.09	0.12	0.18	0.19	0.24	0.32	0.44
1406	0.04	0.06	0.07	0.07	0.11	0.20	0.23	0.38	0.40	0.11
1407	0.11	0.13	0.12	0.13	0.23	0.02	0.02	0.03	0.03	0.03
1408	0.08	0.12	0.12	0.11	0.28	0.29	0.01	0.02	0.02	0.02
1409	0.1	0.16	0.16	0.13	0.01	0.76	0.31	0.01	0.01	0.01
1410	0.11	0.19	0.17	0.19	0.00	0.01	1.14	1.16	1.22	0.70
1411	0.12	0.18	0.17	0.20	0.27	0.00	0.01	0.01	0.01	0.01
1412	0.07	0.11	0.12	0.13	0.17	0.12	0.01	0.06	0.01	0.01
1413	0.13	0.19	0.25	0.22	0.17	0.17	0.19	0.60	0.57	0.55
1414	0.1	0.16	0.22	0.21	0.16	0.18	0.21	0.06	0.07	0.01
1415	0.09	0.15	0.20	0.20	0.15	0.18	0.21	0.77	0.67	0.70
1416	0.08	0.13	0.16	0.19	0.29	0.39	0.35	0.01	0.02	0.02
1417	0.1	0.11	0.12	0.12	0.20	0.01	0.01	0.01	0.02	0.02
1418	0.09	0.14	0.18	0.17	0.02	0.15	0.17	0.19	0.21	0.24
1419	0.09	0.12	0.16	0.18	0.14	0.18	0.20	0.19	0.22	0.23
1420	0.09	0.12	0.17	0.22	0.26	0.11	0.12	0.13	0.17	0.19
1421	0.17	0.13	0.17	0.18	0.21	0.26	0.29	0.33	0.18	0.19
1422	0	0.09	0.12	0.10	0.12	0.15	0.15	0.16	0.18	0.13
1423	0.12	0.10	0.13	0.13	0.17	0.13	0.13	0.14	0.12	0.11
1424	0.11	0.12	0.09	0.08	0.10	0.12	0.11	0.11	0.12	0.12
1425	0.07	0.10	0.12	0.15	0.06	0.08	0.06	0.07	0.08	0.09
1426	0.03	0.05	0.05	0.07	0.06	0.08	0.08	0.09	0.10	0.11
1427	0.05	0.06	0.08	0.08	0.09	0.02	0.12	0.14	0.16	0.19
1428	0.08	0.08	0.10	0.11	0.13	0.14	0.19	0.18	0.10	0.12
1429	0.13	0.16	0.12	0.14	0.17	0.19	0.08	0.09	0.10	0.13
1430	0.12	0.14	0.12	0.14	0.17	0.17	0.19	0.22	0.24	0.11
1431	0.15	0.14	0.13	0.14	0.16	0.06	0.06	0.07	0.06	0.07
1432	0.04	0.05	0.06	0.08	0.11	0.11	0.12	0.16	0.16	0.17
1433	0.09	0.10	0.12	0.14	0.23	0.25	0.27	0.07	0.07	0.08
1434	0.09	0.09	0.11	0.13	0.03	0.03	0.03	0.03	0.03	0.03
1435	0.11	0.10	0.12	0.15	0.18	0.20	0.19	0.23	0.24	0.31
1436	0.04	0.07	0.06	0.09	0.12	0.15	0.17	0.21	0.24	0.38
1437	0.4	0.23	0.27	0.17	0.22	0.25	0.27	0.49	0.53	0.04
1438	0.07	0.09	0.11	0.09	0.13	0.17	0.18	0.08	0.08	0.30
1439	0.05	0.08	0.11	0.12	0.04	0.05	0.06	0.08	0.09	0.09
1440	0.06	0.11	0.07	0.08	0.11	0.16	0.19	0.09	0.10	0.11

1441	0.06	0.11	0.16	0.20	0.11	0.05	0.06	0.07	0.07	0.09
1442	0.13	0.13	0.17	0.15	0.18	0.23	0.33	0.16	0.18	0.08
1443	0.02	0.04	0.07	0.07	0.05	0.07	0.04	0.04	0.05	0.05
1444	0.14	0.15	0.14	0.14	0.16	0.06	0.07	0.07	0.09	0.09
1445	0.03	0.04	0.05	0.06	0.06	0.09	0.10	0.12	0.08	0.09
1446	0.07	0.07	0.08	0.08	0.09	0.06	0.07	0.07	0.07	0.07
1447	0.06	0.10	0.08	0.10	0.13	0.06	0.06	0.06	0.07	0.08
1448	0.07	0.13	0.10	0.13	0.19	0.23	0.16	0.18	0.12	0.13
1449	0.17	0.22	0.13	0.17	0.12	0.14	0.15	0.16	0.17	0.19
1450	0.08	0.13	0.18	0.28	0.13	0.17	0.19	0.21	0.23	0.26
1451	0.05	0.08	0.11	0.06	0.07	0.10	0.12	0.13	0.14	0.17
1452	0.1	0.16	0.15	0.22	0.31	0.09	0.12	0.13	0.14	0.17
1453	0.11	0.12	0.16	0.10	0.07	0.07	0.09	0.09	0.09	0.14
1454	1.18	1.59	1.87	2.10	2.35	2.56	1.41	1.53	1.65	0.75

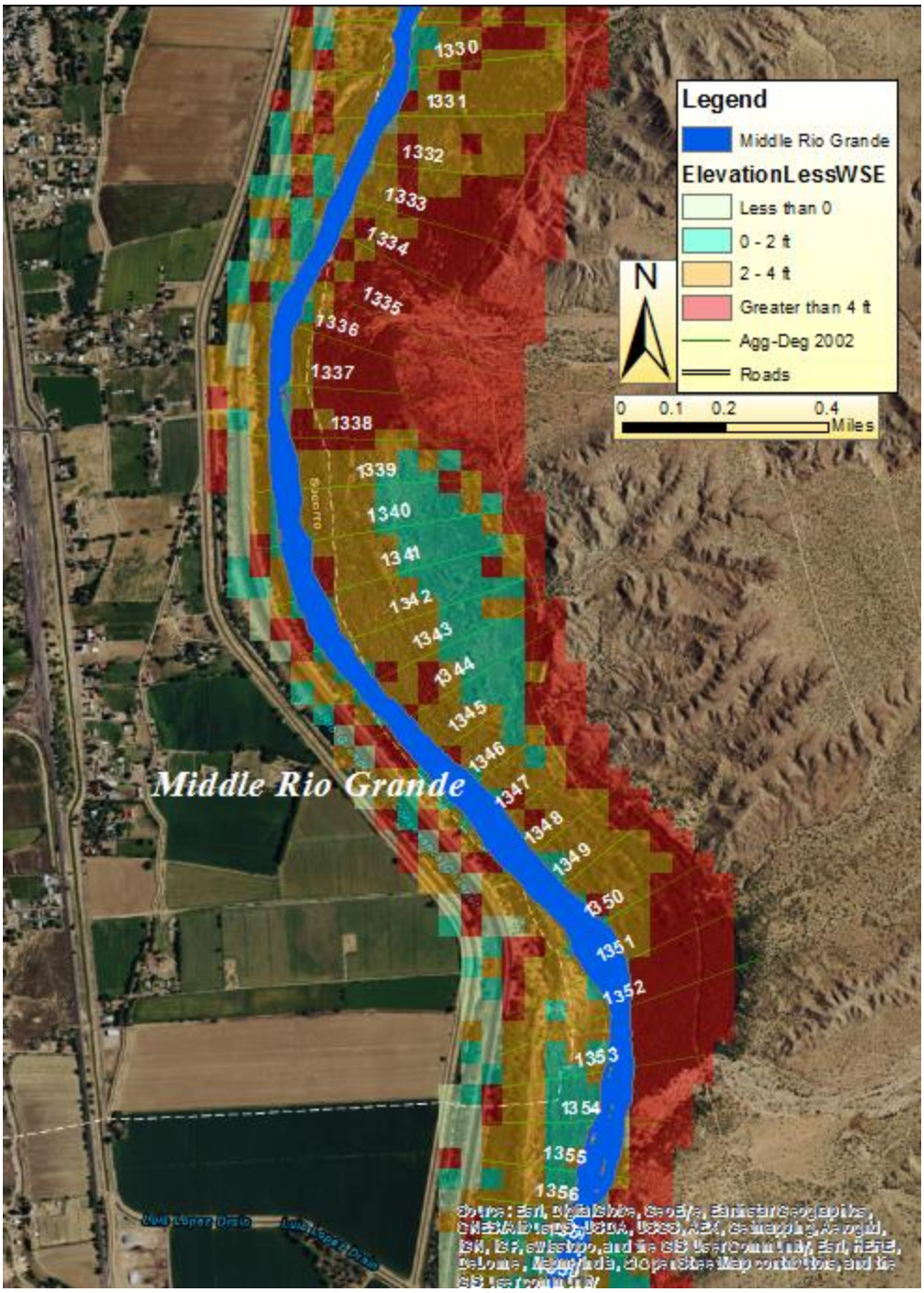

Figure 57 Image of the Terraces near agg-deg lines 1340 to 1352.

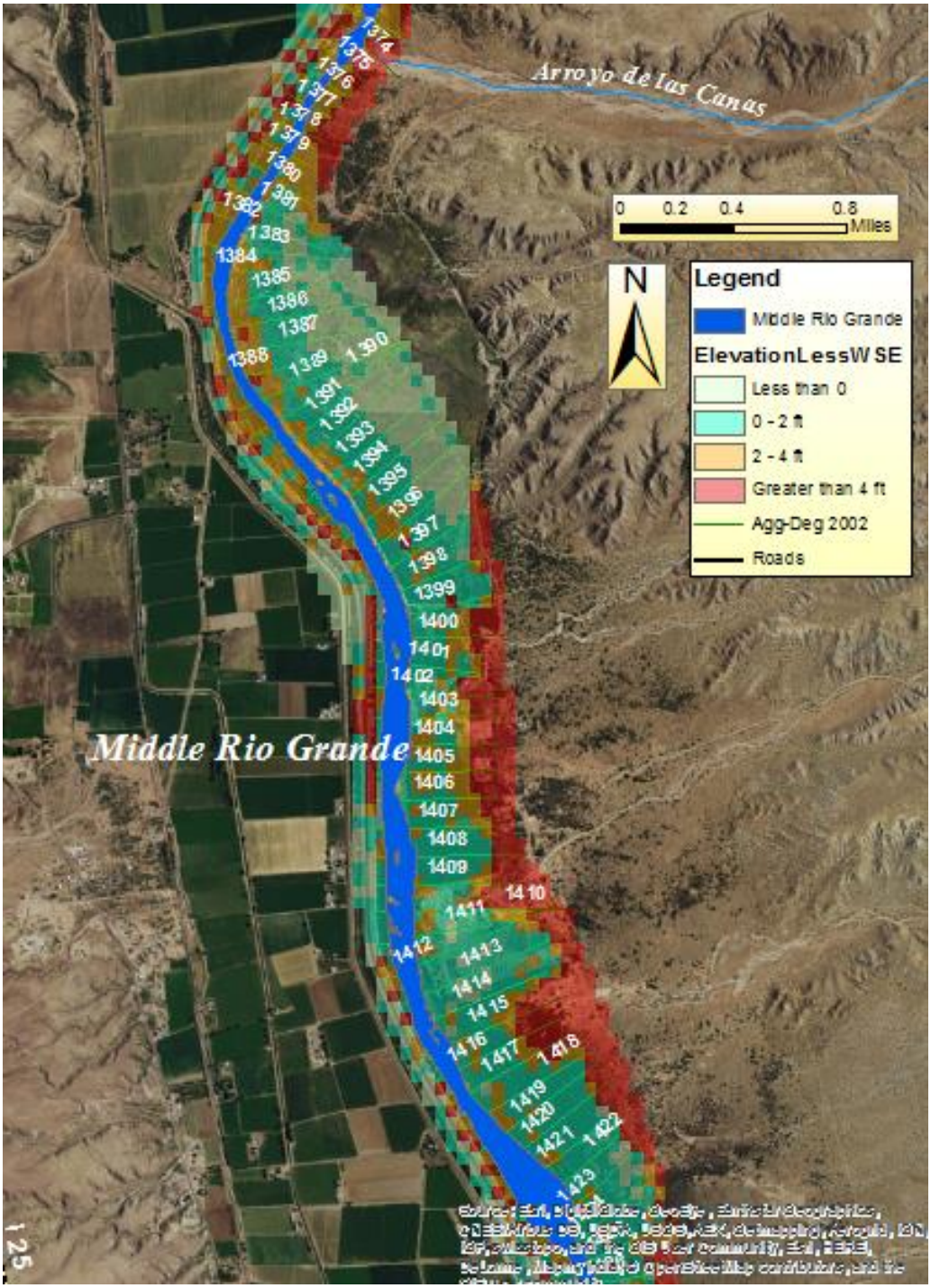

Figure 58 Low-lying terraces below the Arroyo de las Cañas, around agg-deg lines 1380 to 1423.

Appendix B: Bed Material Sample Collection

On June 30, 2016, Jonathan AuBuchon, Aubrey Harris and Eric Gonzales collected sediment samples within the Arroyo de las Cañas study reach of the Rio Grande. The researchers traveled by boat at low flows, and collected sediment samples in bags using a shovel and/or a sediment scoop. The sediment scoop (Figure) was the primary collection tool in the flowing water as it allowed the capture bed material without loss of fines. The shovel was primarily used for samples collected in the dry, such as on exposed bar surfaces. Sediment samples represented a composite of 2-3 samples taken across the cross section. The exception was the collection on exposed sand bars, then the samples would be taken from a couple locations at the downstream end of the bar. Data was collected after the spring run-off, but before monsoonal flows. Figures from the data collection are shown below.

Figure 59. Sediment scoop used for the collection of sediment grab samples in the Cañas study reach (photograph taken by S. Devergie 7/28/2016 on bed material collection south of Belen)

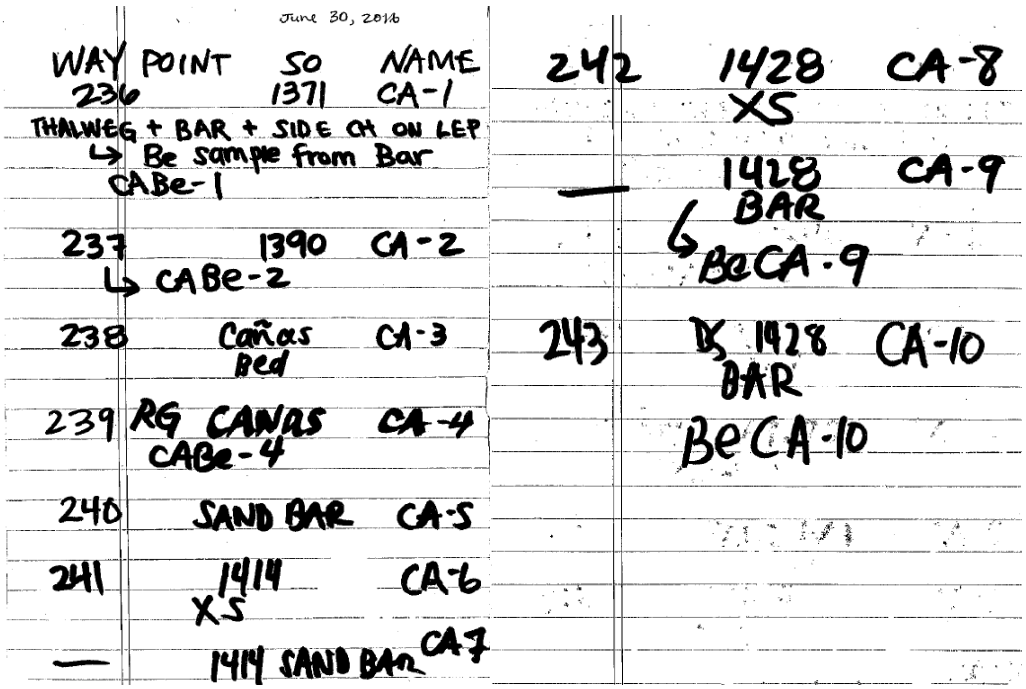

Figure 60 Field notes from the data collection, showing the way point, the sample location, and the sample name. Be-samples were collected for another project.

Table 30 Summary of bed material samples collected on June 30, 2016 on the Arroyo de las Cañas study reach.

PT	NORTHING	EASTING	ELEVATION	RANGELINE (APPX)	SAMPLE	NOTES
236	34.049170	-106.866840	4614	SO-1371	CA-1	GPS points were taken with a hand held etrex Garmin, geographic coordinates NAD83 datum
237	34.024490	-106.866309	4595	SO-1390	CA-2	Samples taken at thalweg, bar and side channel on the LEP
238	34.017270	-106.862560	4592	Arroyo de las Cañas bed	CA-3	30-Jun-16
239	34.017220	-106.862920	4600	Rio Grande at Cañas confluence	CA-4	Confirm pt. 237 is correct, changed easting to *.866 from *.896
240	34.006720	-106.870030	4592	Sand bar	CA-5	
241	33.996530	-106.866950	4590	SO-1414, and then one off a sandbar	CA-6, CA-7	
242	33.980500	-106.860810	4584	SO-1428, and then one off a sandbar	CA-8, CA-9	
243	33.980510	-106.860470	4610	Downstream of SO-1428 on a sandbar	CA-10	

Figure 61 Records of the lab sieve analysis regarding bed materials sampled in June 30, 2016.

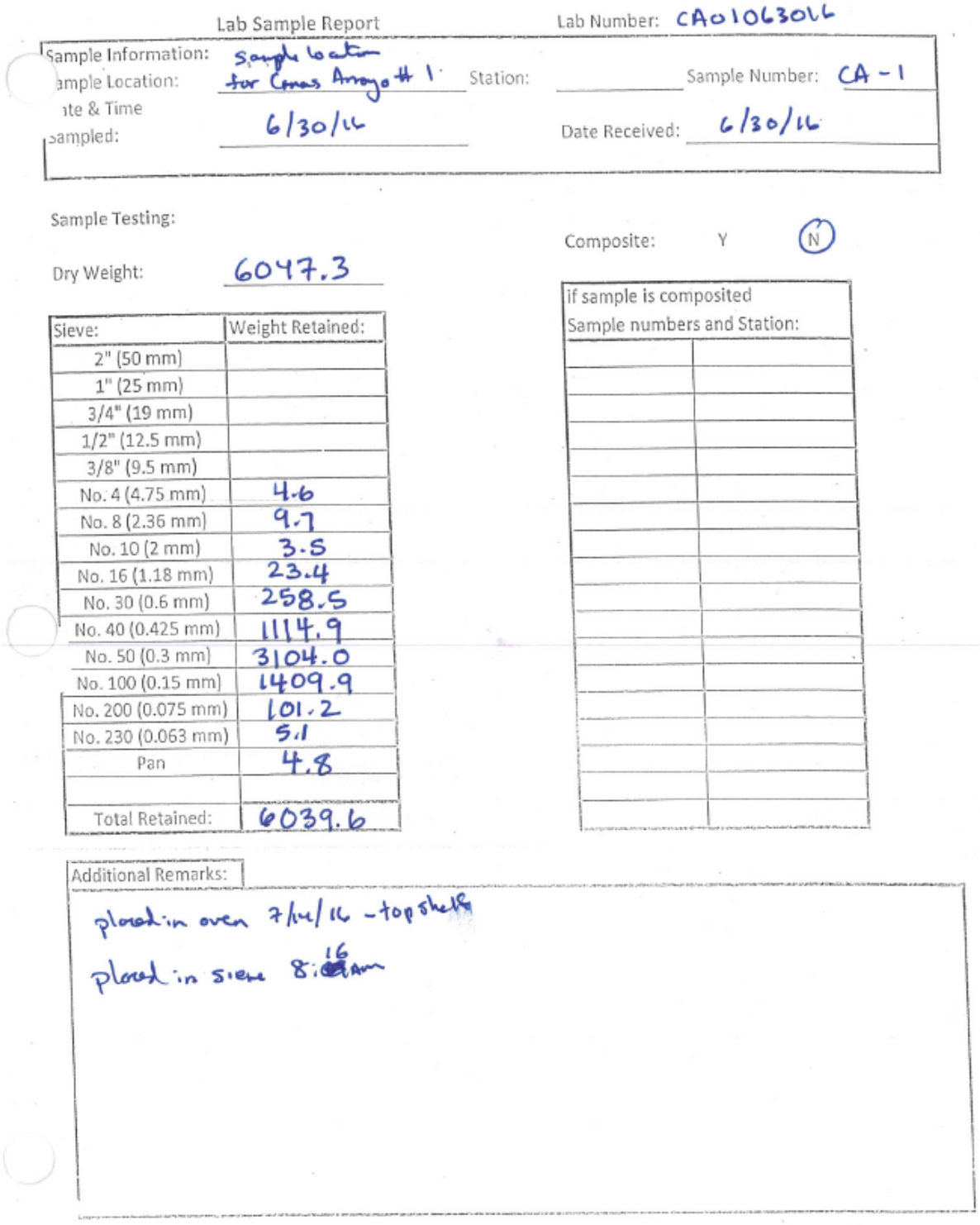

Lab Sample Report

Lab Number: CA01063016

Sample Information:
Sample Location: Sample location for Cross Arroyo # 1
Station:
Sample Number: CA-1
Date & Time Sampled: 6/30/16
Date Received: 6/30/16

Sample Testing:

Composite: Y (N)

Dry Weight: 6047.3

Sieve:	Weight Retained:
2" (50 mm)	
1" (25 mm)	
3/4" (19 mm)	
1/2" (12.5 mm)	
3/8" (9.5 mm)	
No. 4 (4.75 mm)	4.6
No. 8 (2.36 mm)	9.7
No. 10 (2 mm)	3.5
No. 16 (1.18 mm)	23.4
No. 30 (0.6 mm)	258.5
No. 40 (0.425 mm)	1114.9
No. 50 (0.3 mm)	3104.0
No. 100 (0.15 mm)	1409.9
No. 200 (0.075 mm)	101.2
No. 230 (0.063 mm)	5.1
Pan	4.8
Total Retained:	6039.6

if sample is composited Sample numbers and Station:	

Additional Remarks:

placed in oven 7/14/16 - top shelf

placed in sieve 8:16 Am

Lab Sample Report

Lab Number:

Sample Information:

Sample Location: Rio Grande Station: Sample Number: CA-2

Date & Time Sampled: 6-30-2016 Date Received: 7-1-2016

Sample Testing:

Composite: Y N

Dry Weight: 6923.5

Sieve:	Weight Retained:
2" (50 mm)	
1" (25 mm)	
3/4" (19 mm)	
1/2" (12.5 mm)	
3/8" (9.5 mm)	3.5 g
No. 4 (4.75 mm)	24.7
No. 8 (2.36 mm)	77.7
No. 10 (2 mm)	27.0
No. 16 (1.18 mm)	165.9
No. 30 (0.6 mm)	1021.7
No. 40 (0.425 mm)	1722.0
No. 50 (0.3 mm)	2353.1
No. 100 (0.15 mm)	1411.2
No. 200 (0.075 mm)	101.0
No. 230 (0.063 mm)	5.1
Pan	5.5
stem/sticks	1.1
Total Retained:	6918.4

If sample is composited Sample numbers and Station:	

Additional Remarks:

7-5-2016
dry weight w/pan
. 8350.7 g
. 8139.4 g 12:45pm
~~7999.4 g~~ 7990.9 g

Lab Sample Report Lab Number: CA063016

Sample Information:
Sample Location: sample location for Canoa Arroyo #3 Station: bed sample Sample Number: CA-3
Date & Time Sampled: 6/30/16 Date Received: 6/30/16

Sample Testing:
Dry Weight: 9403.2 ~~9403.5~~

Composite: Y (N)

Sieve:	Weight Retained:
2" (50 mm)	1695.6
1" (25 mm)	1986.0
3/4" (19 mm)	588.1
1/2" (12.5 mm)	520.3
3/8" (9.5 mm)	317.0
No. 4 (4.75 mm)	674.4
No. 8 (2.36 mm)	457.6
No. 10 (2 mm)	100.5
No. 16 (1.18 mm)	247.9
No. 30 (0.6 mm)	181.7
No. 40 (0.425 mm)	121.6
No. 50 (0.3 mm)	327.5
No. 100 (0.15 mm)	1371.5
No. 200 (0.075 mm)	550.5
No. 230 (0.063 mm)	103.8
Pan	160.1
Total Retained:	9404.1

if sample is composited Sample numbers and Station:	

Additional Remarks:

placed in oven on 7/13/16 - top shelf ⇒ taken out on 7/14/16
split sample on 7/12/16 ~~oven~~
processed 7/15/16 OA @ 700 AM
performed gradations @ 7:40 AM

largest particle was weighed + measured
mass - 626.1g
axis a - 95mm
axis b - 83mm
axis c - 59mm

Lab Sample Report

Lab Number:

Sample Information:

Sample Location: Rio Grande Station: _____ Sample Number: CA-4

Date & Time Sampled: 6-30-2016 Date Received: 7-1-2016

Sample Testing:

Composite: Y N

Dry Weight: 7564.3

Sieve:	Weight Retained:
2" (50 mm)	922.5
1" (25 mm)	258.6
3/4" (19 mm)	39.7
1/2" (12.5 mm)	19.4
3/8" (9.5 mm)	1.7
No. 4 (4.75 mm)	28.5
No. 8 (2.36 mm)	48.9
No. 10 (2 mm)	15.0
No. 16 (1.18 mm)	90.0
No. 30 (0.6 mm)	534.4
No. 40 (0.425 mm)	1191.3
No. 50 (0.3 mm)	2751.6
No. 100 (0.15 mm)	1274.0
No. 200 (0.075 mm)	232.2
No. 230 (0.063 mm)	46.3
Pan	108.6
Total Retained:	7562.7

if sample is composited Sample numbers and Station:	

Additional Remarks:

7-5-2016

dry weight w/ pan

1. 9191 g
2. 9189.6 g
3. 9037.4 g
4. 8923 g

Lab Sample Report

Lab Number:

mple Information: Rio Grande, Arr
nple Location: de las cañas Reach Station: Sample Number: CA-5
ate & Time
Sampled: 6/30/2016 Date Received: 7/6/2016

Sample Testing:

Composite: Y (N)

Dry Weight: 4408.7

Sieve:	Weight Retained:
2" (50 mm)	—
1" (25 mm)	—
3/4" (19 mm)	—
1/2" (12.5 mm)	—
3/8" (9.5 mm)	0.8
No. 4 (4.75 mm)	3.2
No. 8 (2.36 mm)	8.1
No. 10 (2 mm)	2.6
No. 16 (1.18 mm)	15.2
No. 30 (0.6 mm)	96.7
No. 40 (0.425 mm)	250.6
No. 50 (0.3 mm)	1090.6
No. 100 (0.15 mm)	2507.8
No. 200 (0.075 mm)	337.2
No. 230 (0.063 mm)	37.2
Pan	57.3
Total Retained:	4407.3

wood piece
1 wood piece in rocks
some organics

if sample is composited Sample numbers and Station:	

Additional Remarks:

7/7/2016
put in the oven ~~middle~~ middle shelf - put in again on 7/12/16 bottom shelf

put in shaker 7/13/16 ~ 10:45 am
processed @ 11:15 am

Rio Grande/
Cañas Bed Sampling

Lab Sample Report

Lab Number:

Sample Information:
Sample Location: Rio Grande Station: Sample Number: CA-6
Date & Time Sampled: 6-30-2016 Date Received: 7-1-2016

Sample Testing: Sieve, 7/6/2016

Composite: Y (N)

Dry Weight: 4078.8

Sieve:	Weight Retained:
2" (50 mm)	
1" (25 mm)	
3/4" (19 mm)	
1/2" (12.5 mm)	
3/8" (9.5 mm)	
No. 4 (4.75 mm)	34.5
No. 8 (2.36 mm)	132.7
No. 10 (2 mm)	53.7
No. 16 (1.18 mm)	235.9
No. 30 (0.6 mm)	602.5
No. 40 (0.425 mm)	710.1
No. 50 (0.3 mm)	976.1
No. 100 (0.15 mm)	817.0
No. 200 (0.075 mm)	405.6
No. 230 (0.063 mm)	59.2
Pan	51.8
stems, sticks	0.9
Total Retained:	4097.1

if sample is composited Sample numbers and Station:	

Additional Remarks:

6-30-2016
CA-6 (top shelf)
CA-4 (middle shelf)
CA-2 (bottom shelf)

1st dry weight, w/pan:
5565.5 g
~~5424.8 g~~ 5419.5 g
5306.

Rio Grande at Arroyo de Las Cañas

Lab Sample Report

Lab Number: CA7063016

Sample Information:

Sample Location: CA-7 Station: _____ Sample Number: CA-7

Date & Time Sampled: 6/30/2016 Date Received: 7/6/2016

Sample Testing:

Composite: Y (N)

Dry Weight: 7166.3

Sieve:	Weight Retained:
2" (50 mm)	—
1" (25 mm)	—
3/4" (19 mm)	—
1/2" (12.5 mm)	—
3/8" (9.5 mm)	—
No. 4 (4.75 mm)	0.2
No. 8 (2.36 mm)	1.6
No. 10 (2 mm)	0.4
No. 16 (1.18 mm)	4.6
No. 30 (0.6 mm)	34.9
No. 40 (0.425 mm)	190.7
No. 50 (0.3 mm)	5760.3
No. 100 (0.15 mm)	1076.6
No. 200 (0.075 mm)	77.1
No. 230 (0.063 mm)	9.2
Pan	13.5
Total Retained:	7169.1

organic (wood)

if sample is composited Sample numbers and Station:	

Additional Remarks:

7/7/2016
put in the oven
-top shelf, 2:45 pm

⇒ placed back in oven 7/12/16 top shelf

Still moist (taken out of oven 7/8 ?)

Put in shaker 7/13/16 @ 8:10 AM

8421 g weighed 7/12/2016

Lab Sample Report Lab Number: CA80630L6

Sample Information:
Sample Location: Sample location for Corrals Arroyo #8 Station: Sample Number: CA-8
Date & Time Sampled: 6/30/16 Date Received: 6/30/16

Sample Testing:

Composite: Y (N)

Dry Weight: 6672.3

Sieve:	Weight Retained:
2" (50 mm)	
1" (25 mm)	
3/4" (19 mm)	18.0
1/2" (12.5 mm)	56.3
3/8" (9.5 mm)	47.0
No. 4 (4.75 mm)	112.5
No. 8 (2.36 mm)	95.9
No. 10 (2 mm)	25.8
No. 16 (1.18 mm)	131.5
No. 30 (0.6 mm)	519.6
No. 40 (0.425 mm)	793.9
No. 50 (0.3 mm)	2767.6
No. 100 (0.15 mm)	~~1384.7~~ 1550.2
No. 200 (0.075 mm)	~~178.8~~ 184.1
No. 230 (0.063 mm)	13.0 ~~12.2~~
Pan	27.1
organics	0
Total Retained:	

if sample is composited Sample numbers and Station:	

Additional Remarks:

placed in oven 7/14/16 @ middle shelf
placed in shaker ~ 10:40 pm
processed ~ 11:15 AM

More than 5% error
Re-run sieve analysis on page 2 of 2

1 of 2

Lab Sample Report Lab Number: CA 8063016

Sample Information: Sample location for
Sample Location: Cañas Arroyo # 8 Station: _____ Sample Number: CA-8
Date & Time Sampled: 6/30/16 Date Received: 6/30/16

Sample Testing:

Composite: Y (N)

Dry Weight: 6669.7
4804.1 + 1865.6

Sieve:	Weight Retained:
2" (50 mm)	
1" (25 mm)	
3/4" (19 mm)	18.0
1/2" (12.5 mm)	52.8
3/8" (9.5 mm)	50.2
No. 4 (4.75 mm)	111.1
No. 8 (2.36 mm)	95.3
No. 10 (2 mm)	84.9
No. 16 (1.18 mm)	129.1
No. 30 (0.6 mm)	536.3
No. 40 (0.425 mm)	796.5
No. 50 (0.3 mm)	2874.5
No. 100 (0.15 mm)	1782.5
No. 200 (0.075 mm)	164.6
No. 230 (0.063 mm)	11.4
Pan	24.2
organics	0
Total Retained:	6671.4

if sample is composited Sample numbers and Station:	

Additional Remarks:

Error on 1st sieve analysis - see page 1 of 2
Second sieve analysis run ~ 2 PM
Entered into xls at 2:25.

Lab Sample Report

Lab Number:

Sample Information: Rio Grande on Arr. de las cañas reach

Sample Location:

Site & Time Sampled: 6/30/2016

Station:

Sample Number: CA-9

Date Received: 7/6/2016

Sample Testing:

Composite: Y N

Dry Weight: 3860.4

Sieve:	Weight Retained:
2" (50 mm)	
1" (25 mm)	
3/4" (19 mm)	
1/2" (12.5 mm)	
3/8" (9.5 mm)	
No. 4 (4.75 mm)	
No. 8 (2.36 mm)	0.1
No. 10 (2 mm)	0.8
No. 16 (1.18 mm)	2.3
No. 30 (0.6 mm)	15.4
No. 40 (0.425 mm)	72.3
No. 50 (0.3 mm)	751.3
No. 100 (0.15 mm)	2891.1
No. 200 (0.075 mm)	121.0
No. 230 (0.063 mm)	3.8
Pan	8.3
organics	0.0
Total Retained:	3866.4

if sample is composited Sample numbers and Station:	

Additional Remarks:

7/7/2016
put in oven
bottom shelf

7/8 pulled out of oven, split in half

Entered into xls on 7/8/16 @ 11:25 AM.

Lab Sample Report Lab Number: CA10063016

Sample Information:					
Sample Location:	sample location for Conas Arroyo # 10	Station:	bed sample	Sample Number:	CA-10
Date & Time Sampled:	6/30/16			Date Received:	6/30/16

Sample Testing:

Composite: Y (N)

Dry Weight: 4367.7

Sieve:	Weight Retained:	
2" (50 mm)	—	
1" (25 mm)	—	
3/4" (19 mm)	—	
1/2" (12.5 mm)	—	
3/8" (9.5 mm)	—	
No. 4 (4.75 mm)	0.7	→ some organics (wood & seeds)
No. 8 (2.36 mm)	3.3	→ + sand & org. lumps
No. 10 (2 mm)	1.8	
No. 16 (1.18 mm)	5.8	→ some organics (wood/seeds?)
No. 30 (0.6 mm)	7.8	
No. 40 (0.425 mm)	30.5	
No. 50 (0.3 mm)	496.5	
No. 100 (0.15 mm)	3432.1	
No. 200 (0.075 mm)	319.4	
No. 230 (0.063 mm)	28.0	
Pan	40.8	
Total Retained:	4366.7	

if sample is composited Sample numbers and Station:	

Additional Remarks:

placed in oven 7/13/16 - bottom shelf ⇒ taken out of oven on 7/14/16

placed in shaker @ 8:05 AM 7/15/16

processed @ 8:40 AM 7/15/16

Figure 62 Grain size distribution analysis for the June 30 2016 bed material sampling survey.

Lab Number CA01063016 Sample # CA-1 Station:

Sieve Size and Percent passing for Soil Samples

Sample Size = 6047.3 grams

Sieve No. (US std)	Sieve size (mm)	Mass of soil with pan (g)	Mass of soil w/o pan (g)	* based on Minitial % retained	* based on Minitial sum(% retained)	* based on Minitial % passing
2"	50.80			0.00%	0.00%	100.00%
1"	25.00			0.00%	0.00%	100.00%
3/4"	19.00			0.00%	0.00%	100.00%
1/2"	12.70			0.00%	0.00%	100.00%
3/8"	9.50			0.00%	0.00%	100.00%
#4	4.75		4.6	0.08%	0.08%	99.92%
#8	2.36		9.7	0.16%	0.24%	99.76%
#10	2.00		3.5	0.06%	0.29%	99.71%
#16	1.18		23.4	0.39%	0.68%	99.32%
#30	0.60		258.5	4.28%	4.96%	95.04%
#40	0.425		1114.9	18.46%	23.42%	76.58%
#50	0.30		3104	51.39%	74.82%	25.18%
#100	0.150		1409.9	23.34%	98.16%	1.84%
#200	0.075		101.2	1.68%	99.84%	0.16%
#230	0.063		5.1	0.08%	99.92%	0.08%
pan	--		4.8	0.08%	100.00%	0.00%
	Totals	0	6039.6	--	--	--

Total weight % Difference = 0.1 %

1	0.00		D_{100}			
2	0.00	-1.20	D_{84}	0.49	1 std deviation greater than median	
3	0.00	-1.12	D_{60}	0.38		
4	0.02	-0.82	D_{50}	0.35	Median size	
5	0.25	-0.52	D_{30}	0.31		
6	0.77	-0.37	D_{16}	0.23	1 std deviation less than median	
7	0.95	-0.22	D_{10}	0.19	Effective Size	
8	0.99	0.07	C_u	1.99	Uniformity coefficient	
9	1.00	0.30	C_c	1.32	Coefficient of gradation	
10	1.00	0.37				
11	1.00	0.68	gap graded		Particle size distribution curve	
12	1.00	0.98				
13	1.00	1.10				
14	1.00	1.28				
15	1.00	1.40				
16	1.00	1.71				

Lab Number CA02063016 Sample # CA-2 Station:

Sieve Size and Percent passing for Soil Samples

Sample Size = 6922.4 grams **1.1 g were stems or sticks that were removed.**

Sieve No. (US std)	Sieve size (mm)	Mass of soil with pan (g)	Mass of soil w/o pan (g)	* based on Minitial % retained	* based on Minitial sum(% retained)	* based on Minitial % passing
2"	50.80			0.00%	0.00%	100.00%
1"	25.00			0.00%	0.00%	100.00%
3/4"	19.00			0.00%	0.00%	100.00%
1/2"	12.70			0.00%	0.00%	100.00%
3/8"	9.50		3.5	0.05%	0.05%	99.95%
#4	4.75		24.7	0.36%	0.41%	99.59%
#8	2.36		77.7	1.12%	1.53%	98.47%
#10	2.00		27.0	0.39%	1.92%	98.08%
#16	1.18		165.9	2.40%	4.32%	95.68%
#30	0.60		1021.7	14.77%	19.09%	80.91%
#40	0.425		1722.0	24.89%	43.98%	56.02%
#50	0.30		2353.1	34.01%	77.99%	22.01%
#100	0.150		1411.2	20.40%	98.39%	1.61%
#200	0.075		101.0	1.46%	99.85%	0.15%
#230	0.063		5.1	0.07%	99.92%	0.08%
pan	--		5.5	0.08%	100.00%	0.00%
	Totals	0	6918.4	--	--	--

Total weight % Difference = 0.1 %

1	0.00		D_{100}			
2	0.00	-1.20	D_{84}	0.69	1 std deviation greater than median	
3	0.00	-1.12	D_{60}	0.45		
4	0.02	-0.82	D_{50}	0.40	Median size	
5	0.22	-0.52	D_{30}	0.33		
6	0.56	-0.37	D_{16}	0.24	1 std deviation less than median	
7	0.81	-0.22	D_{10}	0.20	Effective Size	
8	0.96	0.07	C_u	2.25	Uniformity coefficient	
9	0.98	0.30	C_c	1.18	Coefficient of gradation	
10	0.98	0.37				
11	1.00	0.68	gap graded		Particle size distribution curve	
12	1.00	0.98				
13	1.00	1.10				
14	1.00	1.28				
15	1.00	1.40				
16	1.00	1.71				

Lab Number	CA03063016		Sample #	CA-3	Station:	bed material sample					

Sieve Size and Percent passing for Soil Samples

Sample Size = 9403.2 grams

Sieve		Mass of soil		* based on Minitial							
No. (US std)	size (mm)	with pan (g)	w/o pan (g)	% retained	sum(% retained)	% passing					
	83.00					100.00%					
2"	50.80		1695.6	18.03%	18.03%	81.97%	1	0.00		D_{100}	83.00
1"	25.00		1986	21.12%	39.15%	60.85%	2	0.02	-1.20	D_{84}	53.00 1 std deviation greater than median
3/4"	19.00		588.1	6.25%	45.40%	54.60%	3	0.03	-1.12	D_{60}	24.08
1/2"	12.70		520.3	5.53%	50.94%	49.06%	4	0.09	-0.82	D_{50}	13.59 Median size
3/8"	9.50		317.0	3.37%	54.31%	45.69%	5	0.23	-0.52	D_{30}	1.19
#4	4.75		674.4	7.17%	61.48%	38.52%	6	0.27	-0.37	D_{16}	0.21 1 std deviation less than median
#8	2.36		457.6	4.87%	66.34%	33.66%	7	0.28	-0.22	D_{10}	0.16 Effective Size
#10	2.00		100.5	1.07%	67.41%	32.59%	8	0.30	0.07	C_u	150.65 Uniformity coefficient
#16	1.18		247.9	2.64%	70.05%	29.95%	9	0.33	0.30	C_c	0.37 Coefficient of gradation
#30	0.60		181.7	1.93%	71.98%	28.02%	10	0.34	0.37		
#40	0.425		121.6	1.29%	73.27%	26.73%	11	0.39	0.68	gap graded	Particle size distribution curve
#50	0.30		327.5	3.48%	76.76%	23.24%	12	0.46	0.98		
#100	0.150		1371.5	14.58%	91.34%	8.66%	13	0.49	1.10		
#200	0.075		550.5	5.85%	97.19%	2.81%	14	0.55	1.28		
#230	0.063		103.8	1.10%	98.30%	1.70%	15	0.61	1.40		
pan	--		160.1	1.70%	100.00%	0.00%	16	0.82	1.71		
	Totals	0	9404.1	--	--	--					

Total weight % Difference = 0.0 %

Notes

largest particle was weighed with a mass of 626.1 g, dimensions as follows

axis a	95	mm
axis b	83	mm
axis c	59	mm

Lab Number	CA04063016		Sample #	CA-4	Station:					

Sieve Size and Percent passing for Soil Samples

Sample Size = 7564.3 grams

Sieve		Mass of soil		* based on Minitial							
No. (US std)	size (mm)	with pan (g)	w/o pan (g)	% retained	sum(% retained)	% passing					
2"	50.80		922.5	12.20%	12.20%	87.80%	1	0.00		D_{100}	
1"	25.00		258.6	3.42%	15.62%	84.38%	2	0.01	-1.20	D_{84}	20.47 1 std deviation greater than median
3/4"	19.00		39.7	0.52%	16.14%	83.86%	3	0.02	-1.12	D_{60}	0.44
1/2"	12.70		19.4	0.26%	16.40%	83.60%	4	0.05	-0.82	D_{50}	0.39 Median size
3/8"	9.50		1.7	0.02%	16.42%	83.58%	5	0.22	-0.52	D_{30}	0.32
#4	4.75		28.5	0.38%	16.80%	83.20%	6	0.58	-0.37	D_{16}	0.23 1 std deviation less than median
#8	2.36		48.9	0.65%	17.44%	82.56%	7	0.74	-0.22	D_{10}	0.18 Effective Size
#10	2.00		15.0	0.20%	17.64%	82.36%	8	0.81	0.07	C_u	2.40 Uniformity coefficient
#16	1.18		90	1.19%	18.83%	81.17%	9	0.82	0.30	C_c	1.30 Coefficient of gradation
#30	0.60		534.4	7.07%	25.90%	74.10%	10	0.83	0.37		
#40	0.425		1191.3	15.75%	41.65%	58.35%	11	0.83	0.68	gap graded	Particle size distribution curve
#50	0.30		2751.6	36.38%	78.04%	21.96%	12	0.84	0.98		
#100	0.150		1274.0	16.85%	94.88%	5.12%	13	0.84	1.10		
#200	0.075		232.2	3.07%	97.95%	2.05%	14	0.84	1.28		
#230	0.063		46.3	0.61%	98.56%	1.44%	15	0.84	1.40		
pan	--		108.6	1.44%	100.00%	0.00%	16	0.88	1.71		
	Totals	0	7562.7	--	--	--					

Total weight % Difference = 0.0 %

Lab Number	CA05063016		Sample #	CA-5	Station:	bed material sample

Sieve Size and Percent passing for Soil Samples

Sample Size = 4408.7 grams

Sieve		Mass of soil		* based on Minitial		
No. (US std)	size (mm)	with pan (g)	w/o pan (g)	% retained	sum(% retained)	% passing
2"	50.80			0.00%	0.00%	100.00%
1"	25.00			0.00%	0.00%	100.00%
3/4"	19.00			0.00%	0.00%	100.00%
1/2"	12.70			0.00%	0.00%	100.00%
3/8"	9.50		0.8	0.02%	0.02%	99.98%
#4	4.75		3.2	0.07%	0.09%	99.91%
#8	2.36		8.1	0.18%	0.27%	99.73%
#10	2.00		2.6	0.06%	0.33%	99.67%
#16	1.18		15.2	0.34%	0.68%	99.32%
#30	0.60		96.7	2.19%	2.87%	97.13%
#40	0.425		250.6	5.69%	8.56%	91.44%
#50	0.30		1090.6	24.75%	33.30%	66.70%
#100	0.150		2507.8	56.90%	90.20%	9.80%
#200	0.075		337.2	7.65%	97.86%	2.14%
#230	0.063		37.2	0.84%	98.70%	1.30%
pan	--		57.3	1.30%	100.00%	0.00%
	Totals	0	4407.3	--	--	--

Total weight % Difference = 0.0 %

1	0.00		D_{100}			
2	0.01	-1.20	D_{84}	0.38	1 std deviation greater than median	
3	0.02	-1.12	D_{60}	0.28		
4	0.10	-0.82	D_{50}	0.24	Median size	
5	0.67	-0.52	D_{30}	0.19		
6	0.91	-0.37	D_{16}	0.16	1 std deviation less than median	
7	0.97	-0.22	D_{10}	0.15	Effective Size	
8	0.99	0.07	C_u	1.84	Uniformity coefficient	
9	1.00	0.30	C_c	0.89	Coefficient of gradation	
10	1.00	0.37				
11	1.00	0.68	poorly graded		Particle size distribution curve	
12	1.00	0.98				
13	1.00	1.10				
14	1.00	1.28				
15	1.00	1.40				
16	1.00	1.71				

Lab Number	CA06063016		Sample #	CA-06	Station:

Sieve Size and Percent passing for Soil Samples

Sample Size = 4077.9 grams **(0.9 g of stems removed)**

Sieve		Mass of soil		* based on Minitial		
No. (US std)	size (mm)	with pan (g)	w/o pan (g)	% retained	sum(% retained)	% passing
2"	50.80			0.00%	0.00%	100.00%
1"	25.00			0.00%	0.00%	100.00%
3/4"	19.00			0.00%	0.00%	100.00%
1/2"	12.70			0.00%	0.00%	100.00%
3/8"	9.50			0.00%	0.00%	100.00%
#4	4.75		34.5	0.84%	0.84%	99.16%
#8	2.36		132.7	3.24%	4.08%	95.92%
#10	2.00		53.7	1.31%	5.39%	94.61%
#16	1.18		253.9	6.20%	11.59%	88.41%
#30	0.60		602.5	14.71%	26.29%	73.71%
#40	0.425		710.1	17.33%	43.63%	56.37%
#50	0.30		976.1	23.82%	67.45%	32.55%
#100	0.150		817.0	19.94%	87.39%	12.61%
#200	0.075		405.6	9.90%	97.29%	2.71%
#230	0.063		59.2	1.44%	98.74%	1.26%
pan	--		51.8	1.26%	100.00%	0.00%
	Totals	0	4097.1	--	--	--

Total weight % Difference = 0.5 %

1	0.00		D_{100}			
2	0.01	-1.20	D_{84}	0.96	1 std deviation greater than median	
3	0.03	-1.12	D_{60}	0.46		
4	0.13	-0.82	D_{50}	0.39	Median size	
5	0.33	-0.52	D_{30}	0.27		
6	0.56	-0.37	D_{16}	0.17	1 std deviation less than median	
7	0.74	-0.22	D_{10}	0.12	Effective Size	
8	0.88	0.07	C_u	3.66	Uniformity coefficient	
9	0.95	0.30	C_c	1.32	Coefficient of gradation	
10	0.96	0.37				
11	0.99	0.68	gap graded		Particle size distribution curve	
12	1.00	0.98				
13	1.00	1.10				
14	1.00	1.28				
15	1.00	1.40				
16	1.00	1.71				

Lab Number	CA7063016		Sample #	CA-7	Station:	bed material sample					

Sieve Size and Percent passing for Soil Samples

Sample Size = 7166.3 grams

Sieve		Mass of soil		* based on Minitial								
No. (US std)	size (mm)	with pan (g)	w/o pan (g)	% retained	sum(% retained)	% passing						
2"	50.80			0.00%	0.00%	100.00%	1	0.00		D_{100}		
1"	25.00			0.00%	0.00%	100.00%	2	0.00	-1.20	D_{84}	0.40	1 std deviation greater than median
3/4"	19.00			0.00%	0.00%	100.00%	3	0.00	-1.12	D_{60}	0.36	
1/2"	12.70			0.00%	0.00%	100.00%	4	0.01	-0.82	D_{50}	0.35	Median size
3/8"	9.50			0.00%	0.00%	100.00%	5	0.16	-0.52	D_{30}	0.32	
#4	4.75		0.2	0.00%	0.00%	100.00%	6	0.97	-0.37	D_{16}	0.29	1 std deviation less than median
#8	2.36		1.6	0.02%	0.03%	99.97%	7	0.99	-0.22	D_{10}	0.22	Effective Size
#10	2.00		0.4	0.01%	0.03%	99.97%	8	1.00	0.07	C_u	1.62	Uniformity coefficient
#16	1.18		4.6	0.06%	0.09%	99.91%	9	1.00	0.30	C_c	1.25	Coefficient of gradation
#30	0.60		34.9	0.49%	0.58%	99.42%	10	1.00	0.37			
#40	0.425		190.7	2.66%	3.24%	96.76%	11	1.00	0.68	poorly graded		Particle size distribution curve
#50	0.30		5760.3	80.35%	83.59%	16.41%	12	1.00	0.98			
#100	0.150		1076.6	15.02%	98.61%	1.39%	13	1.00	1.10			
#200	0.075		77.1	1.08%	99.68%	0.32%	14	1.00	1.28			
#230	0.063		9.2	0.13%	99.81%	0.19%	15	1.00	1.40			
pan	--		13.5	0.19%	100.00%	0.00%	16	1.00	1.71			
	Totals	0	7169.1	--	--	--						

Total weight % Difference = 0.0 %

Lab Number	CA08063016		Sample #	1	Station:	CA-8					

Sieve Size and Percent passing for Soil Samples

Sample Size = 6669.7 grams

Sieve		Mass of soil		* based on Minitial								
No. (US std)	size (mm)	with pan (g)	w/o pan (g)	% retained	sum(% retained)	% passing						
2"	50.80			0.00%	0.00%	100.00%	1	0.00		D_{100}		
1"	25.00			0.00%	0.00%	100.00%	2	0.00	-1.20	D_{84}	0.59	1 std deviation greater than median
3/4"	19.00		18	0.27%	0.27%	99.73%	3	0.01	-1.12	D_{60}	0.38	
1/2"	12.70		52.8	0.79%	1.06%	98.94%	4	0.03	-0.82	D_{50}	0.35	Median size
3/8"	9.50		50.2	0.75%	1.81%	98.19%	5	0.30	-0.52	D_{30}	0.30	
#4	4.75		111.1	1.67%	3.48%	96.52%	6	0.73	-0.37	D_{16}	0.21	1 std deviation less than median
#8	2.36		95.3	1.43%	4.91%	95.09%	7	0.85	-0.22	D_{10}	0.18	Effective Size
#10	2.00		24.9	0.37%	5.28%	94.72%	8	0.93	0.07	C_u	2.13	Uniformity coefficient
#16	1.18		129.1	1.94%	7.22%	92.78%	9	0.95	0.30	C_c	1.31	Coefficient of gradation
#30	0.60		536.3	8.04%	15.25%	84.75%	10	0.95	0.37			
#40	0.425		796.5	11.94%	27.19%	72.81%	11	0.97	0.68	gap graded		Particle size distribution curve
#50	0.30		2874.5	43.09%	70.28%	29.72%	12	0.98	0.98			
#100	0.150		1782.5	26.72%	97.00%	3.00%	13	0.99	1.10			
#200	0.075		164.6	2.47%	99.47%	0.53%	14	1.00	1.28			
#230	0.063		11.4	0.17%	99.64%	0.36%	15	1.00	1.40			
pan	--		24.2	0.36%	100.00%	0.00%	16	1.00	1.71			
	Totals	0	6671.4	--	--	--						

Total weight % Difference = 0.0 %

Lab Number CA09063016 Sample # 1 Station: CA-9

Sieve Size and Percent passing for Soil Samples

Sample Size = 3860.4 grams

Sieve No. (US std)	Sieve size (mm)	Mass of soil with pan (g)	Mass of soil w/o pan (g)	* based on Minitial % retained	* based on Minitial sum(% retained)	* based on Minitial % passing
2"	50.80			0.00%	0.00%	100.00%
1"	25.00			0.00%	0.00%	100.00%
3/4"	19.00			0.00%	0.00%	100.00%
1/2"	12.70			0.00%	0.00%	100.00%
3/8"	9.50			0.00%	0.00%	100.00%
#4	4.75			0.00%	0.00%	100.00%
#8	2.36		0.1	0.00%	0.00%	100.00%
#10	2.00		0.8	0.02%	0.02%	99.98%
#16	1.18		2.3	0.06%	0.08%	99.92%
#30	0.60		15.4	0.40%	0.48%	99.52%
#40	0.425		72.3	1.87%	2.35%	97.65%
#50	0.30		751.3	19.43%	21.78%	78.22%
#100	0.150		2891.1	74.77%	96.56%	3.44%
#200	0.075		121.0	3.13%	99.69%	0.31%
#230	0.063		3.8	0.10%	99.79%	0.21%
pan	--		8.3	0.21%	100.00%	0.00%
	Totals	0	3866.4	--	--	--

Total weight % Difference = 0.2 %

1	0.00		D_{100}			1.00
2	0.00	-1.20	D_{84}	0.33	1 std deviation greater than median	0.84
3	0.00	-1.12	D_{60}	0.25		0.60
4	0.03	-0.82	D_{50}	0.23	Median size	0.50
5	0.78	-0.52	D_{30}	0.19		0.30
6	0.98	-0.37	D_{16}	0.17	1 std deviation less than median	0.16
7	1.00	-0.22	D_{10}	0.16	Effective Size	0.10
8	1.00	0.07	C_u	1.59	Uniformity coefficient	
9	1.00	0.30	C_c	0.91	Coefficient of gradation	
10	1.00	0.37				
11	1.00	0.68	gap graded		Particle size distribution curve	
12	1.00	0.98				
13	1.00	1.10				
14	1.00	1.28				
15	1.00	1.40				
16	1.00	1.71				

Lab Number CA10063016 Sample # CA-10 Station: bed material sample

Sieve Size and Percent passing for Soil Samples

Sample Size = 4367.9 grams

Sieve No. (US std)	Sieve size (mm)	Mass of soil with pan (g)	Mass of soil w/o pan (g)	* based on Minitial % retained	* based on Minitial sum(% retained)	* based on Minitial % passing
2"	50.80			0.00%	0.00%	100.00%
1"	25.00			0.00%	0.00%	100.00%
3/4"	19.00			0.00%	0.00%	100.00%
1/2"	12.70			0.00%	0.00%	100.00%
3/8"	9.50			0.00%	0.00%	100.00%
#4	4.75		0.7	0.02%	0.02%	99.98%
#8	2.36		3.3	0.08%	0.09%	99.91%
#10	2.00		1.8	0.04%	0.13%	99.87%
#16	1.18		5.8	0.13%	0.27%	99.73%
#30	0.60		7.8	0.18%	0.44%	99.56%
#40	0.425		30.5	0.70%	1.14%	98.86%
#50	0.30		496.5	11.37%	12.51%	87.49%
#100	0.150		3432.1	78.60%	91.11%	8.89%
#200	0.075		319.4	7.31%	98.42%	1.58%
#230	0.063		28	0.64%	99.07%	0.93%
pan	--		40.8	0.93%	100.00%	0.00%
	Totals	0	4366.7	--	--	--

Total weight % Difference = 0.0 %

1	0.00		D_{100}		
2	0.01	-1.20	D_{84}	0.29	1 std deviation greater than median
3	0.02	-1.12	D_{60}	0.24	
4	0.09	-0.82	D_{50}	0.22	Median size
5	0.87	-0.52	D_{30}	0.18	
6	0.99	-0.37	D_{16}	0.16	1 std deviation less than median
7	1.00	-0.22	D_{10}	0.15	Effective Size
8	1.00	0.07	C_u	1.55	Uniformity coefficient
9	1.00	0.30	C_c	0.92	Coefficient of gradation
10	1.00	0.37			
11	1.00	0.68	poorly graded		Particle size distribution curve
12	1.00	0.98			
13	1.00	1.10			
14	1.00	1.28			
15	1.00	1.40			
16	1.00	1.71			

Figure 63 Sand bar where data was collected for CA-1

Figure 64 Near CA-2, red silty clay can be seen on the side channel bars. Likely the clay is attributed to monsoonal rain events.

Figure 65 Near CA-2, high water mark and clay deposits can be seen on the river bank.

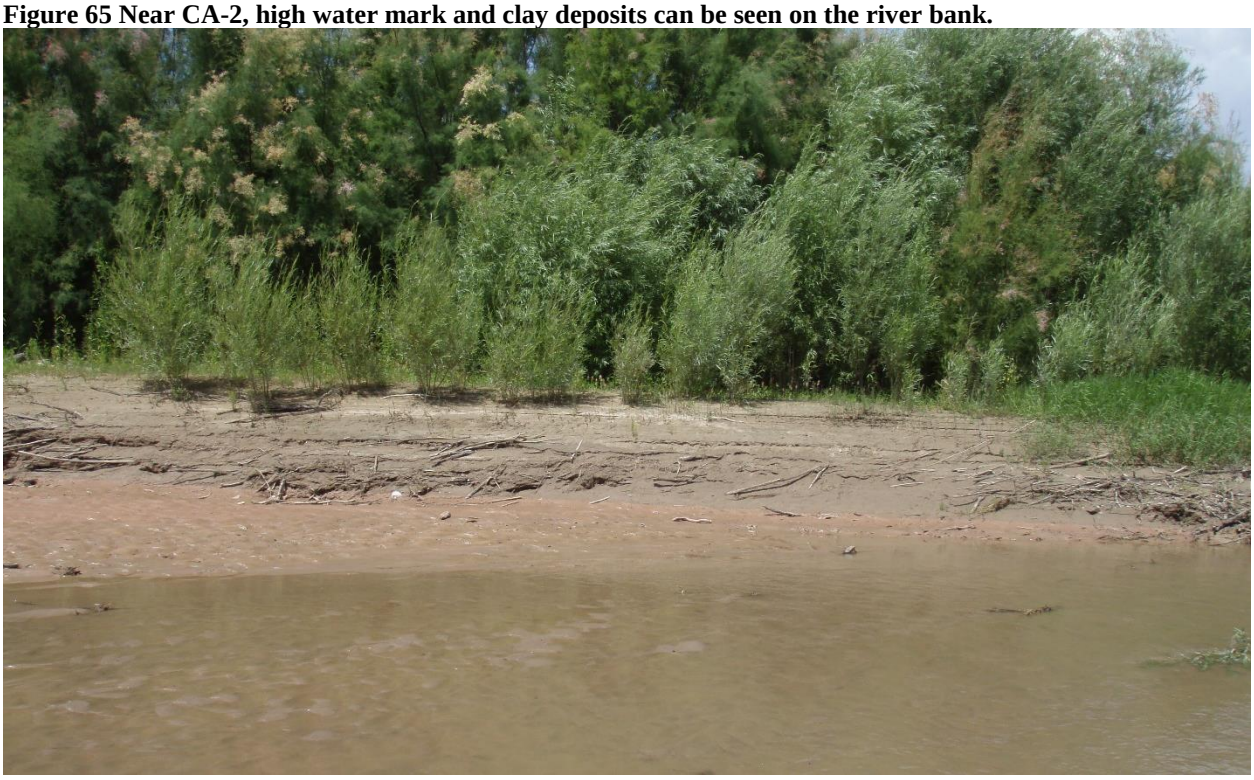

Figure 66 Gravelly sediment deposition found at the Arroyo de las Cañas confluence.

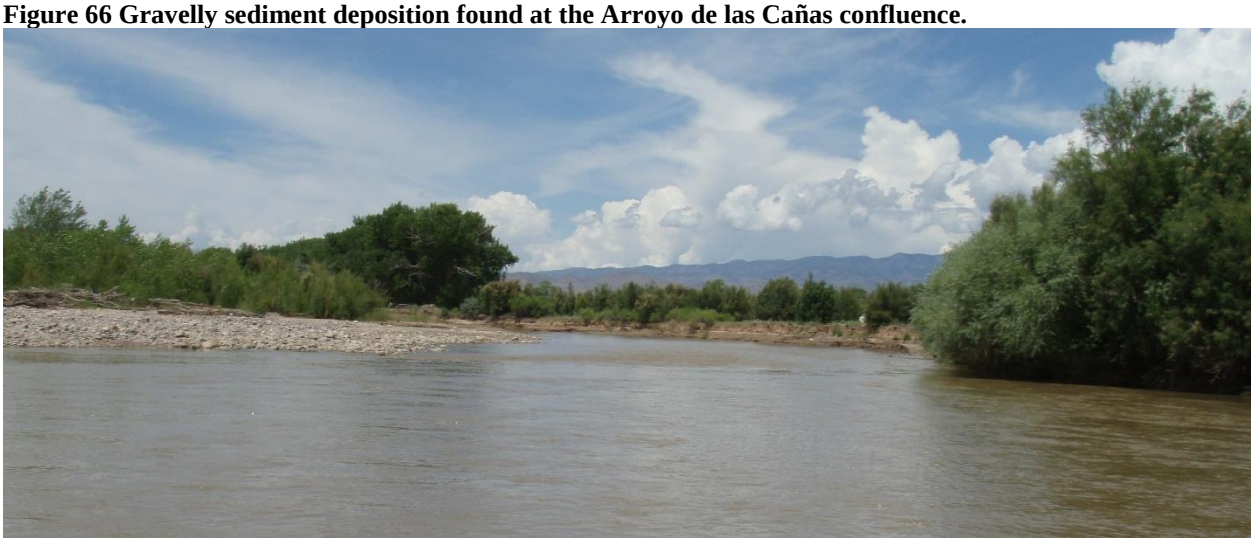

Figure 67 looking upstream, on the alluvial fan of the rocky Arroyo de las Cañas confluence.

Figure 68 From the Arroyo de las Cañas alluvial fan, looking across stream at the erosion occurring at the banks of the Rio Grande.

Figure 69 Eroding side bar opposite the Arroyo de las Cañas confluence (near the collection site for CA-3 and CA-4)

Figure 70 Eroding bank of the Rio Grande, opposite the confluence of the Arroyo de las Cañas

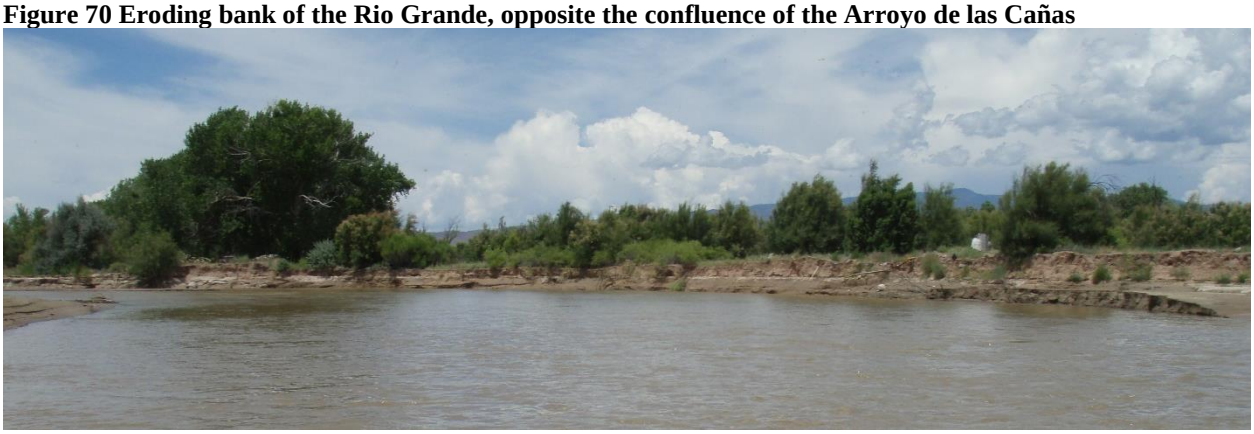

Figure 71 Eroding bank of the Rio Grande, near the confluence of the Arroyo de las Cañas.

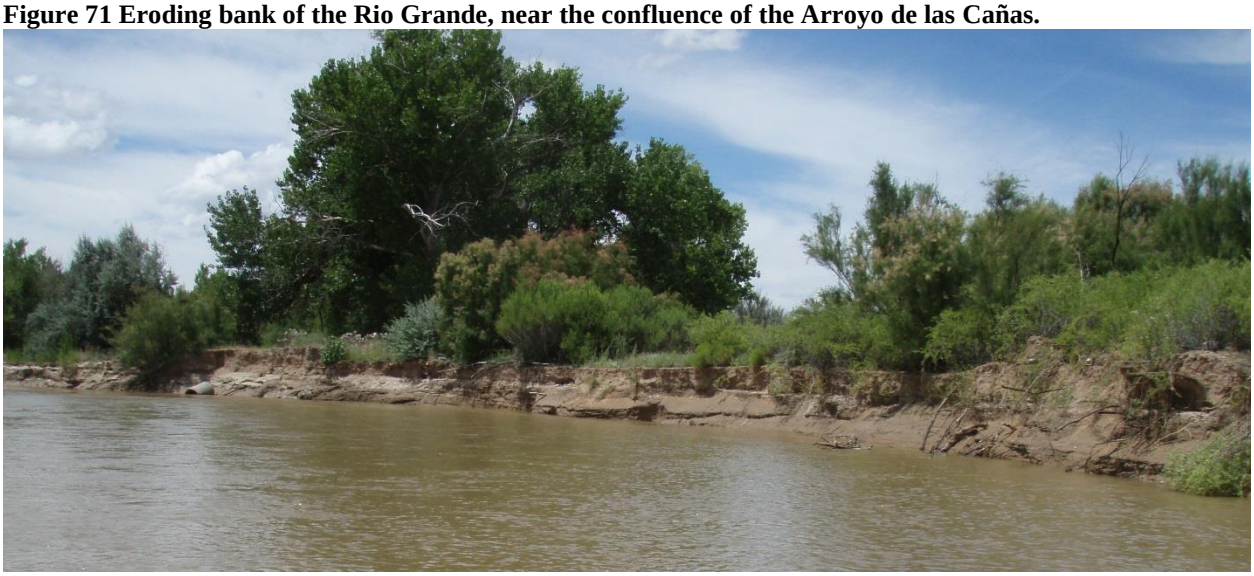

Figure 72 High water mark and the eroding bank of the Rio Grande near the Arroyo de las Cañas confluence.

Figure 73 Sand bar formed below the Arroyo de las Cañas confluence, near the picnic tables.

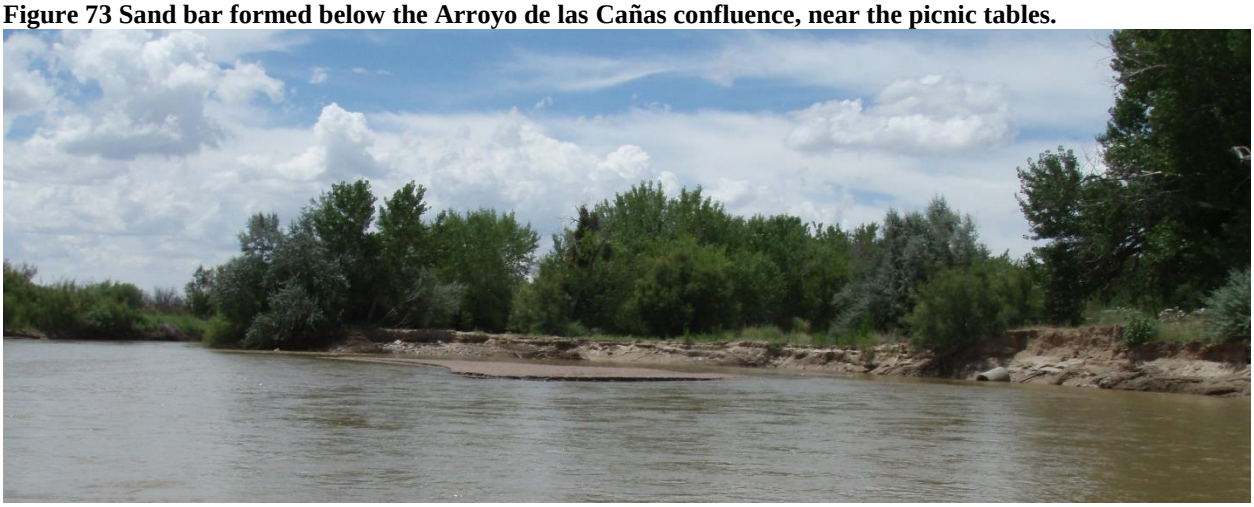

Figure 74 Sand bar near the CA-5 data collection location.

Figure 75 Photograph of the braided channel occurring due to several sand bar and debris near the CA-5 location.

Figure 76 Photograph of the silty clay attributed to monsoon flows on a sand bar. Location is near CA-6 and CA-7.

Figure 77 Eroding sand bar at the CA-8 through CA-10 data collection location.

Figure 78 Approximate location of the sediment samples in the study reach.